

Design and Analysis of Short Packet and Concatenated Coded Communication Systems

by

Kar Peo Yar

A dissertation submitted in partial fulfillment
of the requirements for the degree of
Doctor of Philosophy
(Electrical Engineering: Systems)
in The University of Michigan
2007

Doctoral Committee:

Professor Wayne Stark, Chair
Associate Professor Achilleas Anastasopoulos
Assistant Professor Sandeep Pradhan
Associate Professor Hendrikus Derksen

ABSTRACT

Design and Analysis of Short Packet and Concatenated Coded Communication Systems

by

Kar Peo Yar

Chair: Wayne Stark

For many wireless communication systems it is important to achieve energy efficient operation with a reasonably small delay. Error control coding is an important component of such a system. One commonly used code is a Reed-Solomon (RS) code. RS codes are widely used as outer codes and concatenated with other codes to enhance system robustness against burst errors. They are also widely used with M -ary modulation. In this case the M -ary modulation can be viewed as an inner code. Typically, when an RS code over $\text{GF}(2^m)$ is used with an M -ary modulation, the number of bits per coded symbol m is an integer multiple of $\log_2(M)$. This limits the number of choices of the number of bits used to represent an RS symbol. If m is large, we need to use a large M for orthogonal/biorthogonal modulation. This means a large bandwidth/delay. For M -ary phase shift keying modulation this means a large energy. In this thesis, we provide an analytical method for performance analysis of RS coded systems with arbitrary inner codeword lengths. We derive the bit error performance of RS coded M -ary modulation using Markov Chain analysis. We also demonstrate that the bit/packet error performance of RS codes can be improved with the use of interleaver and iterative decoding.

Energy is consumed in the transmitter in order to radiate an appropriate amplitude

signal as well as the receiver in processing such signals. Most research ignores the effect of amplifier efficiency, distance between transmitter and receiver and processing power of the receiver. If these factors are considered, coding may deteriorate the error probability. In this thesis, we present a study of the energy analysis of short packet data length by using the cutoff rate and capacity theorem in our investigation. We show that there exists an optimum code rate that achieves a minimum total energy consumed. Using the cutoff rate for an additive white Gaussian noise (AWGN) channel, we derive a closed form expression that approximate the optimum code rate. We also present numerical results using practical coding schemes, using RS codes and convolutional codes.

© Kar Peo Yar 2007
All Rights Reserved

To my parents, my wife Valerie and my 2 sons - Matthew and Andrew.

ACKNOWLEDGEMENTS

I am most grateful to my thesis advisor, Professor Wayne Stark, for his guidance and support throughout my graduate study at the University of Michigan. Professor Stark has been a wonderful source of ideas and humor. His extensive knowledge and understanding in the field of wireless communications has been a valuable asset to me; my research has benefited tremendously from our daily discussions.

I would also like to thank the other members of my committee, Professor Achilleas Anastasopoulos and Professor Hendrikus Derksen for teaching me channel coding theory and Professor Sandeep Sadanandarao for introducing information theory to me. This thesis would not have been possible without their instruction and assistance over the years.

I would also like to acknowledge the support which makes this work possible. First, I would like to thank the Department of Electrical Engineering at the University of Michigan for allowing me to enrol during the winter term. Next, I would like to thank the Agency for Science, Technology and Research (A*STAR) for their financial support during these five years.

Finally, I would like to thank my family and friends who have both challenged and supported me throughout the years. To my parents, I thank you for raising me to become an independent adult. To my sisters and brothers, thanks for putting up with me over all the years. To my parents-in-law, thanks for the support for the past few years. I am also grateful to my colleagues Hua Wang, Do-Sik, Ping Cheng Yeh, Chih-Wei Wang, Jinho Kim, SHih-Yu Chang, Changhun Bae and Rong-Terng Juang at the Wireless Communications lab and my friends in Ann Arbor for the unforgettable times we spent together. Finally, I would like to thank Valerie and the little ones,

Matthew and Andrew. You are my source of inspiration, my foundation for courage,
my understanding of love.

TABLE OF CONTENTS

DEDICATION	ii
ACKNOWLEDGEMENTS	iii
LIST OF TABLES	viii
LIST OF FIGURES	ix
LIST OF APPENDICES	xiii
CHAPTERS	
1 Introduction	1
1.1 Energy Efficient System Design	1
1.2 Thesis Overview	4
1.2.1 Reed-Solomon Coded M -ary Modulation With Symbols Overlapping	4
1.2.2 Reed-Solomon Coded Differential Phase Shift Keying Mod- ulation	6
1.2.3 Energy Analysis of Single Hop Communication System for Short Packet Length Data	6
1.2.4 Comparison of Turbo Product Codes and Reed-Solomon Codes	7
1.3 Organization of Thesis	8
2 Analysis of Reed-Solomon Coded M -ary Modulation With Symbols Overlapping	10
2.1 Characteristics of Concatenated Codes	12
2.2 Design Issues of Concatenated Codes	13
2.3 System Model	14
2.4 Markovian Analysis	15
2.5 Performance Over An AWGN Channel	18
2.5.1 Biorthogonal Modulation	18
2.5.2 Orthogonal Modulation with Coherent Demodulation .	23
2.5.3 Orthogonal Modulation with Noncoherent Demodulation	24

2.5.4	Nordstrom-Robinson Code	25
2.5.5	Throughput	27
2.6	Performance Over A Rayleigh Fading Channel	28
2.6.1	Biorthogonal Modulation Over Rayleigh Flat Fading Channel	29
2.6.2	Throughput	32
2.6.3	Block Fading Channel	32
2.7	Low Complexity Coding Strategies for Reed-Solomon Coded M -ary Modulation System	36
2.7.1	RS Coded System with Bits Interleaving	36
2.7.2	RS Coded System With Symbols Interleaving	37
2.7.3	Performance Analysis	38
2.7.4	Performance Over an AWGN Channel	42
2.7.5	Performance Over a Rayleigh Fading Channel	47
2.8	Conclusion	50
3	Analysis of Reed-Solomon With DPSK Modulation	51
3.1	System Description	51
3.2	Derivation of Symbol Error Probability	52
3.3	Derivation of Packet Error Probability over an AWGN Channel	53
3.3.1	Relationship Between Two Adjacent Symbols	55
3.3.2	Decoded Packet Error Probability	57
3.4	Performance of Packet Error Probability over the AWGN channel	58
3.5	Analysis of Symbol Error Probability over a Rayleigh Fading Channel	60
3.6	Performance of RS Codes with DPSK over a Rayleigh Faded Channel	64
3.7	Conclusion	65
4	Energy Analysis of Single Hop Communication System For Short Packet Length Data	66
4.1	System Description	67
4.2	Analysis of Total Energy Consumption Over an AWGN Channel Using Cutoff Rate	69
4.2.1	Derivation of Total Energy Consumed	70
4.2.2	Performance for a Fixed Information Packet Length	71
4.2.3	Derivation of Optimum Code Rate	73
4.2.4	Optimum Code Rate for Large Information Packet	79
4.2.5	Variation of Optimum Code Rate With Packet Error Probability	84
4.2.6	Throughput With Optimum Energy Consumption	87
4.3	Analysis of Total Energy Consumption Over an AWGN Channel Using Capacity	91
4.4	Analysis Using Cutoff Rate for Noncoherent Detection Over Rayleigh Fading Channel	96

4.4.1	Derivation of Total Energy Consumed	96
4.4.2	Performance for a Fixed Information Packet Length . .	96
4.4.3	Derivation of Optimum Code Rate	100
4.4.4	Optimum Code Rate for Large Information Packet . . .	101
4.4.5	Throughput With Optimum Energy Consumption . . .	106
4.5	Energy Performance Using Practical Codes	108
4.5.1	Using RS codes over an AWGN channel	110
4.5.2	Using Convolutional Codes	110
4.6	Conclusion	113
5	Performance Comparison of Product Codes and Reed-Solomon Codes .	118
5.1	Structure of Product Codes	119
5.2	Construction of Rate 1/2 Product Codes	121
5.3	Turbo Decoding of Rate 1/2 Product Codes	123
5.4	System Models	126
5.5	Performance Comparison over BSC	131
5.6	Performance Comparison over AWGN Channel	136
5.7	Performance of RS Codes Over an Erasure Channel	140
5.8	Performance Comparison Over a Bursty Channel	143
5.9	Conclusion	145
6	Conclusions and Future Research	146
6.1	Summary of Contributions	146
6.2	Future Research	148
APPENDICES		149
BIBLIOGRAPHY		155

LIST OF TABLES

Table

4.1	Approximate and exact value of required minimum energy and its respective rate.	77
4.2	Approximate and exact value of required minimum energy and its respective rate.	79
4.3	Approximate and exact values of required minimum energy and its respective code rate for different values of γ , using cutoff rate for noncoherent detection over a Rayleigh fading channel.	106

LIST OF FIGURES

Figure		
2.1	Block diagram of a communications system employing a concatenated code.	12
2.2	Block diagram of RS coded modulation scheme.	14
2.3	Overlapping of RS and biorthogonal symbol.	15
2.4	Bit error probability of RS(96,84) code with (32,6) biorthogonal modulation and RS(255,83) code with (8,4) biorthogonal modulation over an AWGN channel.	22
2.5	Bit error probability of various equivalent RS coded M -ary orthogonal modulation with coherent detection system.	23
2.6	Bit error probability of various equivalent RS coded M -ary orthogonal modulation with noncoherent detection system.	25
2.7	Bit error rate of NR(16,8), 16-ary and 64-ary biorthogonal modulation.	26
2.8	Throughput of RS(96, 84) code with (32,6) biorthogonal modulation and RS(255, 83) code with (8,4) biorthogonal modulation over the AWGN channel.	28
2.9	Bit error probability of RS(96,84) code with (32,6) biorthogonal modulation and RS(255, 83) code with (8,4) biorthogonal modulation over flat fading channel.	31
2.10	Throughput of RS(96, 84) code with (32,6) biorthogonal modulation and RS(255, 83) code with (8,4) biorthogonal modulation over a Rayleigh fading channel.	33
2.11	Bit error probability for block fading channel.	35
2.12	RS coded M -ary orthogonal modulation system with bit interleaving and iterative decoding.	37
2.13	Block coded structure for the RS symbol interleaving system in Fig. 2.12. Each box represents a single bit and there are $k = \log_2 M$ RS codewords in 1 block.	38
2.14	RS coded M -ary orthogonal modulation system with symbols interleaving and iterative decoding.	39

2.15	Packet structure for the RS coded system with symbol interleaving. Here, $M = 16$ and a modulation symbol consists of bits form 2 RS symbols. For example, the first modulation symbol in row 1 consists of bits form RS codeword i and codeword j	40
2.16	Bit error probability of RS(16,6) coded 16-ary orthogonal modulation system using bit interleaving (setup in Fig. 2.12).	43
2.17	Bit error probability of RS(16,6) coded 16-ary orthogonal modulation system using symbol interleaving (setup in Fig. 2.14).	44
2.18	Bit error probability of (i) RS(32,12) coded system with $GF(2^8)$, (ii) RS(16,6) coded system with $GF(2^4)$ and symbol interleaving with 2 iterations, (iii)RS(16,6) coded system with $GF(2^4)$ and bit interleaving with 2 iterations. All the systems employ 16-ary orthogonal modulation. . .	45
2.19	Packet error probability of (i) RS(32,12) coded system with $GF(2^8)$, (ii) RS(16,6) coded system with $GF(2^4)$ and symbol interleaving with 2 iterations, (iii) RS(16,6) coded system with $GF(2^4)$ and bit interleaving with 2 iterations. All the systems employ 16-ary orthogonal modulation.	46
2.20	Bit error probability of (i) RS(32,12) coded system with $GF(2^8)$, (ii) RS(16,6) coded system with $GF(2^4)$ and symbol interleaving with 2 iterations, (iii) RS(16,6) coded system with $GF(2^4)$ and bit interleaving with 2 iterations. All the systems employ 16-ary orthogonal modulation.	48
2.21	Packet error probability of (i) RS(32,12) coded system with $GF(2^8)$, (ii) RS(16,6) coded system with $GF(2^4)$ and symbol interleaving with 2 iterations, (iii) RS(16,6) coded system with $GF(2^4)$ and bit interleaving with 2 iterations. All the systems employ 16-ary orthogonal modulation.	49
3.1	Comparison of symbol error probability for $m=3$ and $m=6$ with Wang's result.	54
3.2	Two Adjacent Symbol a and b. Last bit of symbol a correlates with first bit of symbol b.	55
3.3	Packet Error Probability of RS(15,11) codes with and without interleaver using DPSK over an AWGN channel.	59
3.4	Comparison of bit error probability using (3.2) and (3.27).	62
3.5	Symbol error probability for various values of m using DPSK modulation over a Rayleigh fading channel	63
3.6	Packet Error Probability various RS codes with (denoted by x) and without (denoted by o) interleaver using DPSK over a Rayleigh fading channel.	64
4.1	Variation of $\frac{E_T}{N_0}$ with R with various values of γ	71
4.2	Variation of $\frac{E_T}{N_0}$ with γ when optimum R is used.	72
4.3	Comparison of actual and approximate energy consumed with respect to γ	75
4.4	Comparison of actual and approximate energy consumed with respect to code rate.	76
4.5	Variation of R with respective to γ at the required minimum energy. . .	78

4.6	Variation of $\frac{E_T}{N_0}$ with respect to R ($k=240$).	80
4.7	Variation of γ with respect to code rate at the required minimum energy ($k=240$).	81
4.8	Optimum code rate with respect to number of information bits for $\gamma = 0$ dB.	82
4.9	Optimum code rate for the normalized processing energy when $k \rightarrow \infty$	83
4.10	Total energy vs different code rate for various packet error probabilities (for $\gamma = -5$ dB).	84
4.11	Total energy consumed vs code rate for various packet error probabilities (for $\gamma = 0$ dB).	85
4.12	Total energy consumed vs code rate for various packet error probabilities (for $\gamma = 5$ dB).	86
4.13	Throughput using optimum code rate (for $\gamma = -5$ dB).	88
4.14	Throughput using optimum code rate (for $\gamma = 0$ dB).	89
4.15	Throughput using optimum code rate (for $\gamma = 5$ dB).	90
4.16	Variation of $\frac{E_T}{N_0}$ with R with various values of γ using the capacity for antipodal signalling over an AWGN channel.	93
4.17	Variation of optimum code rate R with γ using the cutoff rate and capacity (for antipodal signalling over an AWGN channel).	94
4.18	Variation of optimum code rate R with γ using the cutoff rate and capacity (for antipodal signalling over an AWGN channel).	95
4.19	Variation of $\frac{E_T}{N_0}$ with R with various values of γ from $-\infty$ to -5 dB using the cutoff rate for noncoherent detection over a Rayleigh fading channel.	97
4.20	Variation of $\frac{E_T}{N_0}$ with R with various values of γ from -5 to 10 dB using the cutoff rate for noncoherent detection over a Rayleigh fading channel.	98
4.21	Optimum code rate using cutoff rate for noncoherent detection over a Rayleigh fading channel.	99
4.22	Comparison of actual energy consumed and the approximation for various γ values using cutoff rate for noncoherent detection over a Rayleigh fading channel.	102
4.23	Variation of $\frac{E_T}{N_0}$ with respect to R for $\gamma = -\infty$ dB to $\gamma = -5$ dB when $k = 240$, using cutoff rate for noncoherent detection over a Rayleigh fading channel.	103
4.24	Variation of $\frac{E_T}{N_0}$ with respect to R for $\gamma = -2.5$ dB to $\gamma = 10$ dB when $k = 240$, using cutoff rate for noncoherent detection over a Rayleigh fading channel.	104
4.25	Optimum code rate with respect to number of information bits k for $\gamma = 0$ dB, using cutoff rate for noncoherent detection over a Rayleigh fading channel.	105
4.26	Optimum code rate for the normalized processing energy when $k \rightarrow \infty$, using cutoff rate for noncoherent detection over a Rayleigh fading channel.	107
4.27	Performance of Throughput Using Optimum Code Rate (for $\gamma = -5$ dB).	108
4.28	Performance of Throughput Using Optimum Code Rate (for $\gamma = 0$ dB).	109

4.29	Total energy consumption for a communication system using RS codes over $GF(2^8)$ with $K = 30$ and packet error rate of 0.01	111
4.30	Total energy consumption for a communication system using RS codes over $GF(2^8)$ with $K = 30$ and packet error rate of 0.001	112
4.31	Performance comparison using cutoff rate and convolutional code over an AWGN channel for $\gamma = -10.10$ dB.	114
4.32	Performance comparison using cutoff rate and convolutional code over an AWGN channel for $\gamma = 1.938$ dB.	115
4.33	Performance comparison using cutoff rate and convolutional code over a Rayleigh channel for $\gamma = 6.94$ dB.	116
5.1	Construction of product code $\mathcal{P} = C_1 \times C_2$	120
5.2	BSC model for communication channel.	127
5.3	System model with BSC and RS codes.	128
5.4	System model with BSC and TP codes.	128
5.5	System model with AWGN channel and RS codes.	129
5.6	System configurations on the AWGN channel using TP codes.	130
5.7	Probability density function of r with given transmitted bits. $ \beta\sqrt{E} $ is the threshold for determine the receive bit as an erasure.	130
5.8	System configurations on the erasure channel using RS codes.	131
5.9	System configurations on the bursty channel using TP codes.	132
5.10	Comparison of performance between (128,64) TP codes and RS codes over BSC.	134
5.11	Comparison on the performance of the product code with a single fixed value of p code	135
5.12	Comparison on the performance of the TP codes with a single fixed value of E_b/N_0 code.	137
5.13	Comparison on the performance of the RS codes, hard and soft decision TP codes over AWGN channel.	138
5.14	Comparison on the performance of the RS codes (with and without genie's help), TP codes over BSC and over AWGN channel.	139
5.15	Optimal value of threshold β	141
5.16	Bit Error Rate for the Three Cases of RS codes	142
5.17	Bit error rate for the three Cases of RS codes	144

LIST OF APPENDICES

APPENDIX

A	Computation of a 8-bits symbol error in block 1, 2th and 3th	150
B	Computation of Bit Error Probability After Decoding	152
C	Proof On the Markov Chain for DPSK Error Probability	154

CHAPTER 1

Introduction

Energy efficiency has always been one of the most important design goals in communications. However, with the advent of the wireless mobile communication era, the demand for energy efficient system design has been growing rapidly. For this reason, there has been a remarkable amount of effort to achieve highly reliable communications with the lowest possible energy consumption. Consequently, there is a vast amount of literature on coding, modulation, and power control techniques that impressively improve energy efficiency. However, there is still room for improvement. In particular, wireless communication system design for short packet transmission has drawn little attention until now. We briefly review the trends and results of previous research in Section 1.1 and discuss our research in Section 1.2. We conclude this chapter in Section 1.3 with a brief overview of this thesis.

1.1 Energy Efficient System Design

In modern digital communications, a sequence of information bits is usually encoded (by source and channel encoders), modulated, amplified and then carried by high-frequency electromagnetic waves over a radio link. At the receiver, the reverse process is carried out by a receiver antenna with a radio frequency tuner, a demodulator, a channel decoder and a source decoder. In this report, we are primarily interested in the channel coding and modulation aspects of digital communications. As is well known, the

energy efficiency depends on the choice of coding, modulation, power control technique as well as on the channel characteristics.

In 1948, Shannon [1] showed that arbitrarily reliable communication is possible as long as the signal transmission rate does not exceed a certain limit called the channel capacity. This stimulated numerous research efforts on error control coding. Following the first class of error control codes, namely Hamming codes [2, 3], powerful algebraic codes such as Golay codes, Bose-Chaudhuri-Hocquenghem (BCH) codes, and Reed-Solomon (RS) codes were found. As coding theory evolved, various important properties of codes were identified and studied such as minimum distance and weight distribution. The discovery of convolutional codes, which were originally called recurrent codes, is another important landmark in the history of error control coding. Convolutional codes have many important properties such as the existence of efficient encoding and decoding algorithms and the impressive performance over an additive white Gaussian noise (AWGN) channels.

Another important landmark of error control coding theory is the discovery of concatenated coding schemes. For example, Forney showed that the weakness of convolutional codes against bursty errors can be compensated with RS codes by serially concatenating a convolutional code with an RS code [4]. The most recent breakthrough in coding theory is the discovery of a class of codes called turbo codes [5] that exhibit near Shannon-limit performance with iterative decoding algorithms. The astounding performance of turbo codes resulted in a surge in the research activity on iterative decoding. For example, Gallager's low parity density check (LDPC) codes [6], discovered with iterative decoding in the 60's by R. G. Gallager, has drawn tremendous attention in the past few years.

Although the above mentioned turbo codes have excellent bit error performance, there still exists some problems. First of all, their error performance tails off, or exhibits an "error floor" at high signal-to-noise ratio (SNR). Moreover, the complexity of the required soft-input, soft-output (SISO) decoder is such that a cost-efficient decoder was unavailable for most commercial applications. For these reasons, RS codes are still be widely employed in many practical applications because of its efficient decoder

implementation [7] and excellent error correction capabilities. In this thesis, we analyze the performance of RS codes under various different situations.

As mentioned earlier, there has been particularly large amount of research efforts on LDPC codes in recent years. Richardson [8] showed that a rate $\frac{1}{2}$ irregular LDPC code performance is less than 0.13 dB away from capacity at bit error probabilities of 10^{-6} for binary-input AWGN. However, to reach that performance, he needed a codeword length of 10^6 . When the codeword length is 1000, its performance is about 1.7 dB away from capacity at a bit error probability of 10^{-4} . He also shows in his simulation that the bit error performance deteriorates as the codeword length becomes smaller. A similar trend was also shown in his paper for a turbo-convolutional code.

From the above, we implied that long packet length generally gives a better bit error performance as compared to short packet length. However, it may not give a better performance in other areas such as system design, time delay, throughput. For example, Nakanishi [9] has shown that the throughput performance of mobile satellite communications using the unslotted-CDMA-ALOHA protocol is better for short packet length as compared to longer packet. Therefore, long packet length is not always a default choice to use in communications.

In some applications the use of short packet lengths are required in their systems. For example, in packet network technology, the Asynchronous Transfer (ATM) mode composed of 53 byte “cells” having 5 byte headers and 48 byte payloads. Because of its short packet length, it is especially good for real time voice and video. Another good example is Bluetooth which was initially created by Ericsson in 1994. Its packet length range from 126 to 2871 bits. In addition to the above two examples, sensor networks generally require short packet lengths. This is because energy is typically more limited in sensor network than in other wireless networks and to avoid the frequent replacement of batteries, long packet data is uncommon since for the same amount of energy per bit, more energy is consumed for large packet length as compared to short packet. The limitations arise from the nature of the sensing devices and the difficulty in recharging their batteries. All the above mentioned systems are widely used in many communication systems. In this thesis, we investigate the energy performance of short

packet length communication, taking into account of receiver processing power, power amplifier efficiency and other factors.

The use of appropriate coding and modulation techniques can also help to achieve energy efficiency in communications. For example, it is well known [10] that M -ary orthogonal signalling can achieve reliable communications over an AWGN channel at the Shannon limit when M approaches infinity. However, as M increases, the bandwidth efficiency decreases and system complexity increases. The performance of different modulation schemes with RS coding is studied in this thesis. Besides coding and modulation, there are other techniques available in improving energy efficiency of communications. Some examples are power control [11], [12] and hybrid ARQ schemes [13], [14].

1.2 Thesis Overview

In this section, we briefly summarize the main contributions of this thesis.

1.2.1 Reed-Solomon Coded M -ary Modulation With Symbols Overlapping

For many wireless communication systems, RS codes are widely used in concatenation with other codes to enhance system robustness against burst errors. In practice, for concatenated codes, RS codes are used as the outer codes and other coding schemes, like convolutional codes, are used as this inner codes [15]. However, for RS coded M -ary orthogonal/biorthogonal modulation, we can view these M -ary modulation schemes as inner codes [16]. An orthogonal modulation can be viewed as mapping (encoding) k information bits into $M = 2^k$ coded bits such that the codewords are orthogonal. Thus, it is possible to consider orthogonal/biorthogonal modulation as a kind of inner code.

For simplicity of discussion, let us call an RS code an M -ary or $\log_2 M$ -bit RS code if the RS symbols belong to $\text{GF}(M)$. For this code, the block length can only be at most $M + 1$. It is natural, though not necessary, to use M -ary modulation for an M -ary RS code. For example, M -ary RS coded systems with M -PSK modulation

can be considered for excellent energy efficiency with reasonably good coding gains [17]. Similarly, M -ary orthogonal or bi-orthogonal modulations have been popular matches with an M -ary RS code. We regard the resultant systems as concatenated coding schemes with the inner code block length equal to a single RS codeword symbol length. Hence, we can say that inner codes of block length m have been popular matches with $M = 2^m$ -ary RS codes. However, it is not always desirable or possible to make such a canonical match between inner codeword length and RS symbol size. For example, it is not very practical to consider 256-PSK to match with a 256-ary RS code when the phase noise is not negligible. Also, even if we can achieve great energy efficiency by employing a 256-ary orthogonal modulation for an 256-ary RS coded system, we have to sacrifice significant amount of bandwidth efficiency. In [17] and [18], RS coded systems are considered in which one inner codeword lengths are integer multiples of the RS symbol size. However, despite the existence of various RS coded system performance analysis (e.g. [17], [19]), the more general case of arbitrary inner codeword length are hardly considered.

In this thesis, we provide an analytical methodology for performance analysis of RS coded systems with arbitrary inner codeword lengths. We derive the bit error performance of the RS coded M -ary modulation using Markov Chain analysis. The performance is analyzed for the cases of orthogonal modulation with coherent and noncoherent demodulation and biorthogonal modulation with coherent demodulation over an AWGN channel. In addition, the bit error probability of RS codes with an NR inner code is simulated and compared with the case of biorthogonal modulation. An example of bit error performance over a Rayleigh flat fading channel is given for the case of biorthogonal modulation. To further improve the bit error and packet error probability of RS codes, we proposed the use of interleaver with iterative decoding, similar to the case of turbo decoding. We demonstrate that by using an interleaver with iterative decoding, there is a performance gain of approximately 0.5 dB over an AWGN channel and a gain of about 1 dB Rayleigh fading channel compare to one that does not use an interleaver.

1.2.2 Reed-Solomon Coded Differential Phase Shift Keying Modulation

A differential phase shift keying (DPSK) modulated signal does not require the estimation of carrier phase for demodulation. Therefore, it eliminates the need for a coherent reference signal at the receiver and does not have cost and complexity associated with carrier phase recovery, as compare to a coherent phase shift keying system. In addition, it has a 3dB performance gain as compare to a noncoherent frequency shift keying system [10]. Hence, to have a low complexity communication system with reasonable error performance, we consider the used of a RS coded DPSK modulation system.

The basic principle of differential modulation is to use the previous symbol as a phase reference for the current symbol, thus avoiding the need for a coherent phase reference at the receiver. That is, the information bits are encoded as the differential phase between the current symbol and the previous symbol. Therefore, differential modulation falls in the more general class of modulation with memory. The analysis of block error probability using DPSK modulation was done by Wang [20]. He shows that the differences in the block error probability are negligible if the received bits are consider to be independent. He analyzed the packet error probability of RS coded DPSK modulation system over an AWGN channel. In our work, we use a different approach to analyze the correlated block error probability. Our analysis arrives at the same result in [20]. We derive the packet error probability of RS coded DPSK modulation over a Rayleigh fading channel and compare its performance with one that uses a bit interleaver.

1.2.3 Energy Analysis of Single Hop Communication System for Short Packet Length Data

In a communication system, energy is consumed by the receiver and transmitter. Most of the communication engineering research ignores the effect of amplifier efficiency, distance between transmitter and receiver and processing power of the receiver. If

these factors are considered, coding may actually deteriorate the error probability. For example, in a wireless sensor network where the distance between the transmitter and the receiver is short, Zorzi [21] demonstrates that the energy spent for decoding may actually exceed that saved due to the coding gain. He uses a block code and simulation of convolutional codes to obtain the total energy required and the error probability.

We present a broader study of the energy analysis by using the cutoff rate and capacity theorem in our analysis. The use of capacity shows the fundamental limit on the minimum energy consumed in a communication system. On the other hand, the cutoff rate shows the “practical limit” on the achievable energy consumption. We analyze the performance over an AWGN channel with binary phase shift keying (BPSK) modulation and Rayleigh fading channel with noncoherent binary frequency shift keying (BFSK). In addition, we present numerical results using practical coding schemes.

1.2.4 Comparison of Turbo Product Codes and Reed-Solomon Codes

Product codes are constructed by the concatenation of two block codes. These codes are shown to have good error performance due to their large minimum distance [22]. However, the optimum decoding of such codes requires an exhaustive comparison of all the possible codewords which implies large amount of computation. Consequently, these codes did not draw much attention until the discovery of iterative decoding. However, even with iterative decoding, turbo product (TP) codes still require a considerable amount of system complexity.

In contrast to TP codes, a vast literature has developed for RS codes and bit error performance of RS coded communication system is still widely research upon. The tremendous amount of research work led to the discovery of an efficient decoding algorithms for RS codes [15]. Consequently, the RS codes have a lower system complexity as compared to the TP codes. The RS codes are a class of maximum distance separable (MDS) codes. This means they have the largest possible minimum distance that a linear code with the same (n, k) parameter, where n, k denote the codeword and information

word length respectively. As the asymptotic bit error performance of linear block code is related to its minimum distance, RS codes have the best asymptotic error correction capability among linear block code of the same (n, k) parameter. Moreover, these codes are also well known for their excellent burst error correction capability. Therefore, these codes are employed in digital audio discs which has high burst error statistics.

Both TP codes and RS codes belong to the same class of block codes and have large minimum distance. Therefore, they are a pair of good candidates for bit error performance over various channels. As decoding of RS codes is less complex than TP codes, our goal is to research on cases when RS codes outperform TP codes in bit error probability. The bit error performance comparisons are made on binary symmetric channel (BSC), AWGN channel, erasure channel and a bursty channel. In the comparisons, we assume that the probability of incorrect decoding for RS codes is negligible. The comparison results show that TP codes are superior to RS codes in all the channels mention above except for one particular case. RS codes have a better performance on binary erasure channel after SNR of 5 dB when the decoder has the knowledge of which symbols are erased and hard decisions are performed for the TP decoder.

1.3 Organization of Thesis

The remainder of this thesis is organized as follows. In Chapter 2, we investigate the bit error performance of RS coded M -ary modulation with symbol overlapping. We begin with a discussion on the characteristics of concatenated codes, followed by a discussion on design issues. Next, we describe the system model we use in our analysis. Then, we provide an analytical methodology for the performance analysis of RS coded system with arbitrarily inner codeword length. After that, we investigate the performance of RS coded system using orthogonal modulation with coherent and noncoherent demodulation and biorthogonal modulation with coherent demodulation. In addition, we also study the performance of concatenated RS codes with Nordstrom-Robinson (NR) codes. The fading case is considered next. We present the performance of a concatenated system using biorthogonal modulation. This is followed by an investiga-

tion on the error performance of the symbol overlapping RS coded M -ary modulation system with the use of interleaving and iterative decoding.

In Chapter 3, we analyze the performance of RS coded DPSK modulation system. We begin with a description of the system model first. The symbol error and packet error probability is derive next. Then, we show the packet error probability over an AWGN channel. We also analyze the symbol error probability over a Rayleigh fading channel and we compare its error probability with one that uses bit interleaving.

In Chapter 4, we perform the energy analysis of single hop communication system for short packet length. We begin with a system description and follow by the analysis over an AWGN channel using cutoff rate. Next, we perform our analysis using the capacity for BPSK over an AWGN channel. We also investigate the energy consumption over a Rayleigh fading channel with noncoherent BFSK detection, using the cutoff rate. Next, we present numerical results using practical coding schemes.

In Chapter 5, we give a detailed description of TP codes and concatenated codes. The structure of product codes is presented. Next, we give a brief description on the construction of product codes with the aid of an example. Then we demonstrate the iterative decoding of the product codes in detail. Following that, we define the system models used in the comparison of TP codes and RS codes. This is followed by a description on the bit error analysis of RS codes over BSC. Then, we perform the comparison over an AWGN channel. After that, we define the meaning of erasure bits and present the comparison result over the erasure channel. We conclude this chapter by a comparison over bursty channel.

In Chapter 6, we give our conclusions and propose some possible future research directions.

CHAPTER 2

Analysis of Reed-Solomon Coded M -ary Modulation With Symbols Overlapping

Several researchers have studied concatenated RS coding systems and analyzed the error probability (e.g. [17] , [19]). It was shown in [17] that by using an RS code as the outer code for M -ary PSK modulation, it is not only possible to achieve large coding gain (or high reliability) with good bandwidth efficiency, but it also can be practically implemented. The case when the length of the inner code (i.e. number of bits in a modulation symbol) is an integer multiple of the outer codes for the AWGN case was investigated in [17] and the fading case is studied in [18].

In this chapter, we study the performance of RS code with M -ary modulation. We examine both cases when an RS symbol consist an integer and non-integer number of the modulated symbols. When a communication system has code words of long block length, to avoid using large bandwidth, an RS symbol can consist a number of modulation symbol. However, for the RS symbol to be aligned with the modulation symbol, the RS symbol size must be an integer multiple of the modulation symbol size. For example, consider an RS code with symbol alphabet $GF(2^m)$ used with M -ary modulation. Then for an integer number of modulation symbols per RS code symbol m has to be equal to $l \log_2 M$ where $l \in \mathbb{Z}$. This limits the number of choices of the number of bits used to represent an RS symbol. For example, if the RS symbol consists of a prime number of bits, then we can only represent one modulation symbol

as one RS symbol (i.e. $l=1$) or as m binary modulation symbols. If this number is large, we need to use a larger M which means a large bandwidth for the case of orthogonal/biorthogonal modulation. Therefore, this motivates us to investigate the case when the RS symbol is not an integer multiple of the modulation symbol. Joiner and Komo [23] have presented a specific case of the performance of RS coded QPSK and 8PSK with symbol overlapping. However, they did not derive a general technique for different modulation schemes. In this paper, we derive the bit error performance of RS coded M -ary modulation using a Markov Chain analysis. This overall code is examined in the case of orthogonal modulation coherent and noncoherent demodulation and biorthogonal modulation with coherent demodulation over an AWGN channel. In addition, the bit error probability of an RS code with the Nordstrom-Robinson (NR) (16,8) code is simulated and compared with the case of biorthogonal modulation. An example of bit error probability over a Rayleigh flat fading channel is given for the case of biorthogonal modulation. We also compute the minimum SNR required for maximum throughput for various code rates.

In Section 2.1, we briefly discuss the characteristics of concatenated codes. Next, we present the design issues of concatenated codes in Section 2.2. In Section 2.3, we introduce the system model that we use for the analysis and assumptions for the RS decoder are also discussed. In Section 2.4, we present the Markovian analysis of the concatenated code when the RS symbol is not an integer multiple of the modulation symbol. The bit error probability after RS decoding, under any modulation is derived. We apply the Markovian technique in Section 2.5 and examine the bit error probability of orthogonal modulation coherent and noncoherent demodulation and biorthogonal modulation with coherent demodulation over an AWGN channel. In addition, we investigate the performance of RS code concatenated with an NR code and compare the bit error probability with biorthogonal modulation. We conclude this section with the study of the throughput. In Section 2.6 the bit error probability of an RS code with biorthogonal modulation under Rayleigh flat fading channel is analyzed. We propose 2 low complexity coding strategies for an RS coded M -ary modulation system in Section 2.7. Finally, we give our conclusion for this chapter in Section 2.8.

2.1 Characteristics of Concatenated Codes

Concatenated coding was first proposed by Forney [4] as a method for achieving large coding gains by combining two or more relatively simple building blocks or component codes. In Fig. 2.1, an example of the concatenation of two block codes is shown. The primary reason for using a concatenated code is to achieve a low error rate with an overall implementation complexity which is less than that which would be required by a single coding operation.

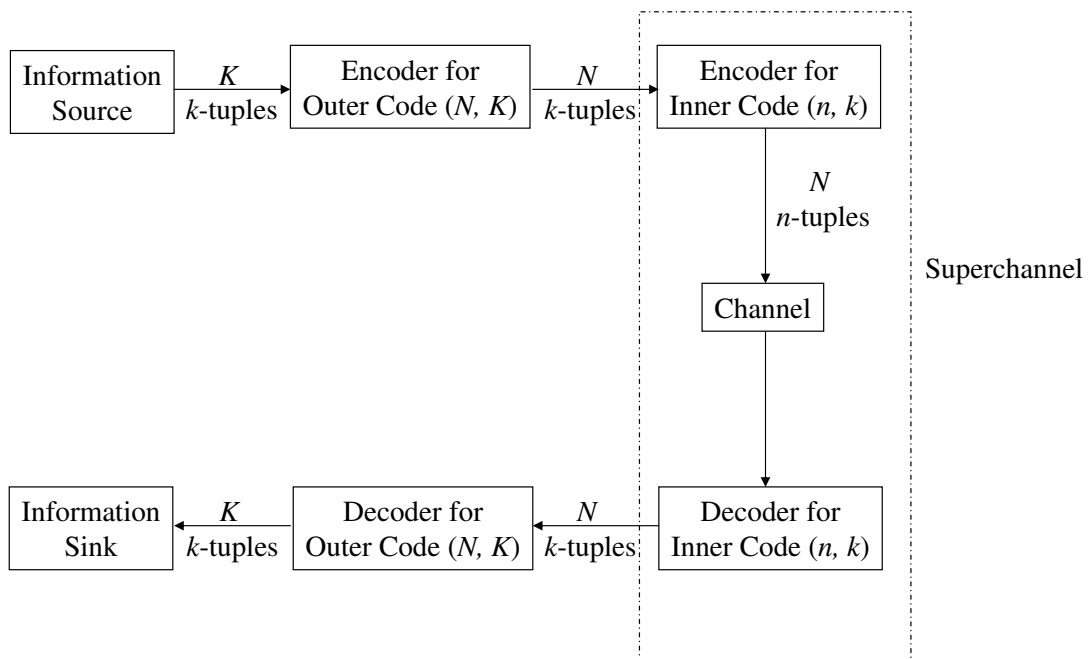


Figure 2.1: Block diagram of a communications system employing a concatenated code.

Consider the arrangement shown in Fig. 2.1. Information to be transmitted is first encoded with an (N, K) encoder, which is labeled as the outer code in the figure. The symbols in an (N, K) code block are then treated as an information stream that is encoded as a sequence of (n, k) inner block code. The combination of inner encoder, channel, and inner decoder can be thought of as forming a new channel, called a “super channel”, which transmits binary k -tuples. Frequently, an RS code is used as the outer code. The overall code is a binary code of length nN , dimension kK . Clearly, if the symbol alphabets of the inner and outer codes are not the same, it is necessary to

reformat the data between the encoders for the inner and outer codes.

The encoding is done as follows. The kK binary information bits are divided into K k -tuples, which are thought of as elements of $\text{GF}(2^k)$. These are then encoded by the outer encoder into the codeword $a_0a_1 \dots a_{N-1}$ with $a_i \in \text{GF}(2^k)$. Each a_i is now encoded by the inner encoder into a binary n -tuples b_i . Then $b_0b_1 \dots b_{N-1}$ is the codeword to be transmitted over the channel. Thus, we obtain a concatenated block code having a block length of Nn bits and containing kK information bits. That is, we have created an equivalent (Nn, Kk) binary code. The rate of the resulting concatenated code is $(\frac{k}{n})(\frac{K}{N})$, which is equal to the product of the two code rates. In addition, the minimum distance of the concatenated code is $d_{min}D_{min}$, where D_{min} is the minimum distance of the outer code and d_{min} is the minimum distance of the inner code.

2.2 Design Issues of Concatenated Codes

From Fig. 2.1, it is clear that the role of the outer code is to correct the errors that remain after decoding the inner code, errors that may exhibit either independent or burst error statistics. Moreover, the rate of the outer code has to be selected carefully due to the following reasons. If the outer code rate is very high, it may not have good error correction capability and thus, errors leaving the inner decoder cannot be reliably corrected. However, if the E_b/N_0 and the rate of the inner code is fixed, then as we reduce the rate of the outer code (to improve its error correction capability), the SNR at the input to the inner code is reduced. If the outer code rate is reduced too much, the SNR may lower to the point where there is a coding loss rather than a gain associated with the inner code. Therefore, we can expect an optimum rate to exist for the outer code.

The design issue for the selection of the inner code of a concatenated code is somewhat different from those for other applications. It is undesirable for the inner code to have a very steep performance characteristic, that is, a waterfall curve with a pronounced knee. If such a code was selected as the inner code and a nominal design point chosen slightly to the right of the knee, an inefficient and unstable design would

result. This is because, should the channel quality degrade even slightly, the error rate at the input to the outer decoder would increase sharply and the outer decoder would be overloaded with errors. On the other hand, if SNR were to increase slightly, the inner code by itself would be capable of providing the desired quality of service. In this case, the outer code causes an overall loss in communication efficiency.

2.3 System Model

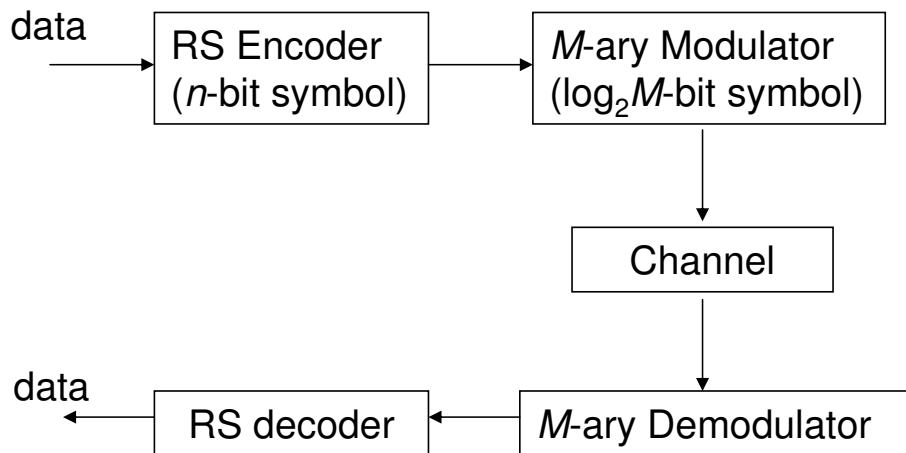


Figure 2.2: Block diagram of RS coded modulation scheme.

We consider the RS coded modulation scheme as shown in Fig. 2.2. Here, a block of information bits is first encoded by a systematic (N, K) RS code where $N \leq 2^n$ and n is the number of bits used to represent a RS symbol. The RS coded bits are passed through an M -ary modulator and a code symbol comprised of $m = \log_2 M$ bits is mapped to one of M signals to be transmitted. For example, considered the case of an RS(255,22) code with symbol alphabet $\text{GF}(2^8)$ and (32,6) biorthogonal modulation. In this case, we use 8 bits to represent an RS symbol and 6 bits to represent a modulation symbol. Therefore, a block of 3 RS symbols consists of 24 bits and they are mapped into 4 modulation symbols. A single RS codeword would get mapped into 340 modulation symbols. Thus, there is an overlapping between an RS symbol and a modulation symbol

and the overlapping is shown in Fig. 2.3.

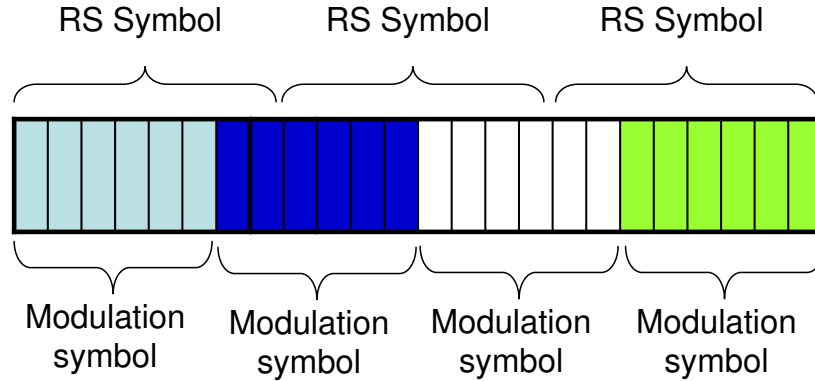


Figure 2.3: Overlapping of RS and biorthogonal symbol.

In analyzing the performance, we assume that the RS decoder can detect with probability 1 when the number of errors is greater than the capability of the code. This assumption yields accurate performance if the detection capability of the RS decoder t is large. The undetected error probability can be calculated using techniques in [24]. When the decoder detects that too many errors have occurred, the decoder strips off the parity symbols and puts out the received information symbols. Therefore, there is no bit/symbol error at the output of the decoder if the number of RS symbol errors is less than t .

In this chapter, the channel models being considered are the (i) AWGN channel and (ii) Rayleigh flat fading channel.

2.4 Markovian Analysis

In this section, we study the performance of concatenated RS systems that group $v = \text{lcm}\{m, n\}$ (lcm denotes least common multiple) bits into one single block of bits. We note that every block would have v/n RS symbols and v/m modulation symbols. For example, if we use 8 bits for an RS symbol (i.e. $n = 8$) and 6 bits to represent a modulation symbol (i.e. $m = 6$), then $v = \text{lcm}\{6, 8\} = 24$. Therefore, we group 24 coded bits into one block and each block consists $v/n = 3$ RS symbols. Consequently,

there are $v/m = 4$ modulation symbols in each block. With this grouping, each block contains the minimum number of RS symbols such that there is no modulation symbol overlapping between each block. Hence, if each modulation symbol experiences independent and identical noise or fading level, then every block of RS symbols experiences independent and identical noise or fading level too. Define $W_i \triangleq$ number of RS symbol errors in the first i blocks. Then W_i is a Markov chain because given the number of errors in the first q blocks, W_{q+1} is independent of W_{q-1}, \dots, W_1 . Thus

$$P(W_{q+1}|W_q, \dots, W_1) = P(W_{q+1}|W_q). \quad (2.1)$$

Making use of the Markovain property of W_q , we can solve for $P(W_q = k)$ via the recursive equation as follows.

$$\begin{aligned} P(W_q = k) &= \sum_{j=\max\{k-v/n, 0\}}^k P(W_q = k, W_{q-1} = j) \\ &= \sum_{j=\max\{k-v/n, 0\}}^k P(W_q = k|W_{q-1} = j)P(W_{q-1} = j). \end{aligned} \quad (2.2)$$

The above equation is true because if there are k RS symbols in the first q blocks, then there is at least $k - v/n$ RS symbol errors in the first $q - 1$ blocks since each block has v/n RS symbol errors. The initial conditions are given as follow.

$$P(W_0 = j) = \begin{cases} 0, & j \neq 0 \\ 1, & j = 0. \end{cases}$$

Let $P_{i,j}$ denotes the probability that there are j symbol errors in i th block. Since the errors in each block of symbols is independent and identically distributed, we can further simplify errors in every other block of symbols $P(W_q = k|W_{q-1} = j)$ as follow:

$$\begin{aligned} P(W_q = k|W_{q-1} = j) &= P_{q,k-j} \\ &= P_{1,k-j}. \end{aligned} \quad (2.3)$$

To analyze the bit error probability after decoding, we define the following events.

- ϵ_d : event that the first bit is in error after decoding,

- ϵ_b : event that the first bit is in error at output of demodulator,
- $\epsilon_{i,j}$: event that i RS symbols are in error in the last j RS symbols of a block of $\frac{v}{n}$ RS symbols,
- $\epsilon_{t,N-1}$: event that t RS symbols are in error in the last $N - 1$ RS symbols of a codeword,
- P_b : bit error probability of the M -ary modulation.

Since RS codes are maximum distance separable codes [7], the minimum distance of an $RS(N, K)$ code is $d_{min} = N - K + 1$. Hence, it is able to correct a maximum of $t = \lfloor \frac{d_{min}-1}{2} \rfloor = \lfloor \frac{N-K}{2} \rfloor$ symbol errors. We assume that the RS decoder can detect with probability 1 when the number of RS symbol errors is greater than the error correction capability of the code [25]. In such a case, it puts out the received information symbols when the number of errors is too many for it to correct. Hence, the probability of bit error after decoding is given as :

$$\begin{aligned}
P(\epsilon_d) &= P(\epsilon_b \cap \epsilon_{t,N-1}) \\
&= \sum_{j=0}^{v/n-1} P(\epsilon_b \cap \epsilon_{j,v/n-1} \cap \{W_{Nn/v-1} \geq t - j\}) \\
&= \sum_{j=0}^{v/n-1} P_b P(\epsilon_{j,v/n-1} \cap \{W_{Nn/v-1} \geq t - j\}) \\
&= P_b \sum_{j=0}^{v/n-1} P(\epsilon_{j,v/n-1}) P(W_{Nn/v-1} \geq t - j). \tag{2.4}
\end{aligned}$$

The first line of (2.4) is true since the event ϵ_b is true when the RS decoder fails and the first bit is in error after demodulation. For the second line of (2.4), we group v/n RS symbols into one block. With this arrangement, we have a total of $N/(v/n) = Nn/v$ blocks of RS symbols. The event ϵ_b implies that the first RS symbol is in error. Hence, if there are j RS symbol errors in the remaining $v/n - 1$ RS symbols of the first block, then the RS decoder fails when there are more than $t - j$ errors in the remaining $Nn/v - 1$ block of RS symbols. Finally, the third and fourth line of (2.4) are true because of independence. This is a generic formula for computing the bit error probability

after RS decoding given any modulation scheme. We will use it to compute the bit error probability of orthogonal modulation coherent and noncoherent demodulation and biorthogonal modulation with coherent demodulation over an AWGN channel. In addition, we will investigate the bit error probability of RS codes using biorthogonal modulation with coherent demodulation over a Rayleigh flat fading channel.

2.5 Performance Over An AWGN Channel

In this section, we first study the bit error probability of RS coded biorthogonal modulation system. We give a detail analysis of the bit error probability after modulation. Next, we investigate the bit error probability of RS coded orthogonal modulation system using coherent and noncoherent demodulation. We conclude this section by a study of bit error probability of RS codes concatenated with NR codes.

2.5.1 Biorthogonal Modulation

We demonstrate the applicability of (2.4) by giving an example of a RS code over $GF(2^8)$ with (32,6) biorthogonal modulation. For this particular system, an 8-bit RS symbol overlaps with a 6-bit modulation symbol as shown in Fig. 2.3.

We let $s_0(t), \dots, s_{M-1}(t)$ be the biorthogonal set where $s_{\frac{M}{2}+l}(t) = -s_l(t)$ for $l = 0, 1, \dots, \frac{M}{2} - 1$. To have a good bit error probability, the mappings of bits to symbols is such that signals with furthest distance signals have largest number of bit errors. To illustrate the mapping, let b_0, \dots, b_{k-1} be the input bits to the modulator. Using the above arrangement, the mappings of b_0, \dots, b_{k-1} to $s_l(t)$ is shown below.

$\underline{b_0, \dots, b_{k-1}}$	$\underline{s_l(t)}$
000 ... 000	$s_0(t)$
000 ... 001	$s_1(t)$
:	
011 ... 111	$s_{M/2-1}(t)$
111 ... 111	$-s_0(t)$
:	

100 ... 000 $-s_{M/2-1}(t)$.

In the course of performance analysis, it is necessary to consider two different types of errors. Therefore, we define an error of the first kind to be an error to a signal orthogonal to the transmitted signal, while an error of the second kind is an error to a signal antipodal to the transmitted signal. The probability of error of the first kind is probability that s_j is chosen given that s_0 is transmitted ($j < M/2$) and is given by

$$\begin{aligned} P_{e,1} &= P\{r_j > |r_0|, r_j > |r_1|, \dots, r_j > |r_{M/2-1}|, r_j > 0 | H_0\} \\ &= \int_0^\infty [F_s(r_j) - F_s(-r_j)][F_n(r_j) - F_n(-r_j)]^{M/2-2} f_n(r_j) dr_j. \end{aligned} \quad (2.5)$$

Here, $f_s(x)$ and $f_n(x)$ are the conditional probability density functions of r_0 and r_1 , respectively, given H_0 . Similarly, $F_s(x)$ and $F_n(x)$ denote the associated probability distribution functions. The expressions for $f_s(x)$, $F_s(x)$, $f_n(x)$ and $F_n(x)$ are given as follows.

$$f_s(x) = \frac{1}{\sigma\sqrt{2\pi}} \exp\left\{-\frac{1}{2\sigma^2}(x - \sqrt{E})^2\right\}, \quad (2.6)$$

$$F_s(x) = \Phi\left(\frac{x - \sqrt{E}}{\sigma}\right), \quad (2.7)$$

$$f_n(x) = \frac{1}{\sigma\sqrt{2\pi}} \exp\left\{-\frac{1}{2\sigma^2}x^2\right\}, \quad (2.8)$$

$$F_n(x) = \Phi\left(\frac{x}{\sigma}\right). \quad (2.9)$$

Note that (2.5) is also the error probability to s_j for $j > M/2$. The error of the second kind is the event that $s_{M/2}$ is chosen given that s_0 is transmitted and is given by

$$\begin{aligned} P_{e,2} &= P\{r_0 < 0, |r_1| < |r_0|, |r_2| < |r_0|, \dots, |r_{M/2-1}| < |r_0| | H_0\} \\ &= \int_{-\infty}^0 f_s(r_0)[F_n(r_0) - F_n(-r_0)]^{M/2-1} dr_0 \\ &= (M-2) \int_0^\infty F_s(-r_0)[F_n(r_0) - F_n(-r_0)]^{M/2-2} f_n(r_0) dr_0 \end{aligned} \quad (2.10)$$

where we have used the fact that the density of noise $f_n(r_0)$ is symmetric. Let P_s, P_b be the probability of symbol and bit error of the M -ary biorthogonal modulation re-

spectively. Therefore, by considering all possible error symbols and error bits, we have

$$\begin{aligned}
P_b &= \frac{M-2}{2}P_{e,1} + P_{e,2} \\
&= \frac{M-2}{2} \int_0^\infty \Phi\left(z - \frac{2E}{N_o}\right) \Phi\left(-z - \frac{2E}{N_o}\right) [2\Phi(z) - 1]^{\frac{M}{2}-2} \frac{1}{\sqrt{2\pi}} \exp\left\{-\frac{z^2}{2}\right\} dz. \tag{2.11}
\end{aligned}$$

$$P_s = (M-2) \int_0^\infty \Phi\left(z - \frac{2E}{N_o}\right) [2\Phi(z) - 1]^{\frac{M}{2}-2} \frac{1}{\sqrt{2\pi}} \exp\left\{-\frac{z^2}{2}\right\} dz. \tag{2.12}$$

In order to compute the bit error probability after decoding, we have to determine $P(\varepsilon_{j,v/n-1})$ according to (2.4). Since we are considering a system with 8-bit RS symbols and 6-bit modulation symbols, we have $v = 24$ bits. Thus, each independent block consist of 3 (4) RS (modulation) symbols. In this case, we have to determine $P(\varepsilon_{0,2})$, $P(\varepsilon_{1,2})$ and $P(\varepsilon_{2,2})$. Denote the first, second and third 8-bit symbols in a block (Fig. 2.3) as A , B and A' . Let E_A , $E_{A'}$, and E_B be the event that symbols A , A' and B are in error respectively. Then, $P(E_A) = P(\overline{E_{A'}})$ due to symmetry since both of them have 2 bits at the end of the block that belongs to another modulation symbol. Denote by $P_{i,j}$ where $i, = 1, \dots, n$ and $j = 0, 1, 2, 3$ to be the probability of j 8-bit symbol errors in block i . Hence, $P_{1,0}$ is the probability that all the 8-bit symbols are correct in the 1st block. That is, all the 6-bit modulation symbols are correct. Hence $P_{1,0} = (1 - P_s)^4$. The error probability $P_{1,1}$, $P_{1,2}$ and $P_{1,3}$ are computed in Appendix A and their results are as follow:

$$\begin{aligned}
P_{1,1} &= P(\overline{E_A}, \overline{E_B}, E_{A'}) + P(\overline{E_A}, E_B, \overline{E_{A'}}) + P(E_A, \overline{E_B}, \overline{E_{A'}}) \\
&= (1 - P_s)^2 [2(1 - P_s)P_s + 6P_{e,1} + (15P_{e,1})(15P_{e,1} + 2 - 2P_s)]. \tag{2.13}
\end{aligned}$$

$$\begin{aligned}
P_{1,2} &= P(\overline{E_A}, E_B, E_{A'}) + P(E_A, E_B, \overline{E_{A'}}) + P(E_A, \overline{E_B}, E_{A'}) \\
&= 2(1 - P_s) \{P_s [15P_{e,1} + (1 - P_s)(59P_{e,1} + P_{e,2})] + (1 - P_s) [15P_{e,1}(47P_{e,1} + P_{e,2}) \\
&\quad + (1 - P_s)(44P_{e,1} + P_{e,2})]\} + P_s^2 (1 - P_s + 3P_{e,1})^2 + [3P_{e,1}(1 - P_s)]^2 \\
&\quad + 6P_s P_{e,1} (1 - P_s) (1 - P_s + 3P_{e,1}). \tag{2.14}
\end{aligned}$$

$$\begin{aligned}
P_{1,3} &= P(E_A, E_B, E_{A'}) \\
&= P_s^2 (59P_{e,1} + P_{e,2})(2 - P_s + 3P_{e,1}) + (1 - P_s)^2 (44P_{e,1} + P_{e,2})(50P_{e,1} + P_{e,2}) \\
&\quad + 2P_s (1 - P_s) [(44P_{e,1} + P_{e,2}) + 3P_{e,1}(59P_{e,1} + P_{e,2})]. \tag{2.15}
\end{aligned}$$

The minimum distance of (N, K) RS codes is $N - K + 1$. Hence, it is able to correct a maximum of t symbol errors. Hence, we have (see Appendix B for detailed analysis),

$$\begin{aligned}
P(\epsilon_d) &= P_b \sum_{j=0}^{v/n-1} P(\varepsilon_{j,v/n-1}) P(W_{Nn/v-1} \geq t - j) \\
&= P_b \sum_{j=0}^2 P(\varepsilon_{j,2}) P(W_{32} \geq 6 - j) \\
&= P_b \left[P(W_{32} \geq 4) \{ P_s (59P_{e,1} + P_{e,2}) (2 - 59P_{e,1} - P_{e,2}) + (1 \right. \\
&\quad - P_s) [(59P_{e,1} + P_{e,2})(47P_{e,1} + P_{e,2}) + (1 - P_s + 3P_{e,1})(44P_{e,1} + P_{e,2})] \} \\
&\quad + P(W_{32} \geq 5) \{ P_s (1 - P_s + 3P_{e,1})^2 + 3P_{e,1} (1 - P_s) (1 - P_s + 3P_{e,1}) \\
&\quad + (1 - P_s) [15P_{e,1} + (1 - P_s)(59P_{e,1} + P_{e,2})] \} \\
&\quad \left. + P(W_{32} \geq 6) (1 - P_s)^2 (1 - P_s + 3P_{e,1}) \right]. \tag{2.16}
\end{aligned}$$

We compare the bit error probability of the RS(96,84) code concatenated with the (32,6) biorthogonal modulation with systems that use the same modulation scheme, block length and equivalent bandwidth and code rate. That is, the systems being compared have the same overall code rate $C = \frac{K}{N} \times \frac{\log_2 M}{M/2}$ and block length of $L = \frac{nMN}{2 \log_2 M}$. With this basis for comparison, it is obvious that for a system that employs a stronger inner code, it needs to have a weaker outer code in order to maintain the same overall code rate. In our study, we compare systems with and without symbol overlapping. However, for a 256-ary biorthogonal system, we need to have an RS code rate to be greater than 1 for the appropriate comparison. Therefore, our next best candidate for the appropriate comparison is an RS(255,83) code with a (8,4) biorthogonal modulation system. This is the non-overlapping case where each RS symbol has exactly 2 modulation symbols. The bit error probability for this system is computed as follows. Let P_{4bs} , P_{8bs} be the symbol error probability of 4-bit symbol and 8-bit symbol respectively. If both the inner and outer code are aligned together, then, each 8-bit symbol will have exactly two 4-bit symbols. Thus

$$P_{8bs} = 2P_{4bs} - P_{4bs}^2. \tag{2.17}$$

Again, assuming the probability of incorrect decoding is negligible the bit error proba-

bility of this system is

$$P(\epsilon_d) = P_b \sum_{l=86}^{254} \binom{254}{l} P_{8bs}^l (1 - P_{8bs})^{254-l}. \quad (2.18)$$

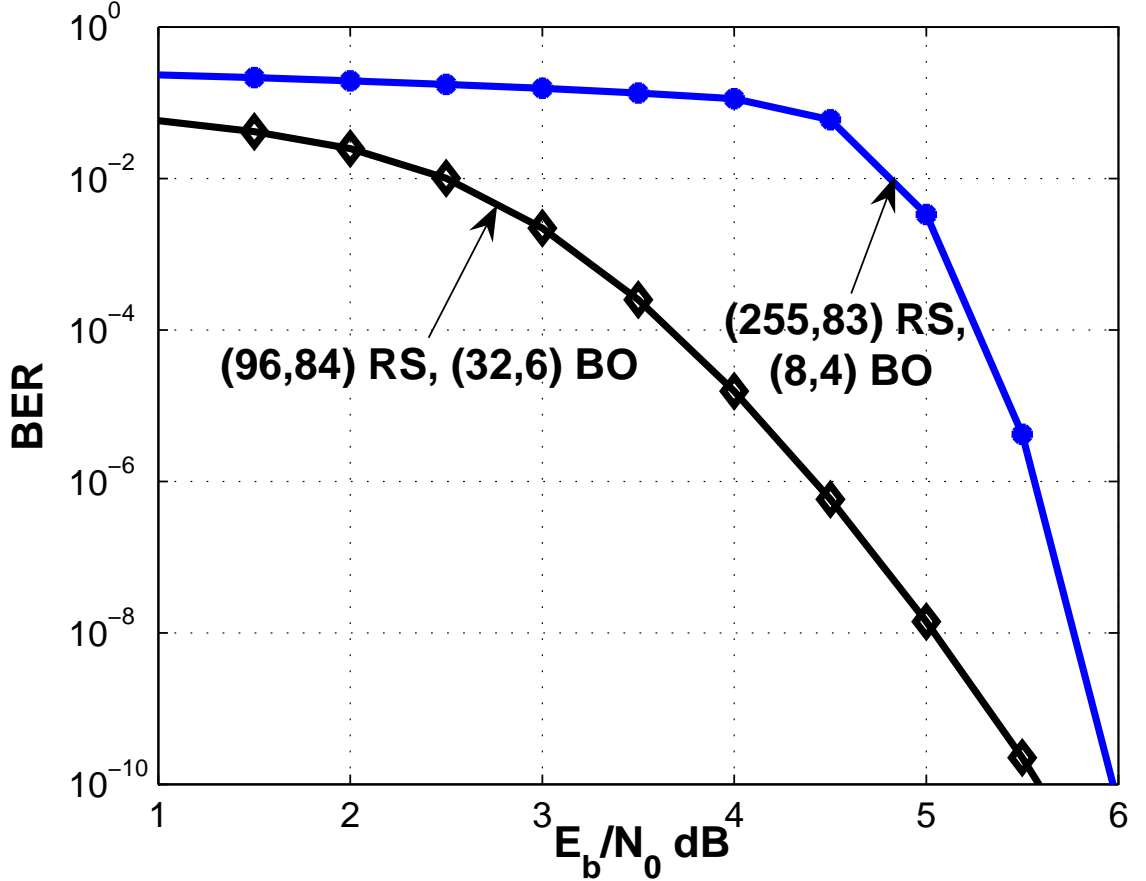


Figure 2.4: Bit error probability of RS(96,84) code with (32,6) biorthogonal modulation and RS(255,83) code with (8,4) biorthogonal modulation over an AWGN channel.

We compare the bit error probability of RS(96,84) code (with (32,6) biorthogonal modulation) with the RS(255,83) code (with (8,4) biorthogonal modulation) in Fig. 2.4. It can be seen that the RS(96,84) codes with (32,6) biorthogonal modulation is about 1.5dB better than the RS(255,83) code with (8,4) biorthogonal modulation at bit error rate of 10^{-5} . This shows that when using biorthogonal modulation over an AWGN channel, there are not too many errors for the outer code to correct at the bit error

rate of 10^{-5} . That is, a stronger inner code is appropriate to achieve a low energy consumption in this case.

2.5.2 Orthogonal Modulation with Coherent Demodulation

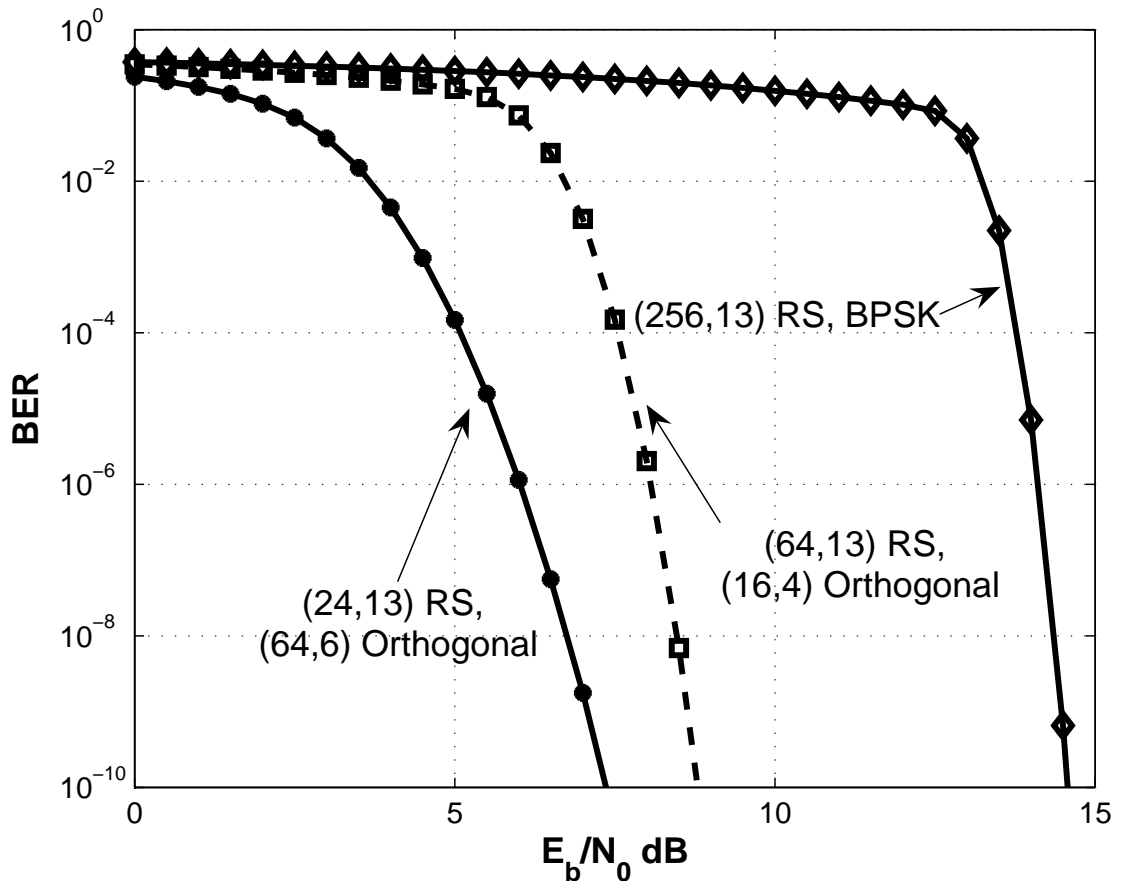


Figure 2.5: Bit error probability of various equivalent RS coded M -ary orthogonal modulation with coherent detection system.

Now consider coherent demodulation of orthogonal signals. The probability of a symbol error for M -ary orthogonal signals with coherent detection is given as [10]:

$$P_M = \frac{1}{\sqrt{2\pi}} \int_{-\infty}^{\infty} \left[1 - \left(\frac{1}{\sqrt{2\pi}} \int_{-\infty}^y e^{-x^2/2} dx \right)^{M-1} \right] \exp \left[-\frac{1}{2} \left(y - \sqrt{\frac{2E_s}{N_0}} \right)^2 \right] dy. \quad (2.19)$$

The bit error probability is

$$P_b = \frac{2^{k-1}}{2^k - 1} P_M. \quad (2.20)$$

Using the Markov chain technique described in Section 2.4, the error probability can be determined for RS codes concatenated with M -ary orthogonal modulation. The results of the analysis is plotted in Fig. 2.5. There is no symbol overlapping for the systems using RS(256,13) with BPSK modulation and RS(64,13) with 16-ary orthogonal modulation in these systems. It can be observed that a stronger inner code gives better performance as compared to a stronger outer code. This observation is consistent with the case of biorthogonal modulation. Consequently, we can conclude that for orthogonal modulation with coherent demodulation, it is best to employ a strong inner code as compared to an a strong outer code to achieve a better bit error probability over an AWGN channel.

2.5.3 Orthogonal Modulation with Noncoherent Demodulation

Now we consider orthogonal modulation with noncoherent demodulation. The symbol error probability for M -ary orthogonal noncoherent detection is given by:

$$P_M = (M - 1) \int_0^\infty [1 - Q(\sqrt{\frac{2E}{N_0}}, \sqrt{2y})] [1 - e^{-y}]^{(M-2)} e^{-y} dy \quad (2.21)$$

where

$$Q(a, b) = \int_{b^2/2}^\infty \exp\{-\left(\frac{a^2}{2} + x\right) I_0(\sqrt{2xa}) dx \quad (2.22)$$

is called Marcum's Q function and I_0 is the modified Bessel function of order 0. The bit error probability is computed using (2.20). The bit error probability of system using 16-ary noncoherent modulation and 64-ary modulation is shown in Fig. 2.6. Similar to the case of coherent orthogonal modulation, we notice that the system has a better performance with a stronger inner code rather than one that uses a stronger outer code. The performance gain from using the RS(24, 13) with 64-ary orthogonal modulation as compared with the RS(64, 13) with 16-ary orthogonal modulation is about 3 dB at

bit error rate of 10^{-5} . These results demonstrate that for RS codes concatenated with orthogonal modulation a good strategy is to place emphasis on the inner code.

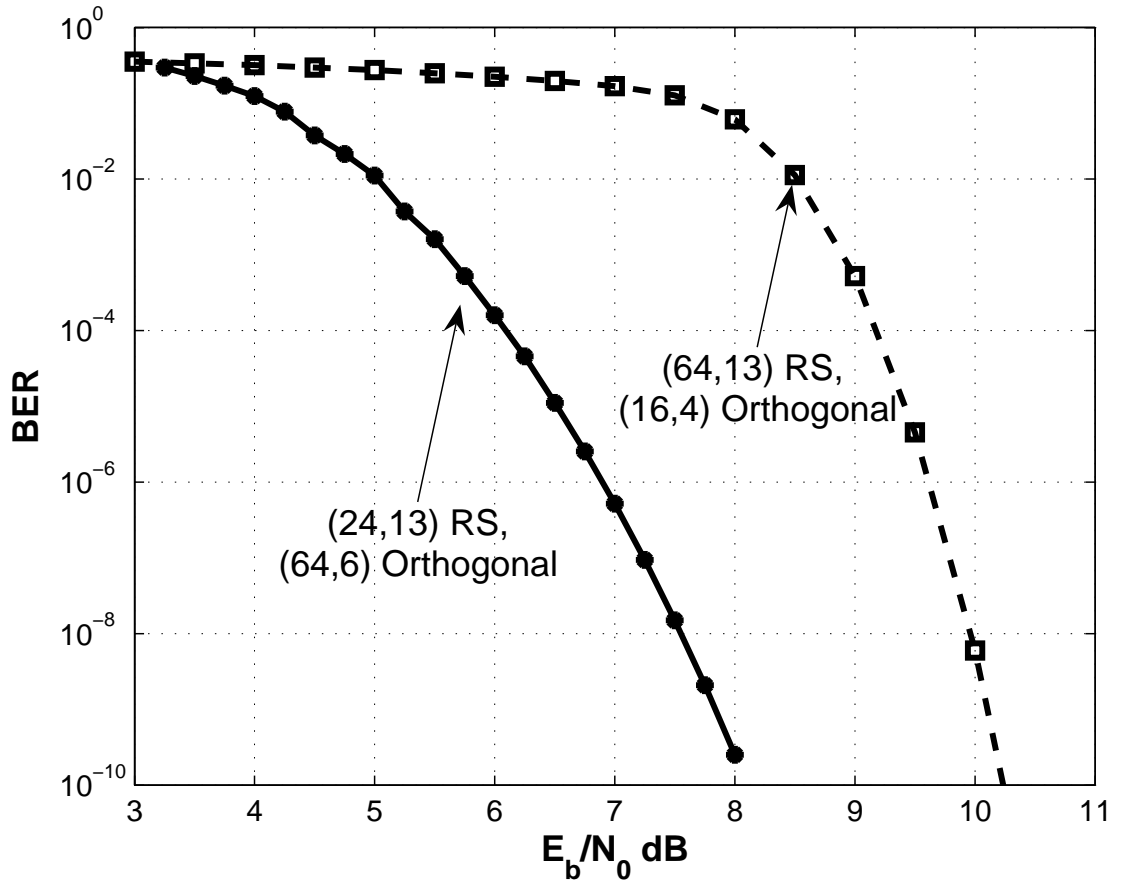


Figure 2.6: Bit error probability of various equivalent RS coded M -ary orthogonal modulation with noncoherent detection system.

2.5.4 Nordstrom-Robinson Code

Next we consider the Nordstrom-Robinson code. The Nordstrom-Robinson(NR) code is a nonlinear code with parameter $(n, k, d) = (16, 8, 6)$. It is constructed by starting with a biorthogonal code of length 16 (with 32 codewords) and adding 7 translates of the code. The minimum distance of the NR code is 6 and it has a total of 256 codewords. Unfortunately, the NR code is difficult to analyze in a way that is computationally

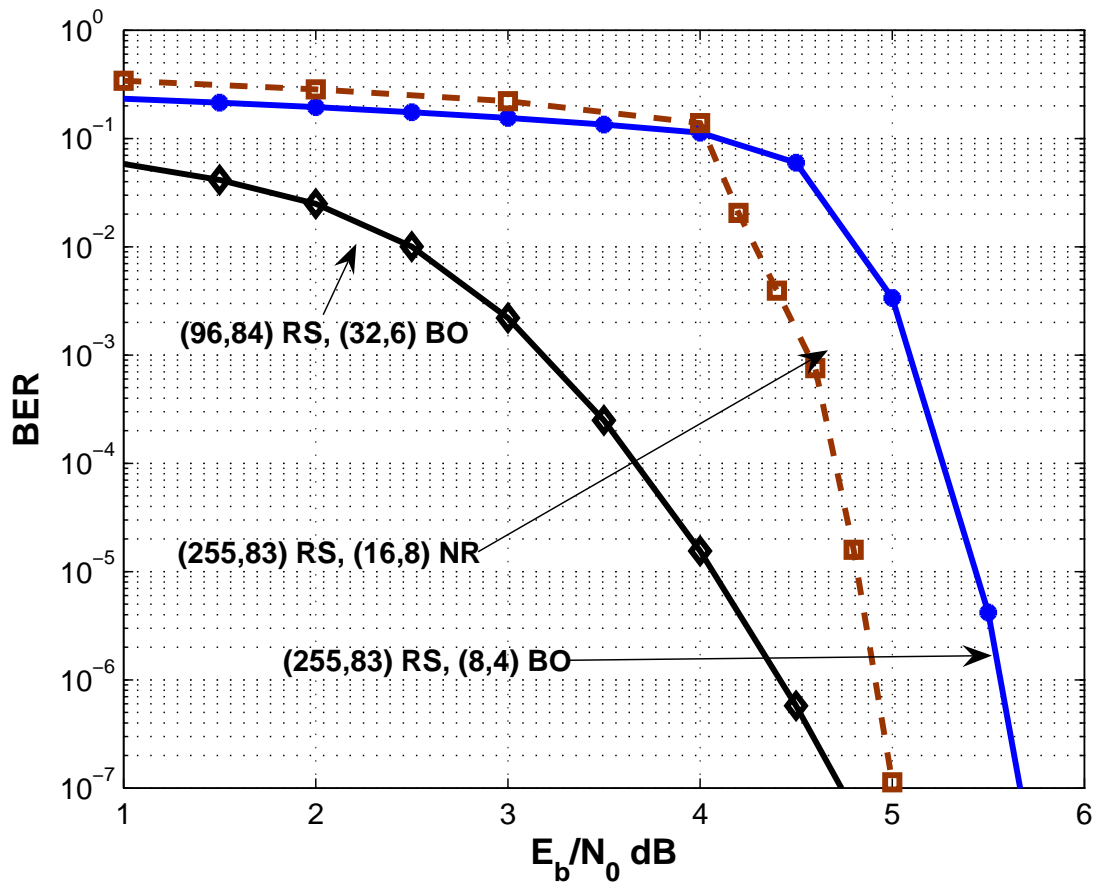


Figure 2.7: Bit error rate of NR(16,8), 16-ary and 64-ary biorthogonal modulation.

efficient. We simulate the performance of the NR code concatenated with RS outer coding and compare it with RS codes concatenated with biorthogonal modulation. In Fig. 2.7, the bit error probability for different RS codes concatenated with biorthogonal modulation and NR modulation is shown. The overall code rate is the same for each of these systems. We note that with the same RS outer code, the NR(16,8) code has a better performance than 8-ary biorthogonal modulation. This is consistent with our previous observation as NR(16,8) code has a better error correction capability than a (8,4) biorthogonal modulation. Therefore, for the AWGN channel, we should place more resources on the inner code rather than the outer code in order to achieve a good bit error probability.

2.5.5 Throughput

Now, we consider the case when the goal of the communication system is not emphasizing low error probability but on high throughput. Denote λ as the number of bits per dimension of an M -ary biorthogonal modulation. Throughput, S , is defined as the expected number of successfully received information bits per dimension and is given by:

$$S = P_s \times r \times \lambda \quad (2.23)$$

where P_s is the probability of success. For length N codes that can correct t errors the probability of success can be written as

$$P_s = \sum_{l=0}^t \binom{N}{l} P_B^l (1 - P_B)^{N-l}. \quad (2.24)$$

We now illustrate the throughput of a system using biorthogonal modulation. The throughput of the RS(96,84) coded system concatenated with a 64-ary biorthogonal modulation and the RS(255,83) coded system concatenated with 16-ary biorthogonal modulation is shown in Fig. 2.8. We note that the minimum SNR required for maximum throughput is around 3dB for the RS(96,84) coded systems with 64-ary biorthogonal modulation and around 5 dB for the RS(255,83) coded systems with 16-ary biorthogonal modulation. That is, they are about 2 dB apart. Hence, the system attains maximum

throughput at a lower SNR for a system using a stronger inner code over AWGN channel for the case of biorthogonal modulation.

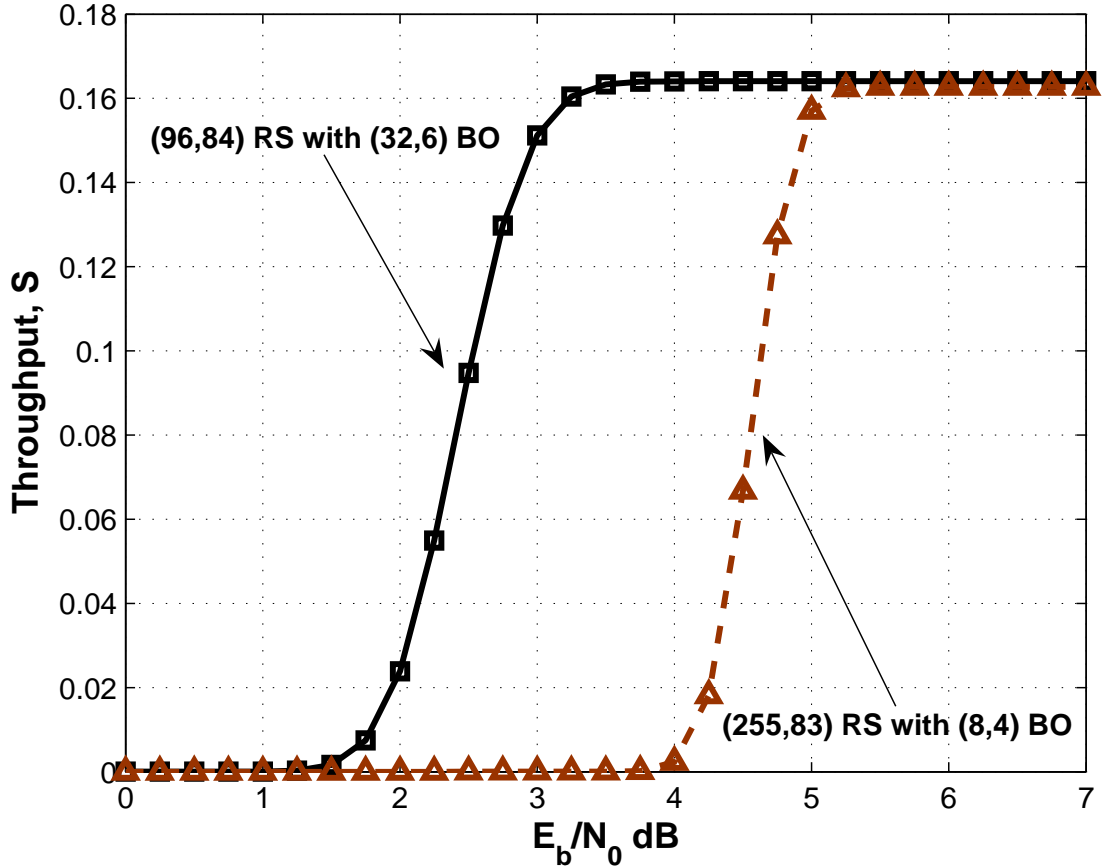


Figure 2.8: Throughput of RS(96, 84) code with (32,6) biorthogonal modulation and RS(255, 83) code with (8,4) biorthogonal modulation over the AWGN channel.

2.6 Performance Over A Rayleigh Fading Channel

In this section, we investigate the bit error probability of RS coded modulation with and without symbol overlapping over a fading channel. We assume that each transmitted bit experience independent fading and we use biorthogonal modulation as an example in studying the bit error probability. The bit error probability after demodulation is derived in following subsection. In addition, we present the bit error

probability after decoding. In the next subsection, we give a description of the block fading channel model considered and derive the bit error probability after decoding. Finally, we present the decoded bit error probability using biorthogonal modulation as an example.

2.6.1 Biorthogonal Modulation Over Rayleigh Flat Fading Channel

Consider a system using binary orthogonal signalling with coherent demodulation and a Rayleigh fading channel. The conditional error probability is given by

$$P_e(R) = Q\left(\sqrt{\frac{ER^2}{N_o}}\right). \quad (2.25)$$

where the random variable R represents the fading and has probability density function

$$f_R(r) = \begin{cases} 0, & r < 0, \\ \frac{r}{\Omega^2} e^{-\frac{r^2}{2\Omega^2}}, & r \geq 0 \end{cases}$$

and $E(R^2) = \Omega^2$. The unconditional probability of error is given by

$$P_e = \int_{r=0}^{\infty} f_R(r) Q\left(\sqrt{\frac{Er^2}{N_o}}\right) dr. \quad (2.26)$$

Now consider M -ary biorthogonal modulation. Let $P_{e,1,c}$ be the conditional probability of error to a signal orthogonal to s_0 , given s_0 is transmitted. As before, we have

$$\begin{aligned} P_{e,1,c} &= P\{r_j > |r_0|, r_j > |r_1|, \dots, r_j > |r_{M/2-1}|, r_j > 0 | H_0\} \\ &= \int_0^{\infty} [F_s(r_j) - F_s(-r_j)][F_n(r_j) - F_n(-r_j)]^{\frac{M}{2}-2} f_n(r_j) dr_j. \end{aligned} \quad (2.27)$$

Hence, an error to an orthogonal signal (see Appendix C for the detailed analysis) is

$$\begin{aligned} P_{e,1} &= \int_{r=0}^{\infty} P_{e,1,c} P_R(r) dr \\ &= \int_{r=0}^{\infty} \frac{r}{\Omega^2} e^{-\frac{r^2}{2\Omega^2}} P_{e,1,c} dr \\ &= \int_{r_j=0}^{\infty} [F_n(r_j) - F_n(-r_j)]^{\frac{M}{2}-2} f_n(r_j) \{F_n(r_j) - F_n(-r_j) \\ &\quad - e^{-\frac{r_j^2}{N_o+1}} \left[F_n\left(\sqrt{\frac{\bar{E}}{N_o} + 1} r_j\right) - F_n\left(-\sqrt{\frac{\bar{E}}{N_o} + 1} r_j\right)\right]\} dr_j. \end{aligned} \quad (2.28)$$

where $\bar{E} = 2E\Omega^2$.

Let $P_{e,2,c}$ be the conditional probability of making an error to the antipodal signal. Then

$$P_{e,2,c} = (M-2) \int_0^\infty F_s(-r_0)[F_n(r_0) - F_n(-r_0)]^{\frac{M}{2}-2} f_n(r_0) dr_0 \quad (2.29)$$

The unconditional error probability is then

$$\begin{aligned} P_{e,2} &= \int_{r=0}^\infty P_R(r) P_{e,2,c} dr \\ &= (M-2) \int_{r=0}^\infty \frac{r}{\Omega^2} e^{-\frac{r^2}{2\Omega^2}} \int_0^\infty F_s(-r_0)[F_n(r_0) - F_n(-r_0)]^{\frac{M}{2}-2} f_n(r_0) dr_0 dr \\ &= (M-2) \int_{r_0=0}^\infty \left[F_n(-r_0) - F_n\left(-\sqrt{\frac{\bar{E}}{N_o}} r_j\right) e^{-\frac{r_0^2}{\frac{\bar{E}}{N_o}+1}} \right] \\ &\quad \cdot [F_n(r_0) - F_n(-r_0)]^{\frac{M}{2}-2} f_n(r_0) dr_0. \end{aligned} \quad (2.30)$$

The bit error probability after demodulation is computed using (2.11). For the case of symbol overlapping, the bit error probability after decoding is found using (2.16). For non-overlapping case, it is computed using (2.17) and (2.18). In Fig. 2.9, we show the bit error probability of the RS(96, 84) code with (32,6) biorthogonal modulation and the RS(255, 83) code with (8,4) biorthogonal modulation. The cross over point is at 10.5 dB, much higher than the case of AWGN. At high SNR, (8,4) biorthogonal modulation performs better than (32,6) biorthogonal modulation and at low SNR, (32,6) biorthogonal modulation is only marginally better. Note that there are 510 independent fading realizations for the RS(255,83)16-ary biorthogonal modulation and 128 independent fading realizations for RS(96,84) 64-ary biorthogonal modulation. In contrast to the AWGN channel case, systems that use a stronger outer code as compare to the inner code have a much better performance. This can be explained as follow. For the AWGN channel case, the number of errors after demodulation is not that large as compare to the fading channel. Therefore, we do not need to have a power error correction code to correct the remaining errors. However, for the case of a fading channel the number of errors produced by the demodulator is much larger than the AWGN channel. Thus, it is necessary to have a strong outer code to correct the vast

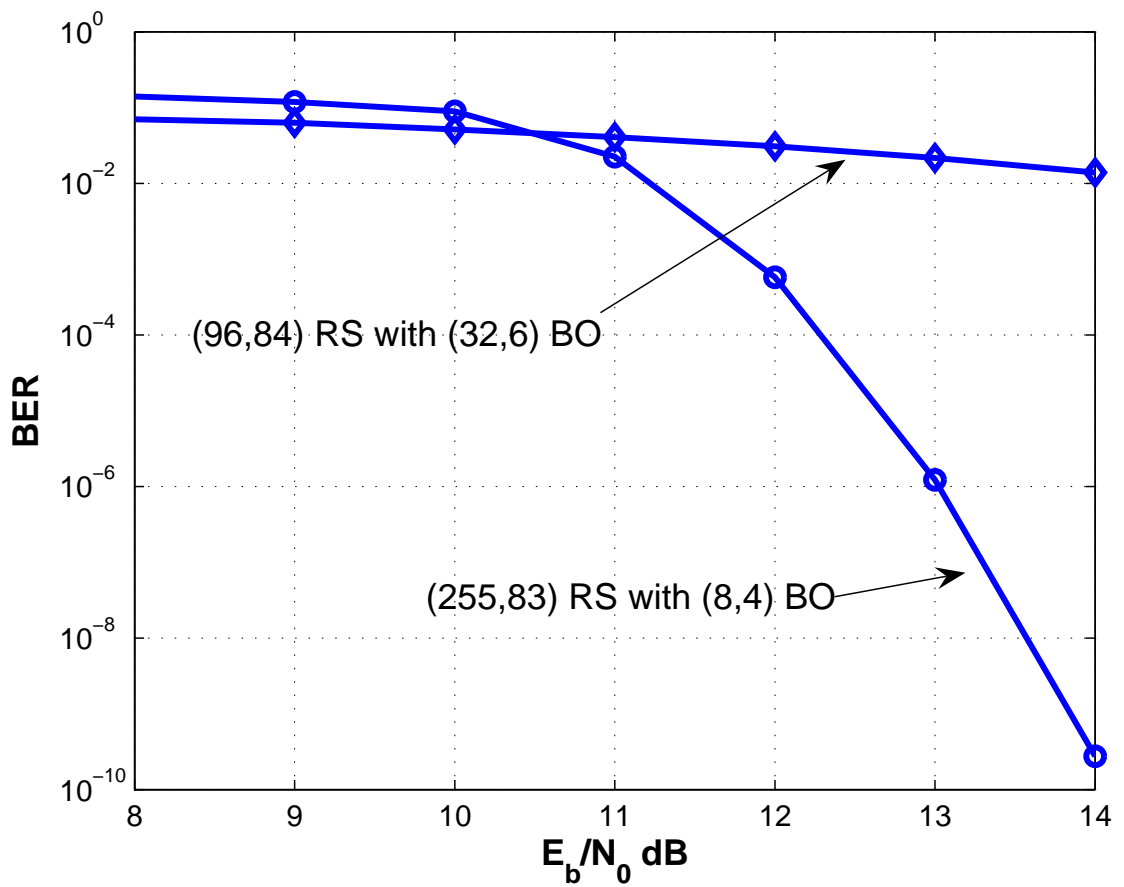


Figure 2.9: Bit error probability of RS(96,84) code with (32,6) biorthogonal modulation and RS(255, 83) code with (8,4) biorthogonal modulation over flat fading channel.

amount of errors after demodulation. Hence, in designing communication system over the Rayleigh fading channel, we need to place more emphasis on the outer code as compared to the inner code.

2.6.2 Throughput

The throughput of systems employing RS coding with biorthogonal modulation over a Rayleigh faded channel is shown in Fig. 2.10. From the figure, the 16-ary modulation system reaches its maximum throughput around 12 dB whereas the 64-ary system reaches its peak around 17 dB. This observation is consistent with the bit error probability seen earlier on.

2.6.3 Block Fading Channel

In this section we consider a simple channel model for a fading channel or a channel with interference. The model is as follows. When a particular modulation symbol is jammed or faded the output of the channel is equally likely to be any of the M symbols. Each symbol is faded or jammed with probability ρ . In addition, a block of length m is either faded or not faded. When the block is not faded the channel is an AWGN channel.

The system we consider is as follows. If we transmit a block of RS symbols such that each block consists of an integer multiple of modulation symbols, then at the demodulator output, during deep fade, each RS symbol in the block is equally likely to be any one of the 2^m symbols given any RS symbol being transmitted, where m denotes the number of bits in one RS symbol. In the following, we give an example for the case when $N = 255$. We divide 255 RS symbols into 17 blocks and this results in each block consisting of 15 RS symbols. In the absence of error control coding, during the deep fade, the information bit is equally likely to be '1' or '0'. Thus, with RS(255,232) code and (128,8) biorthogonal modulation, we have the approximated probability of bit error

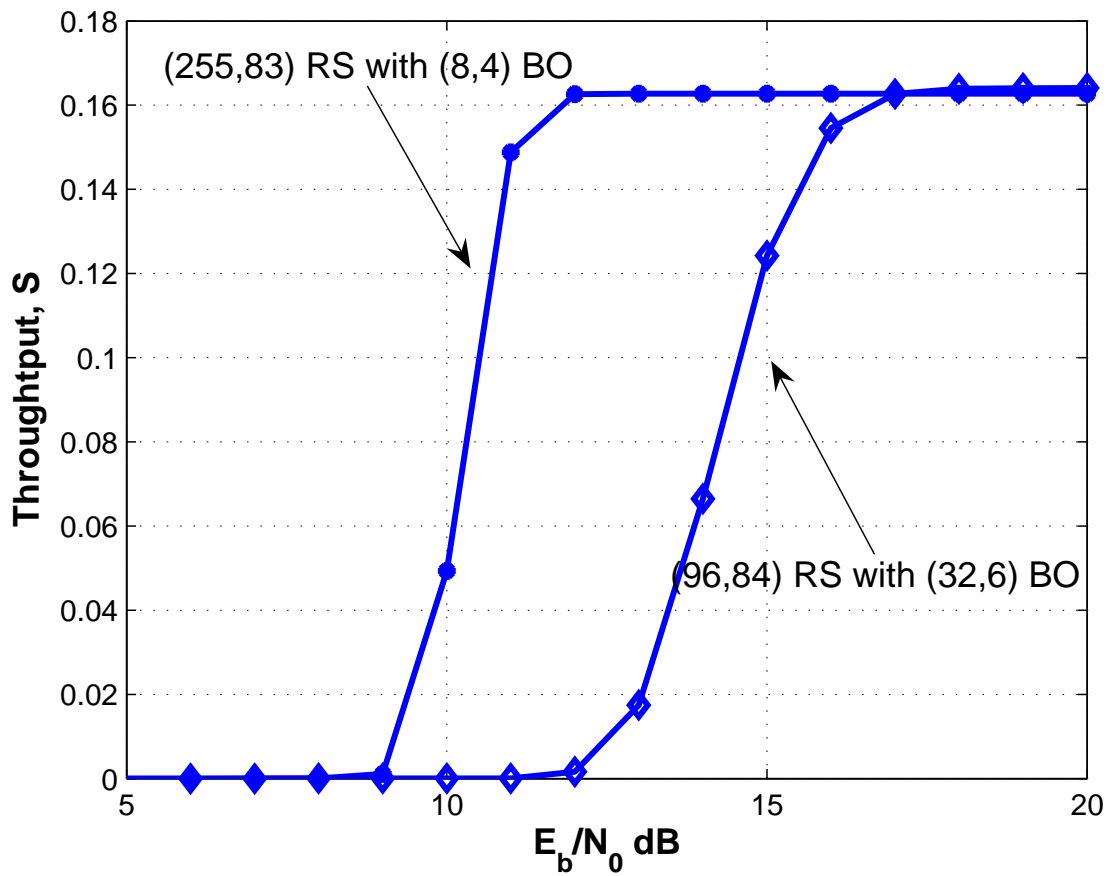


Figure 2.10: Throughput of RS(96, 84) code with (32,6) biorthogonal modulation and RS(255, 83) code with (8,4) biorthogonal modulation over a Rayleigh fading channel.

after decoding as follows

$$P(\epsilon_d) \approx P_b(1 - \rho)^{17} \sum_{i=12}^{254} \binom{254}{i} P_s^i (1 - P_s)^{254-i} + \sum_{j=1}^{17} \binom{17}{j} \rho^j (1 - \rho)^{17-j} 0.5 + \frac{17-j}{17} P_b. \quad (2.31)$$

The first part of (2.31) is the probability of none of the 17 blocks being faded and the second part is the probability of exactly j blocks being faded. When there are exactly j blocks being faded, we assumed that the RS decoder fails and outputs the information bits.

Using a similar expression, we compute the bit error probability for an RS(255,29) code over GF(256) with 16-ary biorthogonal modulation and an RS(255,77) over GF(256) with 64-ary biorthogonal modulation. For these systems, we also divide 255 RS symbols into 17 blocks in order to make an adequate comparison with the RS(255,232) code with (128,8) biorthogonal modulation. For the case of the RS(255,77) code, we use the Markov chain technique described in Section 2.4 and (2.31) to evaluate the bit error probability after decoding. The bit error probability are shown in Fig. 2.11. Here, we are comparing systems using the same number of RS symbols. However, the overall block length is different for each system. From the figure, we observe that there is an error floor for all the three systems being considered. This is due to the fact that ρ is independent of SNR and when there are too many blocks of modulation that experience a deep fade, the decoder fails. In addition, for each system, the higher the probability of encountering a deep fade (i.e. higher ρ) the higher the error floor. Finally, we note that for a fixed ρ , systems that use a stronger outer code has a better bit error probability than one that uses a strong inner code. This is consistence with the previous results for a Rayleigh fading channel. Therefore, we conclude that for fading channel, we should use a stronger outer code as compared to the inner code. However, for the case of AWGN channel, the system should employ a stronger inner code.

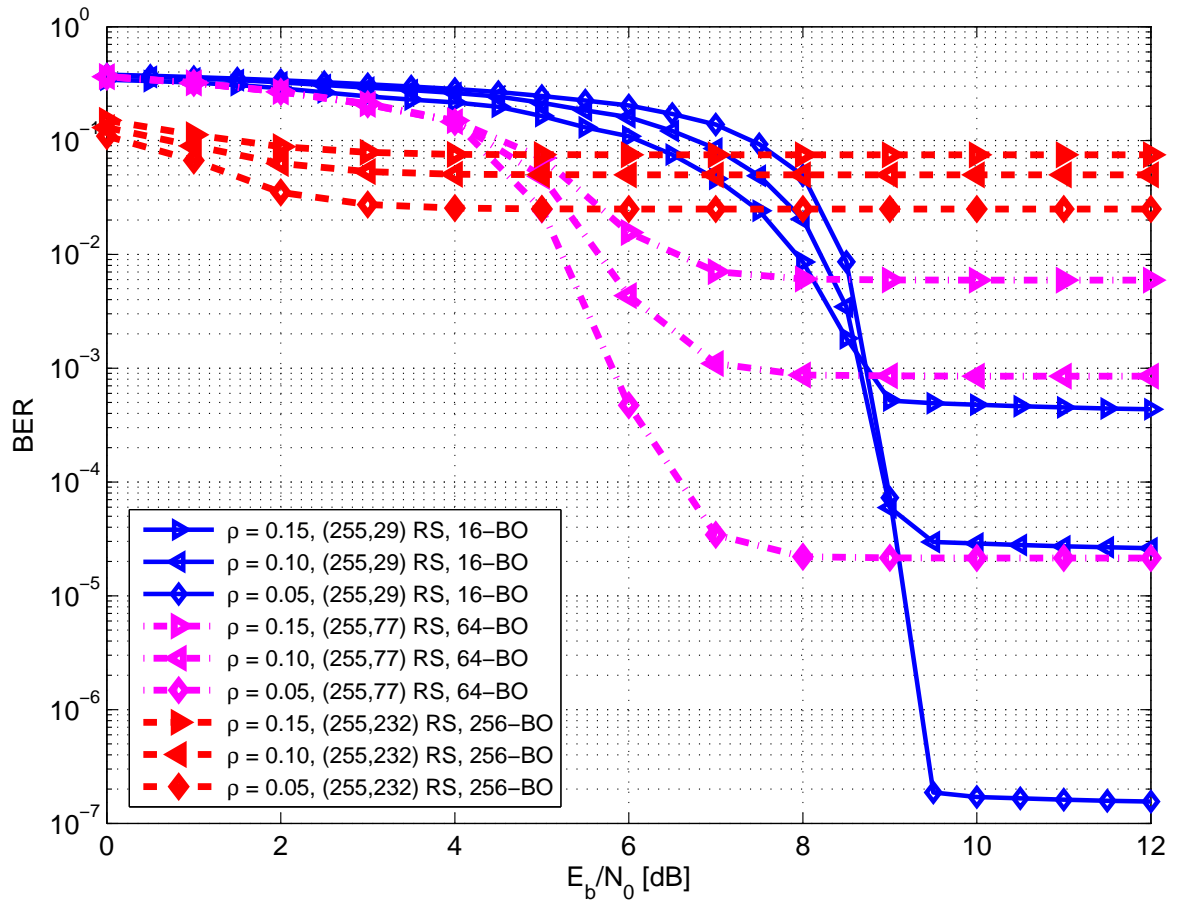


Figure 2.11: Bit error probability for block fading channel.

2.7 Low Complexity Coding Strategies for Reed-Solomon Coded M -ary Modulation System

Recently several techniques to improve the decoded bit/packet error probability of RS codes have been considered. Taipale [26] and Jing [27] develop algorithms for soft-decision decoding for RS codes, Aitsab [28] and Lee [29] suggested methods to decode RS product codes. However, the above algorithms and methods have a much higher complexity as compared to a simple hard decision RS decoding. Here we propose two novel low complexity techniques for decoding RS coded systems with symbol overlapping. The RS decoder still operate with hard decision decoding but use iterative techniques to improve system performance.

We define symbol overlapping to be the case when bits in each modulation symbol belong to 2 or more RS symbols and vice versa. A description of the proposed design is given in this section. We evaluate the bit and packet error probabilities via simulation. We consider both an AWGN channel and an Rayleigh fading channel. Both the bit and packet error probability are compared with an RS code of equal length without interleaving and iterations. We show that the error probability is improve compare to conventional decoding for both the Rayleigh fading channel and AWGN channel.

2.7.1 RS Coded System with Bits Interleaving

The block diagram of the system we consider is shown in Fig. 2.12. The system has an $RS(N, K)$ encoder over $GF(M)$. We considered a packet of $\log_2 M$ codewords. That is, we have $\log_2 M \times K \log_2 M$ information bits. A codeword consists of $\log_2 M \times N \log_2 M$ bits. For example, if $M = 16$ and $K = 6, N = 16$, we will have 4 $RS(16,6)$ codewords with 96 information bits and 256 coded bits. At the output of the RS encoder, the $\log_2 M$ RS codewords are converted back into bits and passed through a matrix interleaver prior to modulation. The block coded structure of this particular system is shown in Fig. 2.13. Note that in this particular structure, each bit in a RS symbol belongs to a different modulation symbol. The received signal is

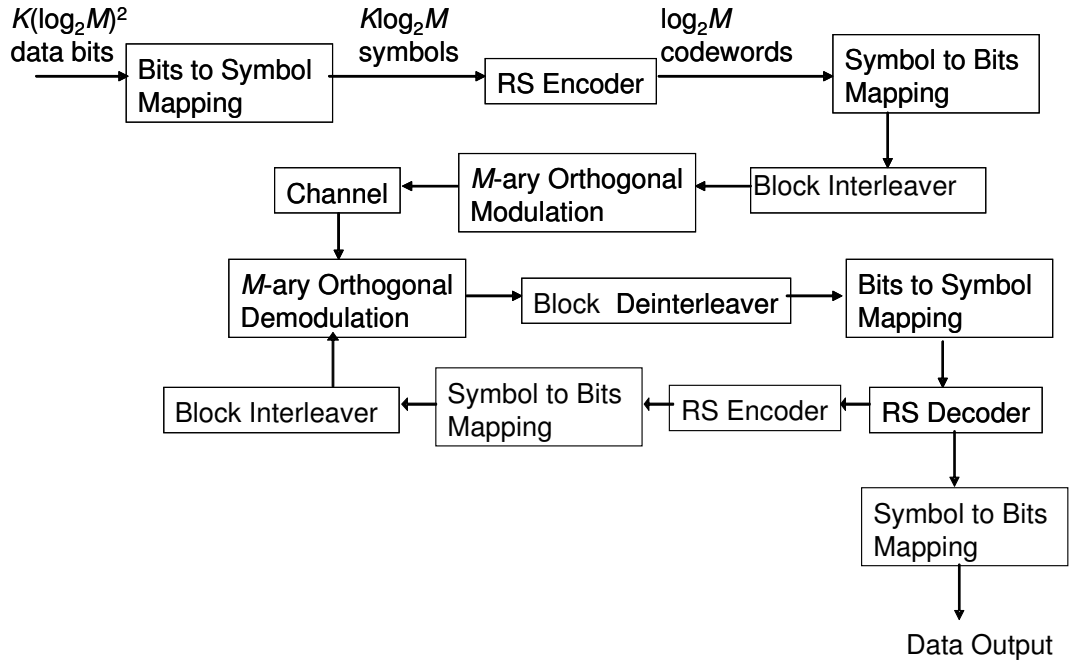


Figure 2.12: RS coded M -ary orthogonal modulation system with bit interleaving and iterative decoding.

demodulated, de-interleaved, mapped into symbols and used as the input to the RS decoder. The decoded symbols are mapped into bits, interleaved and sent back to the demodulator where it can make use of the decoded bits to redemodulate the signals. For example, suppose codeword 1 in Fig. 2.13 is decoded correctly by the RS decoder. Then this information is sent to the demodulator. Then, based on this information, the demodulator can make a better decision on the modulation symbol since it only needs to consider $\frac{M}{2}$ possible symbols since it knows the value of the first bit. This process is repeated for a fixed number of times.

2.7.2 RS Coded System With Symbols Interleaving

The RS coded system with symbol interleaving is illustrated in Fig. 2.14. At the output of the RS encoder, we have $\log_2 M$ RS codewords. That is, we have $\log_2 M \times N$ RS symbols. We perform matrix interleaving on this block of RS symbols. This set of symbols are converted to bits and as a result, we have a block of $N \times (\log_2 M)^2$

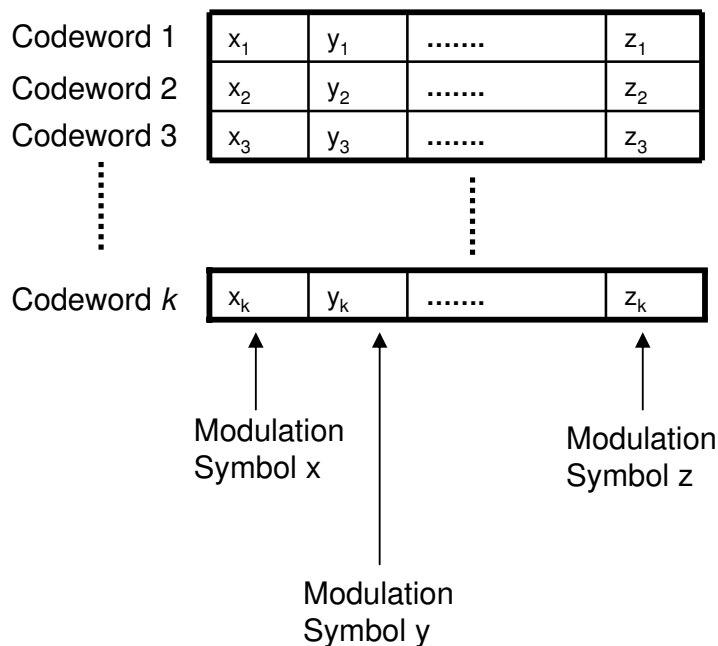


Figure 2.13: Block coded structure for the RS symbol interleaving system in Fig. 2.12. Each box represents a single bit and there are $k = \log_2 M$ RS codewords in 1 block.

coded bits. Prior to modulation, a circular shift of $\frac{\log_2 M}{2}$ bits is performed on each row of $(\log_2 M)^2$ bits. The purpose of the circular shift is to cause overlapping between RS symbols and modulation symbols. The transmitted block structure for $M = 16$ is shown in Fig. 2.15.

The received signal is demodulated, circularly shifted by $\frac{\log_2 M}{2}$ bits for each row of bits, mapped into symbols, deinterleaved and sent to the RS decoder. Similar to the case of bit interleaving, the decoded symbols are interleaved, mapped into bits, each row is circularly shifted by $\frac{\log_2 M}{2}$ bits and sent back to the demodulator where it can make use of the decoded bits to re-demodulated the signals. This process is repeated for a fixed number of times.

2.7.3 Performance Analysis

We compare the performance of the systems in Fig. 2.12 and Fig. 2.14 with a RS code using error-only decoding (without interleaving and iterating) with the same M -

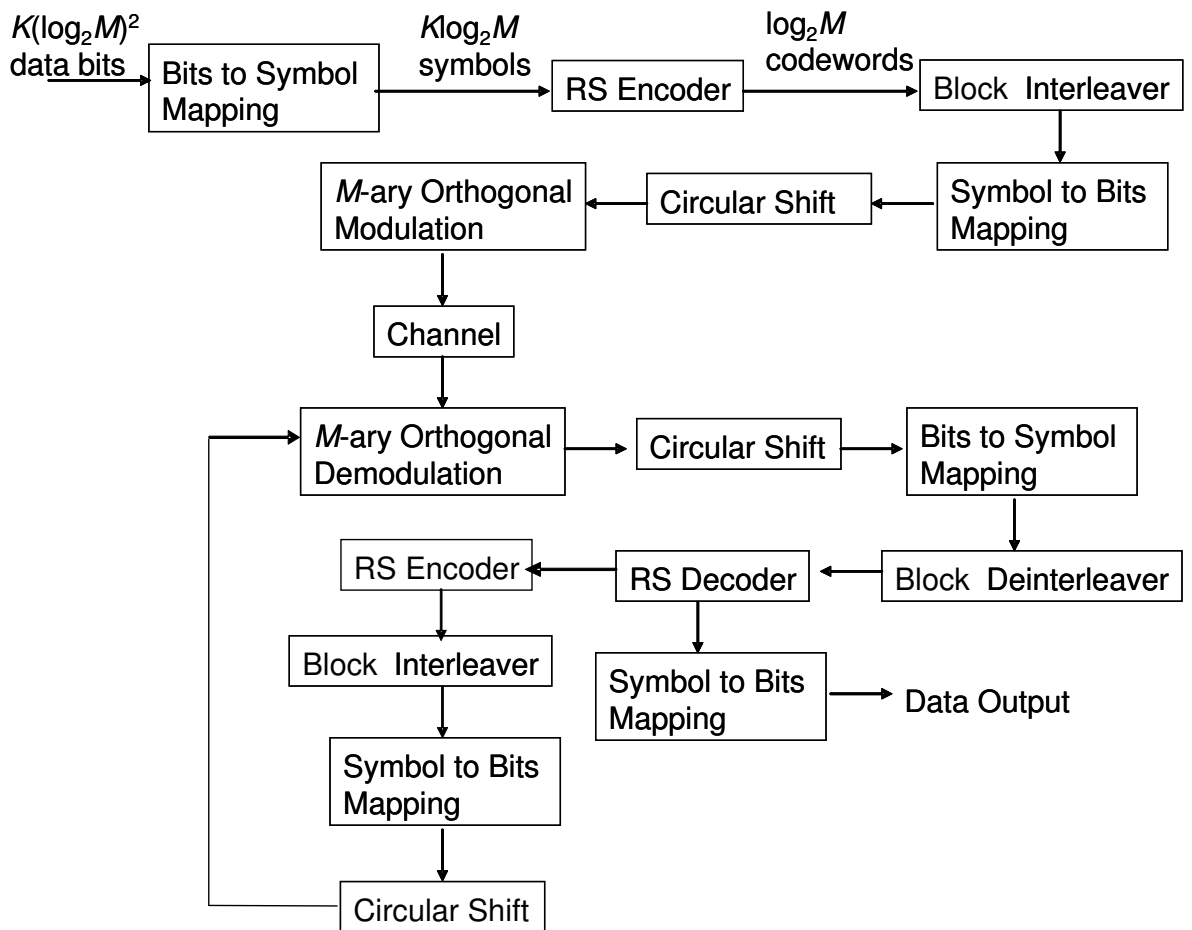


Figure 2.14: RS coded M -ary orthogonal modulation system with symbols interleaving and iterative decoding.

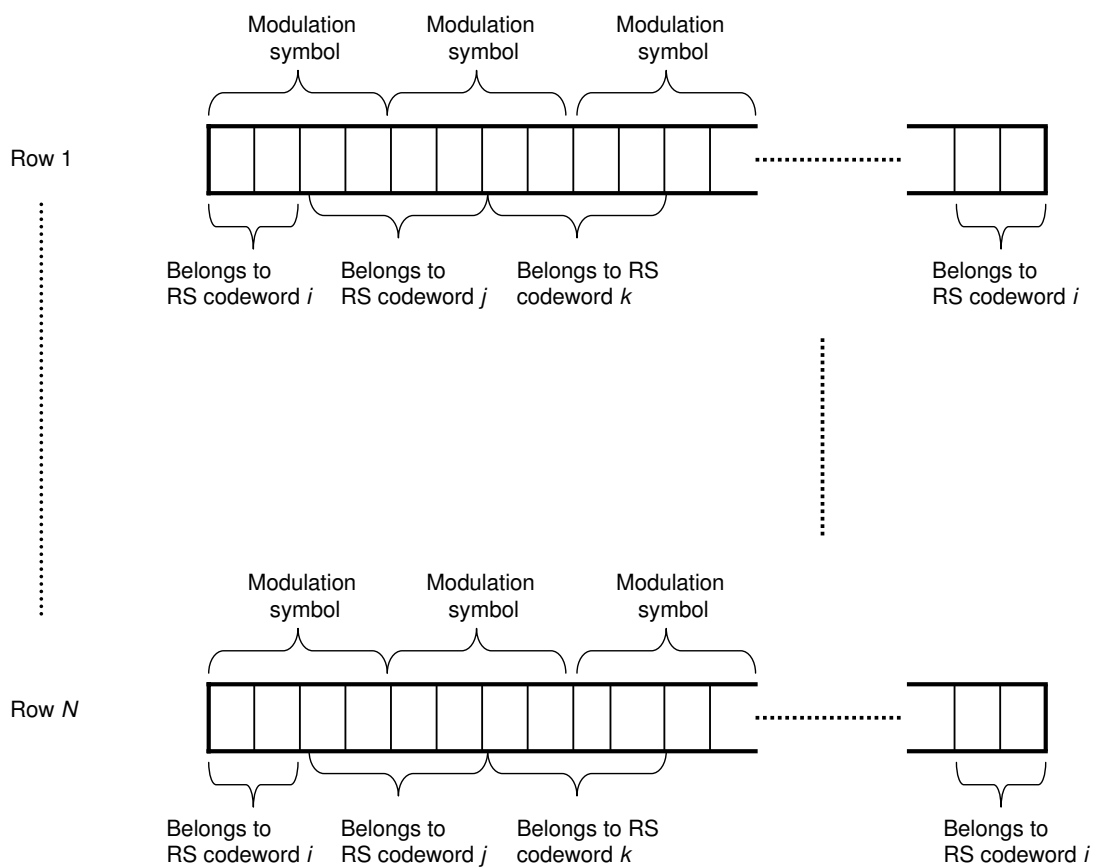


Figure 2.15: Packet structure for the RS coded system with symbol interleaving. Here, $M = 16$ and a modulation symbol consists of bits from 2 RS symbols. For example, the first modulation symbol in row 1 consists of bits from RS codeword i and codeword j .

ary modulation. Using $M = 16$ and RS(16,6) codes for the proposed system, we have a total of 96 information bits 256 coded bits. In order to provide a fair comparison, the packet size has to be the same for the non-interleaved, no iteration RS code. Therefore, a good candidate would be an RS(32,12) codes over GF(2^8). In this case, not only we have the same packet length, the code rate is also the same. For the results presented in this thesis, it is assumed that the codes are systematic and the RS decoder can detect all decoding errors. This is because decoding errors are rare for RS codes and errors-only decoding unless $N - K$ is very small [25]. In addition, probability of an undetected error is very small if a good error-detecting code is used. As a result, the probability of an undetected decoding error is negligible.

To analysis the standard bit error probability of (N, K) RS codes after decoding, we define the following events.

- ϵ_d : event that the first bit is in error after decoding,
- ϵ_b : event that the first bit is in error at output of demodulator,
- $\epsilon_{t,L}$: event that t RS symbols are in error in the last L RS symbols of a codeword.

Since RS codes are maximum distance separable codes [7], the minimum distance of an (N, K) RS code is $d_{min} = N - K + 1$. Hence, it is able to correct a maximum of $t = \lfloor \frac{d_{min}-1}{2} \rfloor$ symbol errors. Based on the above assumptions, when the number of RS symbol errors is greater than the error correction capability of the code, the decoder puts out the received information symbols. Hence, ϵ_d occurs if the first received bit is in error and there are at least t errors out of the last $N - 1$ symbols. Since ϵ_b and $\epsilon_{t,L}$ are independent, we have

$$\begin{aligned} P(\epsilon_d) &= P(\epsilon_b \cap \epsilon_{t,L}) = P(\epsilon_b)P(\epsilon_{t,L}) \\ &= p \sum_{l=t}^{N-1} \binom{N-1}{l} P_B^l (1 - P_B)^{N-1-l} \end{aligned} \quad (2.32)$$

where p, P_B are the bit error probability of 16-ary orthogonal modulation and RS symbol error probability respectively. Denote by P_4 the symbol error probability of 16-ary

orthogonal modulation, then P_B is given by

$$P_B = 1 - (1 - P_4)^2. \quad (2.33)$$

2.7.4 Performance Over an AWGN Channel

For AWGN channel, p and P_4 are given by [10]

$$P_4 = \frac{1}{\sqrt{2\pi}} \int_{-\infty}^{\infty} \left[1 - \left(\frac{1}{\sqrt{2\pi}} \int_{-\infty}^y e^{-x^2/2} dx \right)^{M-1} \right] \exp \left[-\frac{1}{2} \left(y - \sqrt{\frac{2E_s}{N_0}} \right)^2 \right] dy, \quad (2.34)$$

$$p = \frac{2^{4-1}}{2^4 - 1} P_4 = \frac{8}{15} P_4 \quad (2.35)$$

where $E_s = E_b \log_2 M$.

The bit error probability of the RS(16, 6) codes with 16-ary orthogonal modulation using the setup in Fig. 2.12 and Fig. 2.14 over an AWGN channel is shown in Fig. 2.16 and Fig. 2.17 respectively with zero, one and two iterations. From these figures, we note that the bit error probability does not improve significantly from one iteration to two iterations. We performed simulations with up to ten iterations and the bit error probability is about the same as two iterations. Therefore, we believe that for this system setup, two iterations are enough. The performance gain for both the systems considered from zero to two iterations is about 1 dB over the AWGN channel.

We compare the bit error probability of both systems using two iterations with no symbol overlapping RS(32,12) code over GF(2^8). The result is given in Fig. 2.18. We note that the RS coded system with symbol interleaving has the best performance among the three and it has a gain of about 0.5 dB compared to the RS(32,12) code without interleaving and iteration at bit error rate of 10^{-3} . We do not expect a large gain as the RS decoder is a hard decision decoder. However, this particular proposed setup has a lower decoding complexity compared to soft decision RS decoding as it only require up to 2 iterations.

The comparison of packet error probability of the systems considered is given in Fig. 2.19. The packet error probability, P_{pck} for the RS(32,12) code over GF(2^8) is

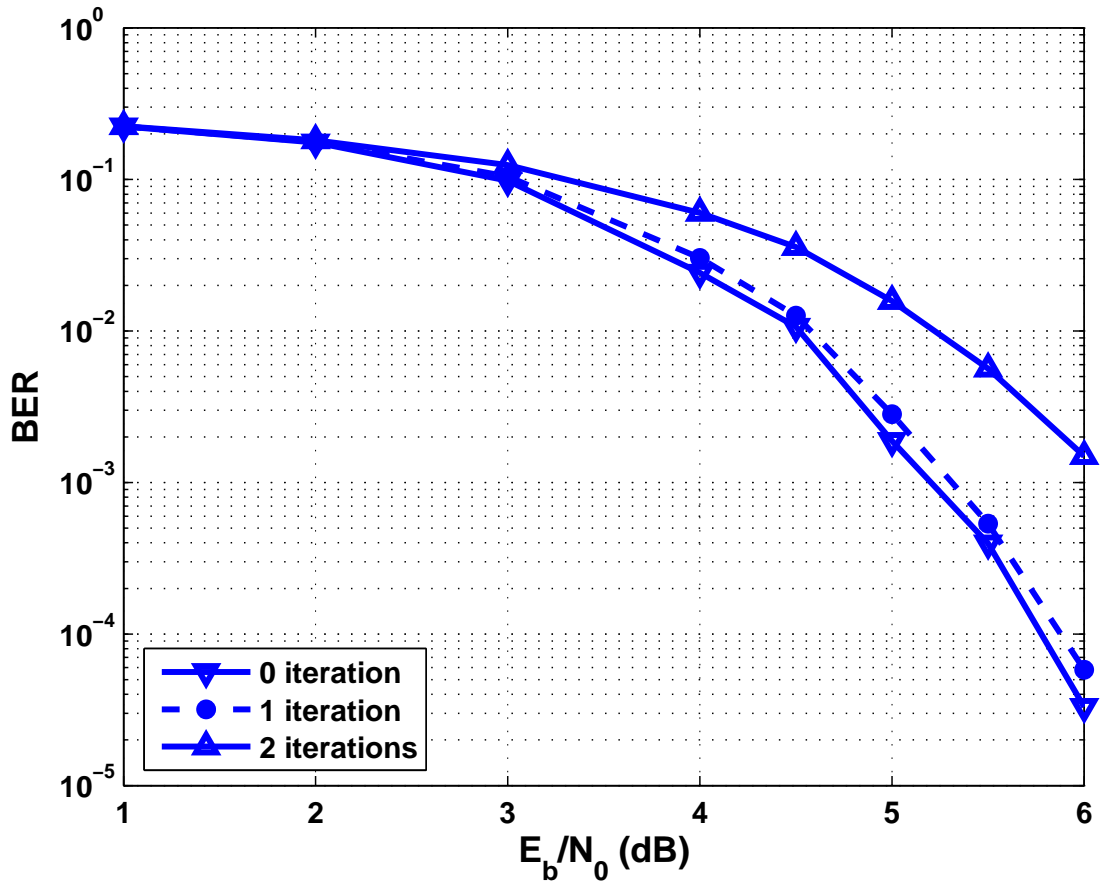


Figure 2.16: Bit error probability of RS(16,6) coded 16-ary orthogonal modulation system using bit interleaving (setup in Fig. 2.12).

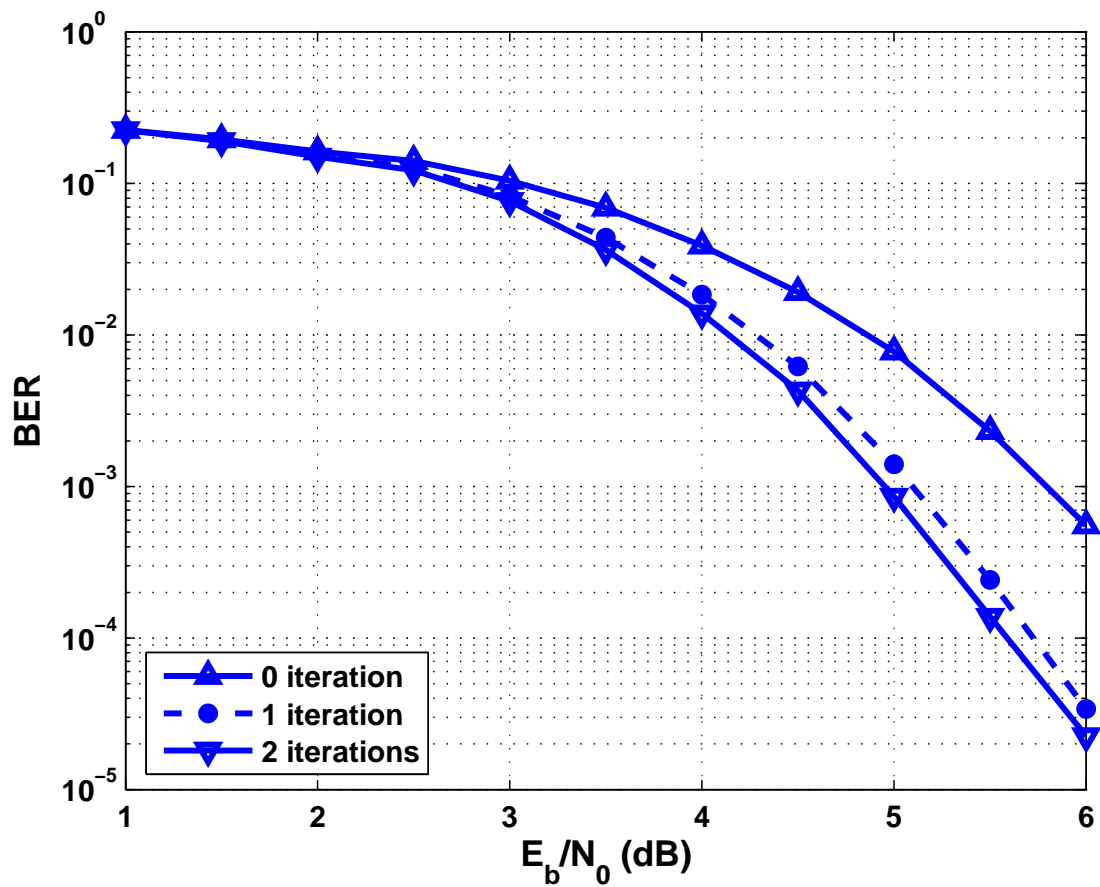


Figure 2.17: Bit error probability of RS(16,6) coded 16-ary orthogonal modulation system using symbol interleaving (setup in Fig. 2.14).

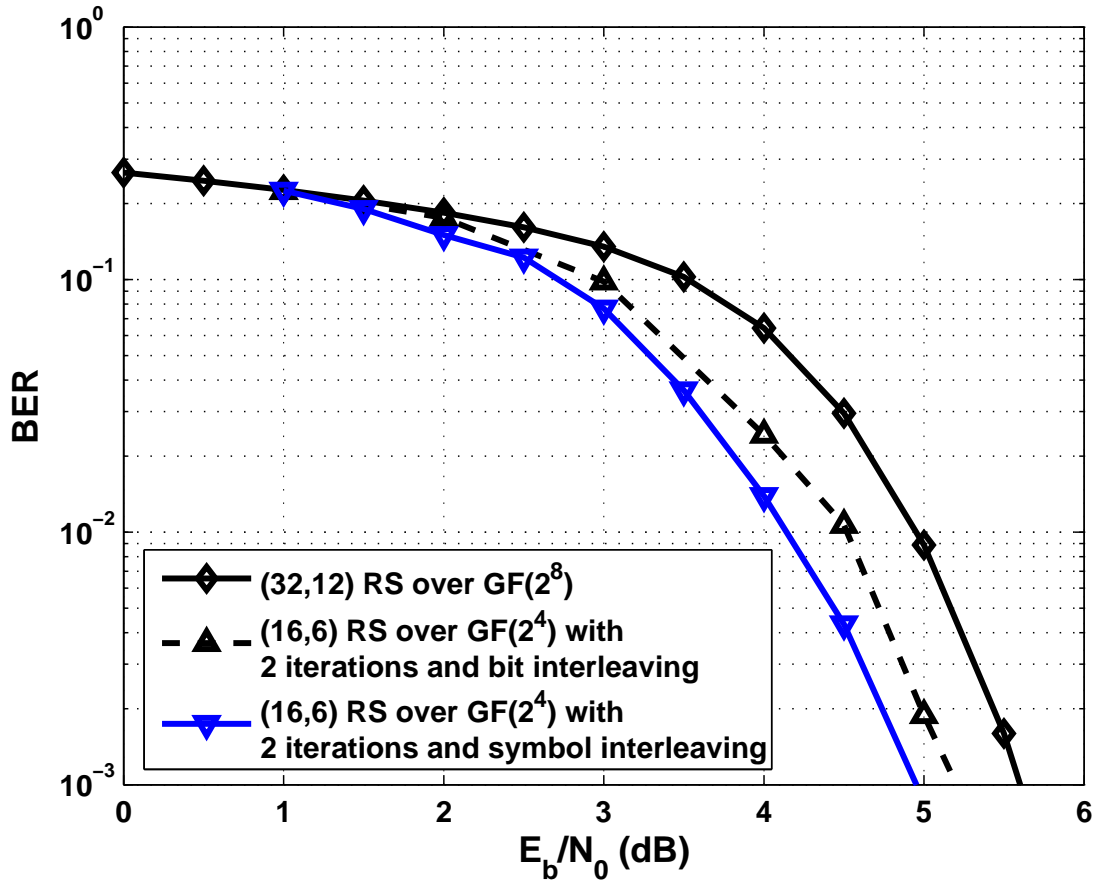


Figure 2.18: Bit error probability of (i) RS(32,12) coded system with $GF(2^8)$, (ii) RS(16,6) coded system with $GF(2^4)$ and symbol interleaving with 2 iterations, (iii)RS(16,6) coded system with $GF(2^4)$ and bit interleaving with 2 iterations. All the systems employ 16-ary orthogonal modulation.

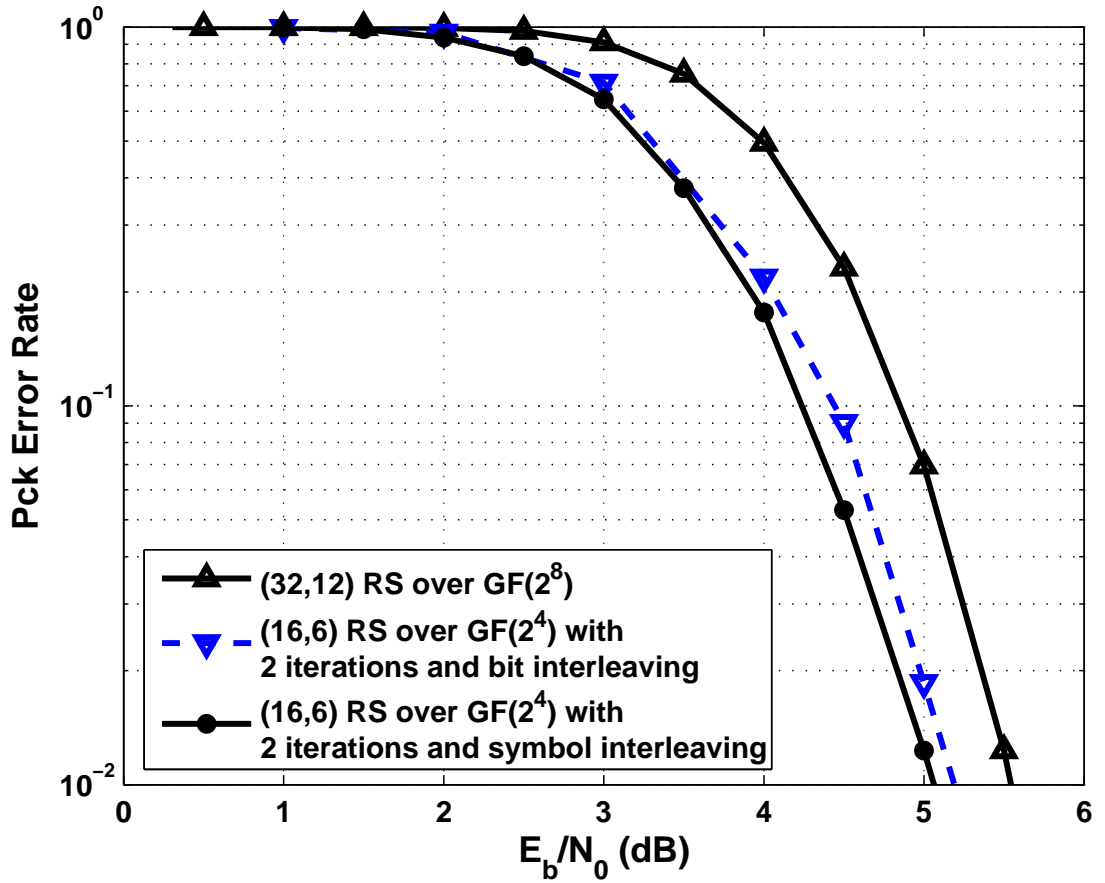


Figure 2.19: Packet error probability of (i) RS(32,12) coded system with $GF(2^8)$, (ii) RS(16,6) coded system with $GF(2^4)$ and symbol interleaving with 2 iterations, (iii) RS(16,6) coded system with $GF(2^4)$ and bit interleaving with 2 iterations. All the systems employ 16-ary orthogonal modulation.

given by

$$P_{pck} = \sum_{l=11}^{32} \binom{31}{l} P_B^l (1 - P_B)^{31-l}. \quad (2.36)$$

Similar to the case of bit error probability, the RS(16,6) coded system with symbol interleaving and 2 iterations have the best performance. At packet error rate of 10^{-2} , it out performs the RS(32,12) code over GF(2^8) system by about 0.4 dB.

2.7.5 Performance Over a Rayleigh Fading Channel

Now consider the case where every modulation symbol is faded independently. For an orthogonal signaling system with fading channel, the conditional symbol error probability is given by

$$P_4(R) = \frac{1}{\sqrt{2\pi}} \int_{-\infty}^{\infty} \left[1 - \left(\frac{1}{\sqrt{2\pi}} \int_{-\infty}^y e^{-x^2/2} dx \right)^{M-1} \right] \cdot \exp \left[-\frac{1}{2} \left(y - \sqrt{\frac{2R^2 E_s}{N_0}} \right)^2 \right] dy \quad (2.37)$$

where the random variable R represents the fading and has density

$$P_R(r) = \begin{cases} 0, & r < 0, \\ \frac{r}{\Omega^2} e^{-\frac{r^2}{2\Omega^2}}, & r \geq 0, \end{cases}$$

and $E(R^2) = \Omega^2$. Hence, the probability of symbol error over a Rayleigh fading channel is given by

$$P_e = \int_{r=0}^{\infty} P_R(r) P_4(r) dr. \quad (2.38)$$

The bit error probability of three systems considered over a Rayleigh fading channel is shown in Fig. 2.20. Similar to the case of AWGN channel, the RS(16,6) over GF(2^4) with 2 iterations and symbol overlapping has the best bit error probability. It has a gain of approximately 1 dB at bit error rate of 10^{-3} compared to the RS(32,12) code over GF(2^8). Comparison of packet error probability is given in Fig. 2.21. As we can see, the performance follows a similar trend from the earlier results. However, the performance gain is small compared to the AWGN case. At a packet error rate of 10^{-2} , the RS coded system with symbol overlapping is only marginally better than the RS(32,12) coded system.

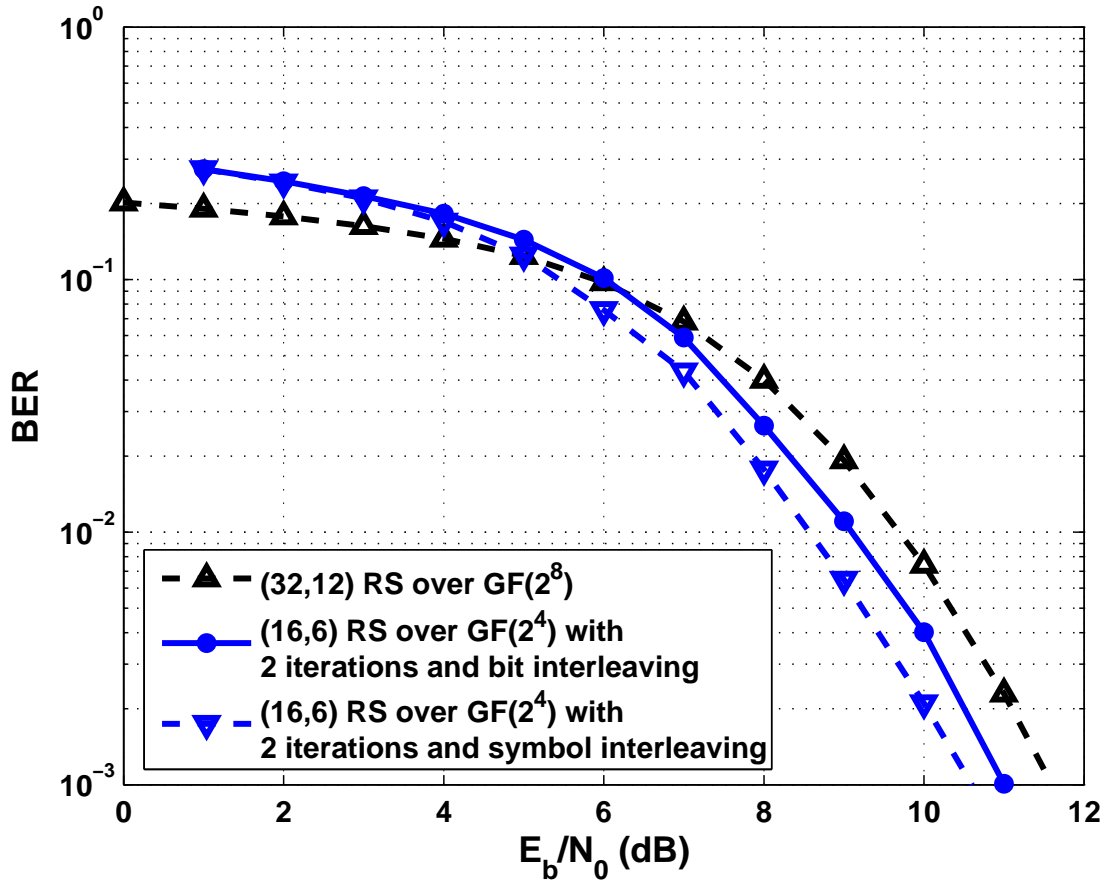


Figure 2.20: Bit error probability of (i) RS(32,12) coded system with $GF(2^8)$, (ii) RS(16,6) coded system with $GF(2^4)$ and symbol interleaving with 2 iterations, (iii) RS(16,6) coded system with $GF(2^4)$ and bit interleaving with 2 iterations. All the systems employ 16-ary orthogonal modulation.

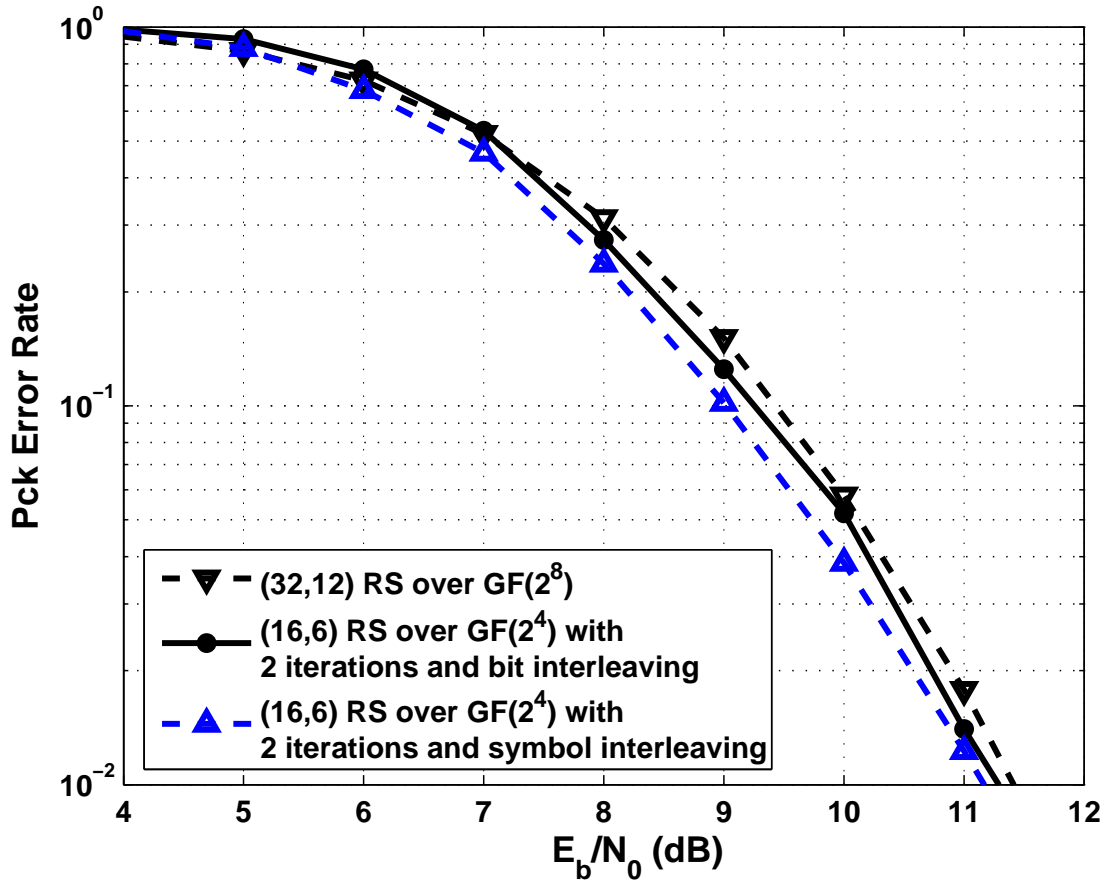


Figure 2.21: Packet error probability of (i) RS(32,12) coded system with $GF(2^8)$, (ii) RS(16,6) coded system with $GF(2^4)$ and symbol interleaving with 2 iterations, (iii) RS(16,6) coded system with $GF(2^4)$ and bit interleaving with 2 iterations. All the systems employ 16-ary orthogonal modulation.

2.8 Conclusion

In this chapter, we developed a technique for analyzing the bit error and codeword error probability of RS coded M -ary modulation system with symbol overlapping using a Markov chain technique. We gave examples of bit error probability of the coded system using orthogonal with coherent and noncoherent demodulation. We also considered biorthogonal modulation with coherent demodulation. The bit error probability of RS code concatenated with an NR code is simulated and compared with the equivalent RS coded biorthogonal modulation. For a Rayleigh flat fading channel, we demonstrated the effect of RS coded modulation on the bit error probability using biorthogonal modulation. It was found that over an AWGN channel, a stronger inner code gives better bit error probability. However, in the case of a Rayleigh flat fading and block fading channel, a stronger outer code gave a better bit error probability as there is a large number of errors present. Next, we analyzed the throughput of a system using biorthogonal modulation over an AWGN channel and a Rayleigh fading channel. The minimum SNR in attaining maximum throughput is the lowest for system employing strong inner code for the case of AWGN channel. But, for Rayleigh fading channel, a strong outer code would result in the lowest SNR for maximum throughput. We proposed two novel low complexity coding strategies for RS coded modulation system - (i) bit interleaving with iterations and (ii) symbol interleaving with iterations. We found that the system with symbol interleaving has better bit error and packet error probability as compared to the case with bit interleaving over an AWGN channel and a Rayleigh channel. In comparison to a system that did not employ symbol overlapping, we have a gain about 1 dB at bit error rate of 10^{-3} at a marginal increase in complexity (i.e. only 2 iterations).

CHAPTER 3

Analysis of Reed-Solomon With DPSK Modulation

Differential phase shift keying (DPSK) is a modulation technique that does not require a coherent reference at the receiver and thus can be noncoherently demodulated. In DPSK modulation the change in the information (rather than the information) is encoded into the phase of the transmitted signal. In this way, for the detection of DPSK modulated signals, a decision is made on the phase difference measured on adjacent symbols. For bit error probability, it is well known that DPSK is 3 dB better than frequency shift keying (FSK) [10, 30, 31, 32]. Although phase shift keying (PSK) has better performance than DPSK, the receiver for PSK is more complex as it is necessary to synchronize the oscillator at the receiver with the received signal. Nafie [33] and Poh [34] proposed the use of M -ary DPSK in Bluetooth for high rate communications.

3.1 System Description

In this chapter we consider an RS(N, K) coded communication system using DPSK modulation. Each RS symbol consists of m bits and $N \leq 2^m$. Let p_e be the bit error probability of the system. If the events of error on each bit are independent then the symbol error probability, p_E is given by

$$p_E = 1 - (1 - p_e)^m. \quad (3.1)$$

This is true if we are using BPSK or BFSK. However, for DPSK modulation, the above formula is not applicable as adjacent decision errors are not mutually independent.

Wang [20] has shown that the actual symbol error probability (by considering error correlation in DPSK) is slightly worse off than the memoryless model when $m = 3$ and $m = 6$. In the analysis he assumed that the nonadjacent decision errors are mutually independent. In the next section, we will derive the exact symbol error probability, p_E , and compare with Wang's result.

3.2 Derivation of Symbol Error Probability

The probability density function (pdf) of the phase error, ϕ , of a received signal over an AWGN channel relative to the transmitted signal is [35]

$$f(\phi) = \frac{1}{2\pi} \exp\left(-\frac{E_c}{N_0}\right) + \sqrt{\frac{E_c}{\pi N_0}} \exp\left(-\frac{E_c}{N_0} \sin^2 \phi\right) \cos \phi \left[1 - Q\left(\sqrt{\frac{2E_c}{N_0}} \cos \phi\right)\right], \quad (3.2)$$

where $-\pi \leq \phi \leq \pi$ and $\frac{E_c}{N_0}$ is the *SNR* per coded bit. The probability of error for the j th decision conditioned on the phase error in the j th bit for binary DPSK is [36]

$$p_{e_j|\phi} = Q\left(\sqrt{\frac{2E_c}{N_0}} \cos \phi\right). \quad (3.3)$$

Therefore, the probability of error for the j th decision (i.e. bit error probability) for DPSK over an AWGN channel is

$$\begin{aligned} p_{e_j} &= \int_{-\pi}^{\pi} p_{e_j|\phi} f(\phi) d\phi \\ &= \int_{-\pi}^{\pi} Q\left(\sqrt{\frac{2E_c}{N_0}} \cos \phi\right) f(\phi) d\phi. \end{aligned} \quad (3.4)$$

Wang [20] assumed that the nonadjacent decision errors are mutually independent and derived the expression for symbol error probability as

$$p_E = 1 - \left(1 - \frac{1}{2} \exp\left(-\frac{E_c}{N_0}\right)\right) \left\{ \frac{\int_{-\pi}^{\pi} \left[1 - Q\left(\sqrt{\frac{2E_c}{N_0}} \cos \phi\right)\right]^2 f(\phi) d\phi}{1 - \frac{1}{2} \exp\left(-\frac{E_c}{N_0}\right)} \right\}^{m-1}. \quad (3.5)$$

In the following, we derive the symbol error probability, p_E , and arrive at the same result as Wang. Let c_j be the event of correct decision for the j th bit. Therefore, for a

m -bit symbol, the probability of symbol error is

$$\begin{aligned}
p_E &= 1 - P(c_0, c_1, \dots, c_{m-1}) \\
&= 1 - P(c_{m-1}|c_{m-2}, \dots, c_0)P(c_{m-2}, \dots, c_0) \\
&= 1 - P(c_{m-1}|c_{m-2})P(c_{m-2}, \dots, c_0) \\
&= 1 - P(c_0) \prod_{j=1}^{m-1} P(c_j|c_{j-1}). \tag{3.6}
\end{aligned}$$

The above derivation is true because given the event c_{j-1} , the event c_j is independent of the event c_{j-2}, \dots, c_0 since the decision on j bit is only depends on itself and the previous bit. The proof is given in Appendix C. Since $P(c_j|c_{j-1})$ is identical for any j , we can simplify (3.6) as

$$p_E = 1 - P(c_0)P^{m-1}(c_1|c_0) \tag{3.7}$$

where

$$P(c_0) = 1 - p_e = 1 - \int_{-\pi}^{\pi} p_{e|\phi} f(\phi) d\phi \tag{3.8}$$

and

$$P(c_1|c_0) = \frac{P(c_0, c_1)}{P(c_0)} = \frac{1 - 2p_e + P(e_0, e_1)}{P(c_0)}. \tag{3.9}$$

The above expression requires us to evaluate the double error probability, $P(e_0, e_1)$. Oberst [36] has shown that

$$P(e_i, e_j|\phi) = \left[Q\left(\sqrt{\frac{2E_c}{N_0}} \cos \phi \right) \right]^2 \tag{3.10}$$

and we can evaluate $P(e_0, e_1)$ using (3.2) and (3.10)

$$P(e_1, e_0) = \int_{-\pi}^{\pi} P(e_i, e_j|\phi) f(\phi) d\phi \tag{3.11}$$

In Fig. 3.1, we show the symbol error probability for $m = 3$ and $m = 6$.

3.3 Derivation of Packet Error Probability over an AWGN Channel

The derivation of packet error probability for RS codes using DPSK modulation over the AWGN channel is not trivial. This is because the adjacent symbols in a codeword

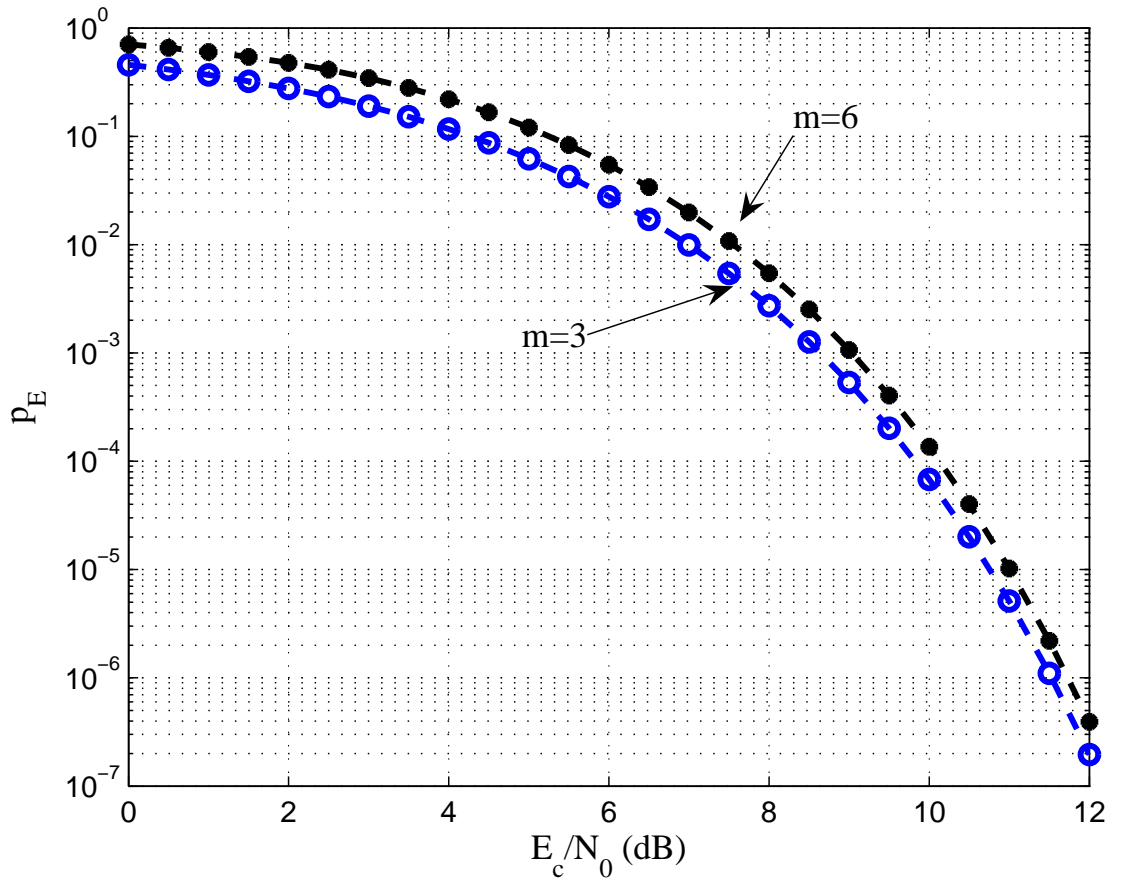


Figure 3.1: Comparison of symbol error probability for $m=3$ and $m=6$ with Wang's result.

are dependent. The event of an error on the last bit of a symbol is not independent of the event of an error on the first bit of the next symbol. To derive the packet error probability using RS codes, we need to understand the relationship between 2 adjacent symbols in a RS codeword.

3.3.1 Relationship Between Two Adjacent Symbols

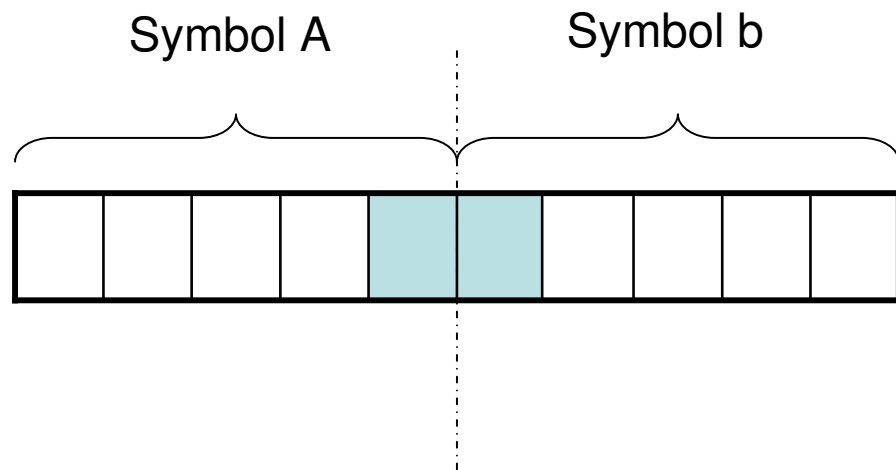


Figure 3.2: Two Adjacent Symbol a and b. Last bit of symbol a correlates with first bit of symbol b.

The relationship between 2 adjacent symbols is shown in Fig. 3.2. The event of an error on the last bit in symbol a is not independent of the event of an error of the first bit in symbol b . Therefore, the error events of symbol a and b are not independent. We define the following events and probabilities:

- E_i : event that symbol i is in error,
- C_j : event that symbol j is correct,
- e_a : event that the last decision in block a is wrong,
- c_a : event that the last decision in block a is correct,

- e_b : event that the first decision in block b is wrong,
- c_b : event that the first decision in block b is correct,
- p_e : probability for the occurrence of one decision error,
- p_c : probability of a correct decision,
- p_{ee} : probability for the occurrence of two consecutive errors,
- p_E : probability for one symbol error,
- p_C : probability for one correct symbol,
- $p_{E|E}$: probability for one symbol error, condition on the previous one being in error,
- $p_{C|E}$: probability for one correct symbol, condition on the previous one being in error,
- $p_{C|C}$: probability for one correct symbol, condition on the previous one being correct,
- $P_{E|C}$: probability for one symbol error, condition on the previous one being correct.

The probability that symbol b is in error, given that symbol a is in error is

$$\begin{aligned}
P(E_b|E_a) &= P(E_b, e_a, e_b|E_a) + P(E_b, e_a, c_b|E_a) + P(E_b, c_a, e_b|E_a) + P(E_b, c_a, c_b|E_a) \\
&= \frac{1}{P(E_a)} [P(E_a|e_a, e_b, E_b)P(E_b|e_a, e_b)P(e_a, e_b) \\
&\quad + P(E_a|e_a, c_b, E_b)P(E_b|e_a, c_b)P(e_a, c_b) + P(E_b|c_a, e_b, E_a)P(E_a|c_a, e_b)P(c_a, e_b) \\
&\quad + P(E_a|c_a, c_b, E_b)P(E_b|c_a, c_b)P(c_a, c_b)] \\
&= \frac{1}{P(E_a)} [P(e_a, e_b) + P(E_b|c_b)P(e_a, c_b) + P(E_a|c_a)P(c_a, e_b) \\
&\quad + P(E_a|c_a)P(E_b|c_b)P(c_a, c_b)]. \tag{3.12}
\end{aligned}$$

Since every decision and every symbol has the same error probability, that is, $P(e_a) = P(e_b) = p_e, P(c_a) = P(c_b) = p_c, P(E_a) = P(E_b) = p_E$, we may omit the subscripts a, b and simplify (3.12). as follow

$$\begin{aligned}
p_{E|E} &= \frac{p_{ee}}{p_E} + \frac{2p_{E|c}p_{ec}}{p_E} + [p_{E|c}]^2 p_{cc} \\
&= \frac{p_{ee}}{p_E} + \frac{2(p_E - p_e)(p_e - p_{ee})}{p_E(1 - p_e)} \\
&\quad + \frac{(p_E - p_e)^2(1 - 2p_e + p_{ee})}{p_E(1 + p_e)^2}.
\end{aligned} \tag{3.13}$$

With $p_{E|E}$ known, we can express the probabilities $p_{C|E}, p_{C|C}$ and $p_{E|C}$ as

$$p_{C|E} = 1 - p_{E|E}, \tag{3.14}$$

$$p_{C|C} = 1 - \frac{p_{C|E}p_E}{p_C}, \tag{3.15}$$

$$p_{E|C} = 1 - p_{C|C}. \tag{3.16}$$

3.3.2 Decoded Packet Error Probability

We use the approach in [37] to evaluate the decoded packet error probability with the error correlation taken into account. The following three functions are introduced to describe the approach:

- $G(k)$: conditional probability for k correct symbols given one erroneous leading symbol (written as $p_{C^k|E}$),
- $R(m, n)$: given that the first symbol in an n -symbol sequence is in error, the conditional probability for the occurrence of $(m - 1)$ errors in the remaining $(n - 1)$ symbols,
- $p(n, m)$: probability for the occurrence of m errors in an n -symbol sequence.

The initial condition is defined as

$$G(0) = 1, \tag{3.17}$$

$$R(1, 1) = 1. \tag{3.18}$$

By definition,

$$G(k) = p_{C|E} p_{C|C}^{k-1} \quad k = 1, 2, \dots \quad (3.19)$$

The recursive expression for $R(m, n)$ is

$$R(1, n) = p_{C^{n-1}|E} = G(n-1) \quad n \geq 1 \quad (3.20)$$

$$R(m, n) = p_{E|E} R(m-1, n-1) + p_{E|C} \sum_{i=2}^{n-m+1} G(i-1) R(m-1, n-i), \quad 2 \leq m \leq n. \quad (3.21)$$

When $m = n$, $R(m, n)$ is simplified as

$$R(n, n) = p_{E|E}^{n-1}. \quad (3.22)$$

The probability of m errors in an n -symbol sequence is given by

$$p(n, m) = p_E \sum_{i=1}^{n-m+1} G(i-1) R(m, n-i+1). \quad (3.23)$$

Therefore, for a t -error correcting capability RS codes, the packet error probability is

$$P_{pck} = \sum_{i=t+1}^N p(N, i) \quad (3.24)$$

3.4 Performance of Packet Error Probability over the AWGN channel

We can make the error events of the bits to be independent if the coded bits were interleaved before the modulation. With bit interleaving, the error events are independent and the symbol error probability is given in (3.1). Therefore, the error probability of a $RS(N, K)$ code capable of correcting t errors is

$$P_{pck} = \sum_{i=t+1}^N \binom{N}{i} p_E^i (1 - p_E)^{N-i}. \quad (3.25)$$

The packet error performance for the $RS(15,11)$ codes with and without interleave is shown in Fig. 3.3. At packet error rate of 10^{-3} , the use of bit interleaver has a gain of 0.5 dB compared to one that does not use an interleaver. As the packet error decreases, the gain in dB with the use of bit interleaver increases.

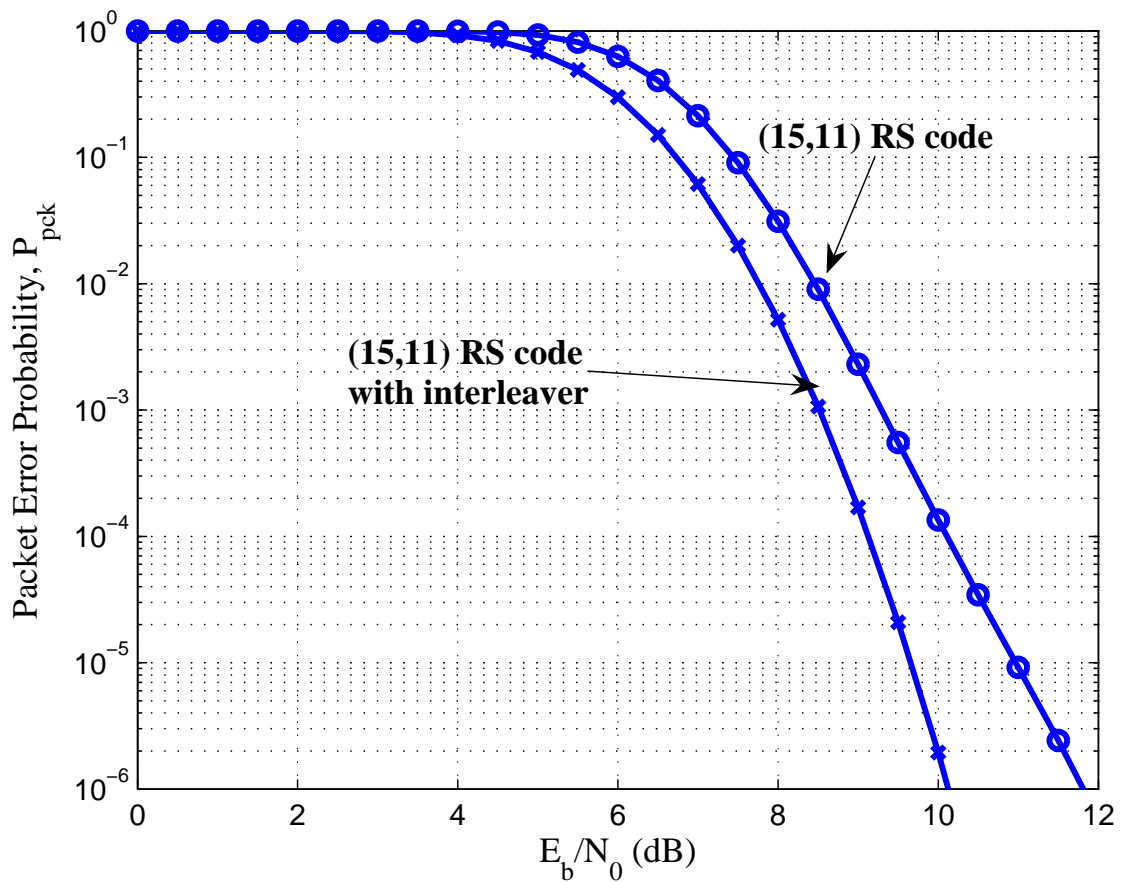


Figure 3.3: Packet Error Probability of RS(15,11) codes with and without interleaver using DPSK over an AWGN channel.

3.5 Analysis of Symbol Error Probability over a Rayleigh Fading Channel

The probability of error for the j th decision conditioned a particular fading level and on a particular phase error in the j th bit for binary DPSK is

$$p_{e_j|\phi,r} = Q\left(\sqrt{\frac{2E_c}{N_0}}R \cos \phi\right). \quad (3.26)$$

The pdf of ϕ is given in (3.2). From Section 2.6, the pdf for the random variable R is

$$P_R(r) = \begin{cases} 0, & r < 0, \\ \frac{r}{\Omega^2} e^{-\frac{r^2}{2\Omega^2}}, & r \geq 0 \end{cases}$$

and $E(R^2) = \Omega^2$. Therefore, from the above equations, we can evaluate the probability of error for the j th decision conditioned on a particular phase error in the j th bit for

binary DPSK, $p_{e|\phi}$, over the Rayleigh fading channel as

$$\begin{aligned}
p_{e_j|\phi} &= \int_{r=0}^{\infty} p_R(r) Q\left(\sqrt{\frac{2E_c}{N_0}} r \cos \phi\right) dr \\
&= \int_{r=0}^{\infty} \frac{r}{\Omega^2} e^{-\frac{r^2}{2\Omega^2}} Q\left(\sqrt{\frac{2r^2 E_c \cos^2 \phi}{N_0}}\right) dr \\
&= \int_{r=0}^{\infty} \frac{r}{\Omega^2} \frac{1}{\sqrt{2\pi}} \int_{u=\sqrt{\frac{2r^2 E_c \cos^2 \phi}{N_0}}}^{\infty} e^{-\frac{r^2}{2\Omega^2}} e^{-u^2/2} du dr \\
&= \int_{u=0}^{\infty} \frac{e^{-u^2/2}}{\sqrt{2\pi}} \int_{r=0}^{u/\sqrt{\frac{2E_c \cos^2 \phi}{N_0}}} \frac{r}{\Omega^2} e^{-\frac{r^2}{2\Omega^2}} du dr \\
&= \int_{u=0}^{\infty} \frac{\exp\left(-\frac{u^2}{2}\right)}{\sqrt{2\pi}} \int_{r=0}^{u/\sqrt{\frac{2E_c \cos^2 \phi}{N_0}}} \frac{r}{\Omega^2} \exp\left(-\frac{r^2}{2\Omega^2}\right) dr du \\
&= \int_{u=0}^{\infty} \frac{\exp\left(-\frac{u^2}{2}\right)}{\sqrt{2\pi}} \left[1 - \exp\left(-\frac{u^2}{\frac{4\Omega^2 E_c \cos^2 \phi}{N_0}}\right)\right] du \\
&= \frac{1}{2} - \int_{u=0}^{\infty} \frac{1}{\sqrt{2\pi}} \exp\left[-\frac{u^2}{2}\left(1 + \frac{1}{\frac{2\Omega^2 E_c \cos^2 \phi}{N_0}}\right)\right] du \\
&= \frac{1}{2} - \gamma \int_{u=0}^{\infty} \frac{1}{\gamma\sqrt{2\pi}} \exp\left[-\frac{u^2}{2\gamma^2}\right] du, \quad \gamma = \sqrt{\frac{\frac{2\Omega^2 E_c \cos^2 \phi}{N_0}}{1 + \frac{2\Omega^2 E_c \cos^2 \phi}{N_0}}} \\
&= \frac{1}{2} - \frac{1}{2} \sqrt{\frac{\frac{2\Omega^2 E_c \cos^2 \phi}{N_0}}{1 + \frac{2\Omega^2 E_c \cos^2 \phi}{N_0}}} \\
&= \frac{1}{2} - \frac{1}{2} \sqrt{\frac{\frac{\bar{E}_c}{N_0} \cos^2 \phi}{1 + \frac{\bar{E}_c}{N_0} \cos^2 \phi}} \tag{3.27}
\end{aligned}$$

where $\frac{\bar{E}_c}{N_0} = \frac{2\Omega^2 E_c}{N_0}$. Therefore, from (3.2) and (3.27), the bit error probability of DPSK over a Rayleigh fading channel is

$$\begin{aligned}
p_{e_j} &= \int_{-\pi}^{\pi} p_{e_j|\phi} f(\phi) d\phi \\
&= \int_{-\pi}^{\pi} \left(\frac{1}{2} - \frac{1}{2} \sqrt{\frac{\frac{\bar{E}_c}{N_0} \cos^2 \phi}{1 + \frac{\bar{E}_c}{N_0} \cos^2 \phi}}\right) f(\phi) d\phi. \tag{3.28}
\end{aligned}$$

In [10], the classical result for bit error probability for DPSK over a Rayleigh channel is given as

$$p_{e_j} = \frac{1}{2\left(1 + \frac{\bar{E}_c}{N_0}\right)}. \tag{3.29}$$

To verify that our derivation is correct, we plot the bit error probability for DPSK over a Rayleigh channel using (3.28) and (3.29) in Fig. 3.4. It is obvious that our derivation is correct as the numerical result matches perfectly with (3.29).

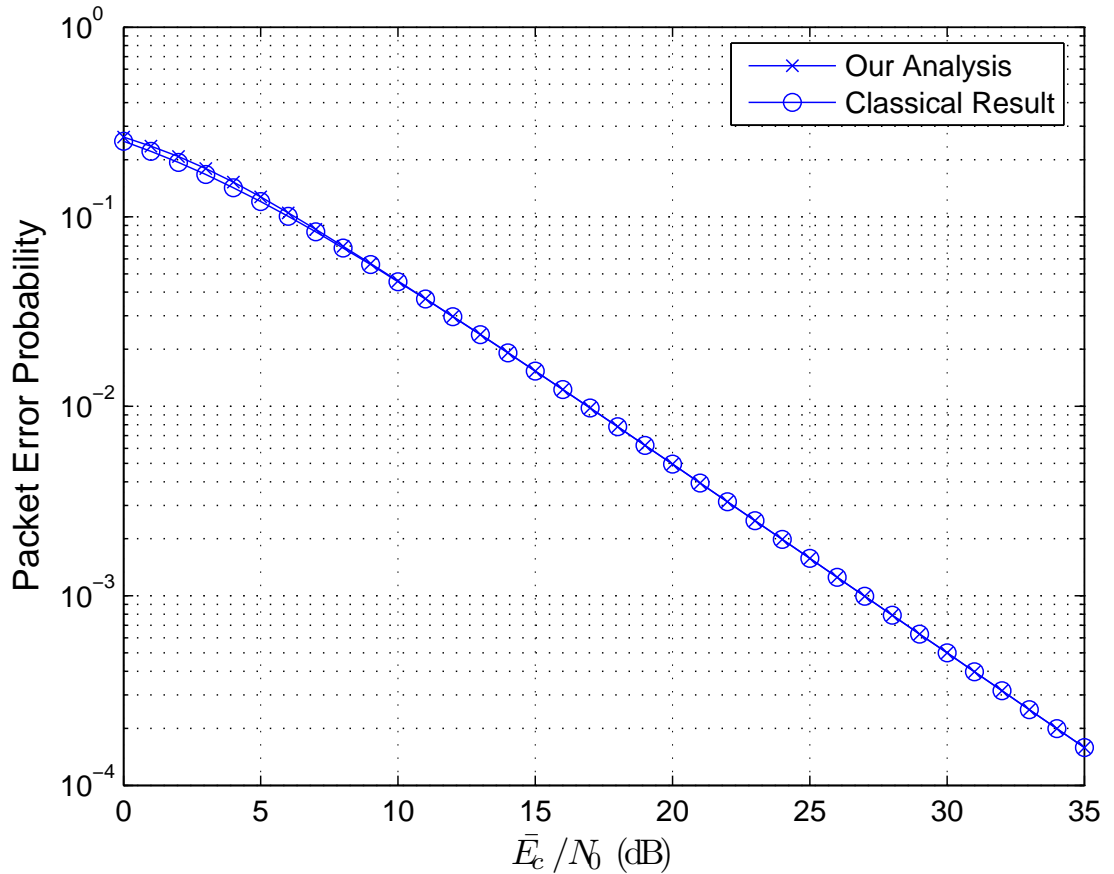


Figure 3.4: Comparison of bit error probability using (3.2) and (3.27).

We use (3.6), (3.7), (3.8), (3.9), (3.10) and (3.11) with (3.28) to compute the m -bit symbol error probability for DPSK over the Rayleigh channel. The results are shown in Fig. 3.5 for $m = 4, 5, 6, 7$ and 8. From the figure, the energy required for a fixed packet error probability increases with m .

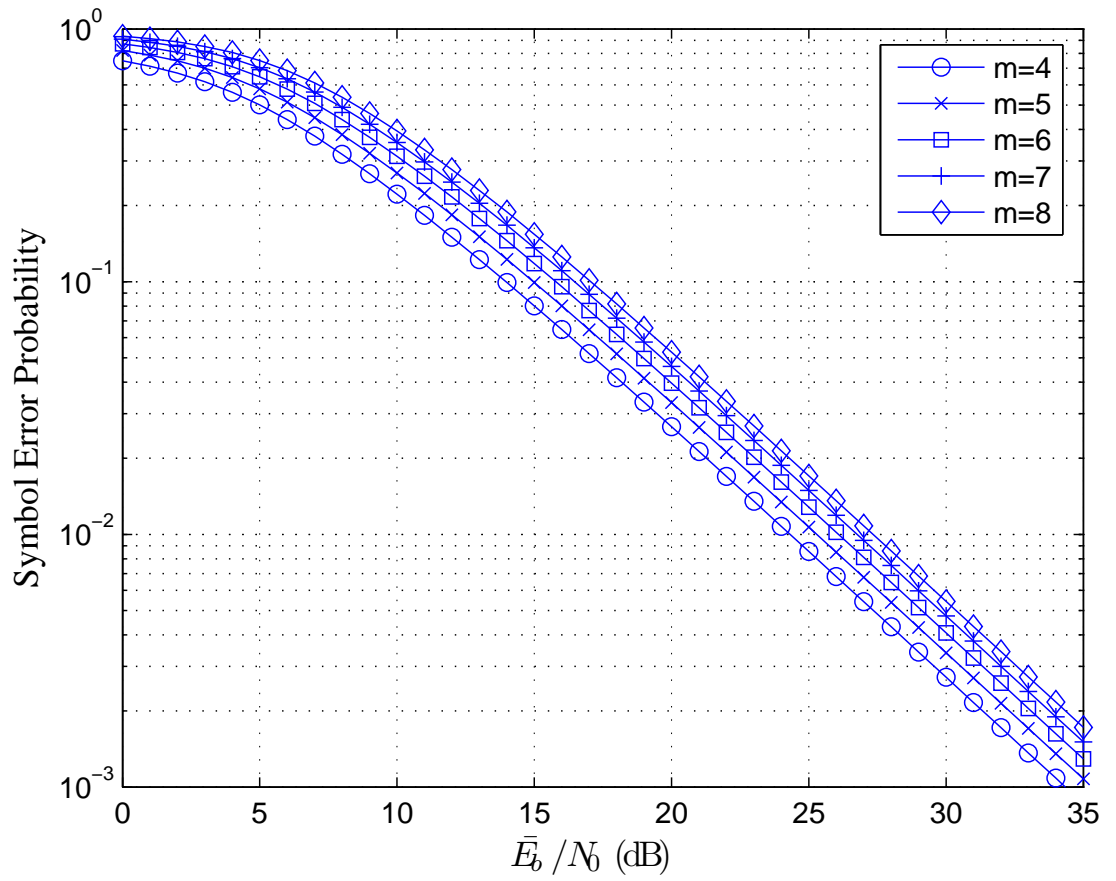


Figure 3.5: Symbol error probability for various values of m using DPSK modulation over a Rayleigh fading channel .

3.6 Performance of RS Codes with DPSK over a Rayleigh Faded Channel

We compared the packet error probability of an (N, K) RS codes using DPSK modulation over the Rayleigh fading channel with and without interleaver in Fig. 3.6 for $N = 16, 32, 64, 128$. We observe that there is no performance difference between RS codes with and without interleaver. Therefore, the use of interleaver does not result in any coding gain for these codes.

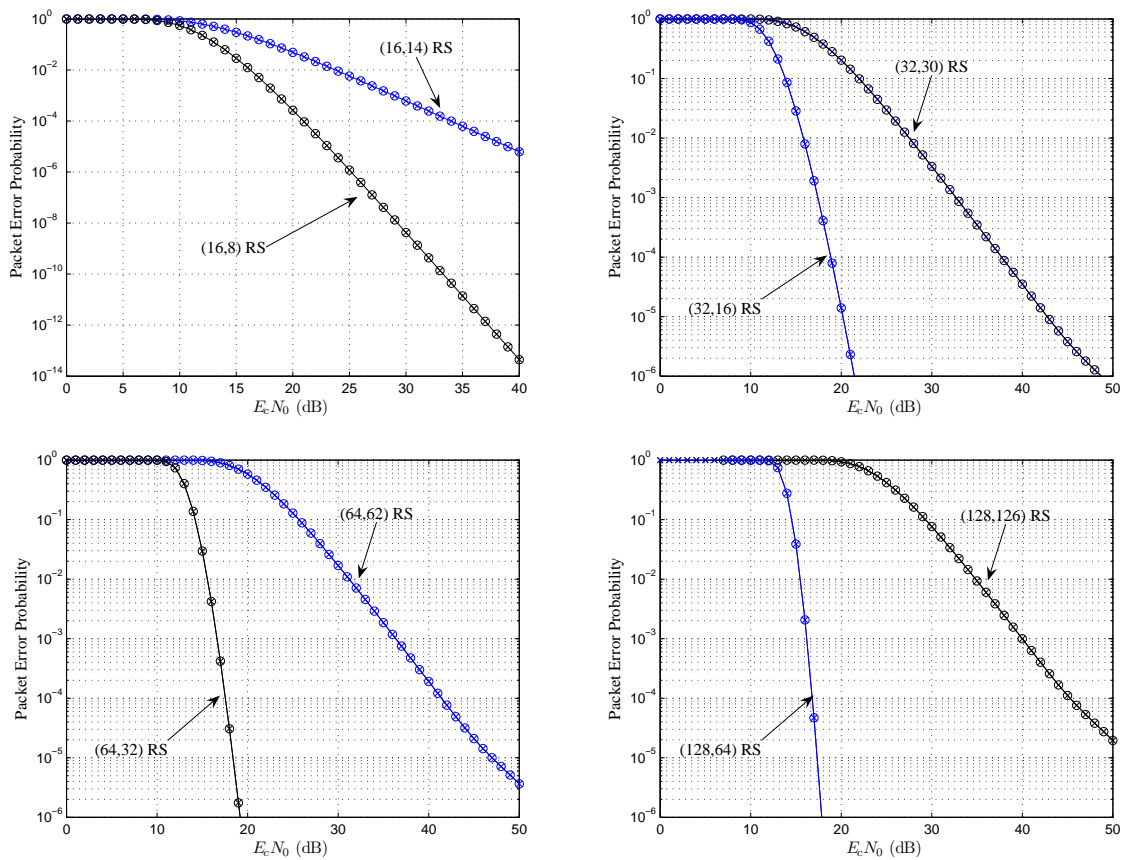


Figure 3.6: Packet Error Probability various RS codes with (denoted by x) and without (denoted by o) interleaver using DPSK over a Rayleigh fading channel.

3.7 Conclusion

In this section, we described the method to analyze the symbol error probability of an RS codes with DPSK modulation, taking into account of the correlation between the coded bits. In addition, we outlined the methodology to derive the packet error performance over an AWGN channel. The use of a bit interleaver breaks the dependency between the coded bits. We shown that by interleaving, we can achieve a coding gain over an AWGN channel.

We derived and analyzed the symbol error probability of a RS symbol over a Rayleigh fading channel. In addition, the packet error probability was also studied. We demonstrate that the bit interleaver would not result in coding gain for packet error probability over the Rayleigh fading channel.

CHAPTER 4

Energy Analysis of Single Hop Communication System For Short Packet Length Data

Cellular networks, WiFi and many communications systems use single-hop networks. Some of the advantages of a single hop networks compared to multi-hop networks are as follows:

- no need to design routing algorithms implying a simple protocol stack and no overhead for routing information
- low delay
- simpler time synchronization
- possibility to use centralized media access control (MAC) schemes (like pooling).

Most of the computing and communication devices in a single hop network are usually battery-powered. Therefore, improving the energy efficiency can extend the operating time of these devices. In [38]- [41] work has been done on minimizing the energy consumption of the processing units. In traditional communications systems, coding is almost always beneficial in reducing the required transmission energy when the transmission range is long. However, in application like wireless sensor networks where the range is short, the energy spent for decoding may actually exceed that saved due to the coding gain. This is because error control coding add parity bits to protect the information bits. For low rate code, the number of parity bits maybe greater

than the number of information bits. The parity bits result in a longer packets to be transmitted. Therefore, the duration of a packet is longer as compared to an uncoded packet. Hence, the receiver is on for a longer period of time. If there is a fixed power consumption when the receiver is on then the energy consumed at the receiver varies inversely with the code rate. In this environment, interesting tradeoffs can be identified. Zorzi [21] consider the design of error control schemes in wireless sensor networks. He investigated the total energy consumption in both single and multi-hop systems using hard-decision binary linear block codes and convolutional codes.

In this chapter, we describe the model of the communication system which we analyze. We investigate the channel coding aspect of energy efficiency of the system. We analyze the energy consumption over an AWGN channel by examining the “practical limits” [42] of coding using the cutoff rate. The cutoff rate is the rate above which the number of steps per decoded digit becomes very high with sequential decoding [43]. In addition, we consider the case when RS codes are used over the AWGN channel.

In Section 4.1, we present the model for the energy consumption analysis. We consider an AWGN channel and analyze the total energy consumed using the cutoff rate. The optimum code rate is used to investigate the system’s throughput. In Section 4.2, we use the capacity theorem to analyze the total energy consumption. The results obtained are compared with the results obtained using the cutoff rate. In Section 4.3 we consider the case of a Rayleigh fading channel. The energy-code rate relation is investigated via the cutoff rate for noncoherent detection. In Section 4.4, we study the energy consumption using RS codes over an AWGN channel. We also compare the performance of convolutional codes over an AWGN and a Rayleigh fading channel with the cutoff rate. We give our conclusions in Section 4.5.

4.1 System Description

In our model, we considered a packet of K information symbols. The information bits pass through a channel encoder. The channel encoder introduces controlled redundancy (parity bits) into the information bits in such a manner that errors caused

by the channel would be corrected. At the output of the channel encoder, we have N coded symbols. That is, the channel encoder introduces $N - K$ parity symbols to the information bits. Therefore, the code rate, R , of this packet is $\frac{K}{N}$. Next, each coded bit is modulated using phase shift keying (PSK) or frequency shift keying (FSK). Prior to transmission, the signals pass through an amplifier. We assumed that the efficiency of the amplifier is η . That is, energy $\frac{E}{\eta}$ is consumed in order to radiate energy E for transmission of each coded bit. The receiver is located at a distance d from the transmitter. It has a thermal noise N_0 . In addition, we assume the receiver uses power P_{pr} while actively receiving and processing the signal.

With the above system model, we can compute the energy required at the transmitter and the energy required at the receiver. In analyzing the transmitter's energy per bit (E_t) of the system. We take into account of the attenuation, $f(d)$, of the transmitted signal. That is, The received signal power depends on the distance d between the transmitter and receiver. For example, one model for attenuation is, for sufficiently large d , $f(d) = \zeta/d^4$, where ζ is a constant related to the square of the product of height of the transmitting and receiving antenna [44]. We define $\frac{E_b}{N_0}_{req}$ as the required received energy per bit-to-noise power density for a given codeword error probability P_E . Based on the required received signal-to-noise ratio, the attenuation, and the power efficiency the energy consumed at the receiver can be determined as

$$E_t = \frac{N_0}{\eta f(d)} \left(\frac{E_b}{N_0} \right)_{req} \quad (4.1)$$

Now we compute the energy required per bit E_r at the receiver. In some communication systems most of the energy is consumed by the receiver's radio frequency (RF) front end. The RF front end is the part of the receiver that amplifies the signal, mixes the signal to an appropriate frequency and converts to digital samples. In our model, we ignore the energy consumed by the DSP processor and assume the front end dominates the energy consumed. Therefore, our receiver does not take into account the complexity of channel decoding. The energy consumed depends only on the duration that the front end is turned on. We assumed that the system uses a transmission rate

μ bits/second. For a transmission rate μ , the energy consumed per information bit by the receiver (E_r) with processing power P_{pr} is

$$E_r = \frac{NP_{pr}}{K\mu} \quad (4.2)$$

. Note that for binary information bits, we denote the information packet length as k bits and the transmitted packet length to be n bits. Hence, $R = K/N = k/n$. Therefore, the total energy required (E_{tot}) is

$$\begin{aligned} E_{tot} &= E_t + E_r \\ &= \frac{N_0}{\eta f(d)} \left(\frac{E_b}{N_0}\right)_{req} + \frac{NP_{pr}}{K\mu} \end{aligned} \quad (4.3)$$

We normalize the total energy as follows

$$E_T = \eta f(d) E_{tot} \quad (4.4)$$

to isolate the term $\left(\frac{E_b}{N_0}\right)_{req}$ for the ease of analysis. Hence, the normalized total signal-to-noise ratio is given by

$$\frac{E_T}{N_0} = \left(\frac{E_b}{N_0}\right)_{req} + \frac{\gamma}{R} \quad (4.5)$$

where $\gamma = \frac{\eta f(d) P_{pr}}{\mu N_0}$. We can view γ as processing energy to noise ratio as seen at the transmitter end. This single parameter allows engineer at the transmitter end to select an appropriate channel encoder for a required energy consumption.

In our investigations, we study two different channels. The first one we consider is an additive white Gaussian noise (AWGN) channel with power spectral density $\frac{N_0}{2}$ and the second one is the Rayleigh fading channel. The analysis on the AWGN channel is presented in next section.

4.2 Analysis of Total Energy Consumption Over an AWGN Channel Using Cutoff Rate

In this section, we analyze the total energy consumption over an AWGN channel using the cutoff rate and random coding bound. We first derive the expression for

the total energy consumed and follow by an example using a fixed information packet length. Next, we derive a closed form expression for the optimum code rate when the code rate is very low. A Taylor's series approximation is used when the code rate is not too low. After that, we investigate the optimum code rate for large packet length. Next, we study the variation of optimum code rate with packet error probability. We conclude this subsection with the throughput of the system using the optimum code rate.

4.2.1 Derivation of Total Energy Consumed

The channel cutoff rate, R_0 , provides a useful tool in assessing the performance/complexity tradeoffs associated with the design and implementation of modulation/coding systems. It gives a tradeoff between error probability, signal-to-noise ratio and code rate that is easily trackable as compared to Gallager error exponent [45]. For binary antipodal signalling over an AWGN channel, the cutoff rate assuming maximum likelihood decoding is known to be given by [10]

$$R_0 = 1 - \log_2 \left(1 + \exp\left(-\frac{E_c}{N_0}\right) \right) \quad (4.6)$$

where E_c is the energy per coded bit, $\frac{N_0}{2}$ is the two-sided noise power spectral density. If a code of rate R information bits/channel bit is used, then the energy per information bit is $E_b = \frac{E_c}{R}$. The random coding bound guarantees existence of codes of length N and rate R with average codeword error probability bounded by

$$P_e \leq 2^{-N(R_0-R)}. \quad (4.7)$$

We consider a code that has error probability exactly the upper bound described in (4.7). Then from (4.6) we have

$$\left(\frac{E_b}{N_0}\right)_{\text{req}} = -\frac{1}{R} \ln \left(2^{1-R+\frac{1}{N} \log_2 P_e} - 1 \right). \quad (4.8)$$

Therefore, from (4.1), the total normalized energy required (E_{tot}) is

$$\frac{E_T}{N_0} = -\frac{1}{R} \ln (2^\delta - 1) + \frac{\gamma}{R} \quad (4.9)$$

where $\delta = 1 - (R - \frac{R}{K} \log_2 P_e)$.

4.2.2 Performance for a Fixed Information Packet Length

The variation of $\frac{E_T}{N_0}$ with R and γ is shown in Fig. 4.1 below with information word length, $K = k = 24$ bits and codeword error probability, $P_e = 0.01$. We observe

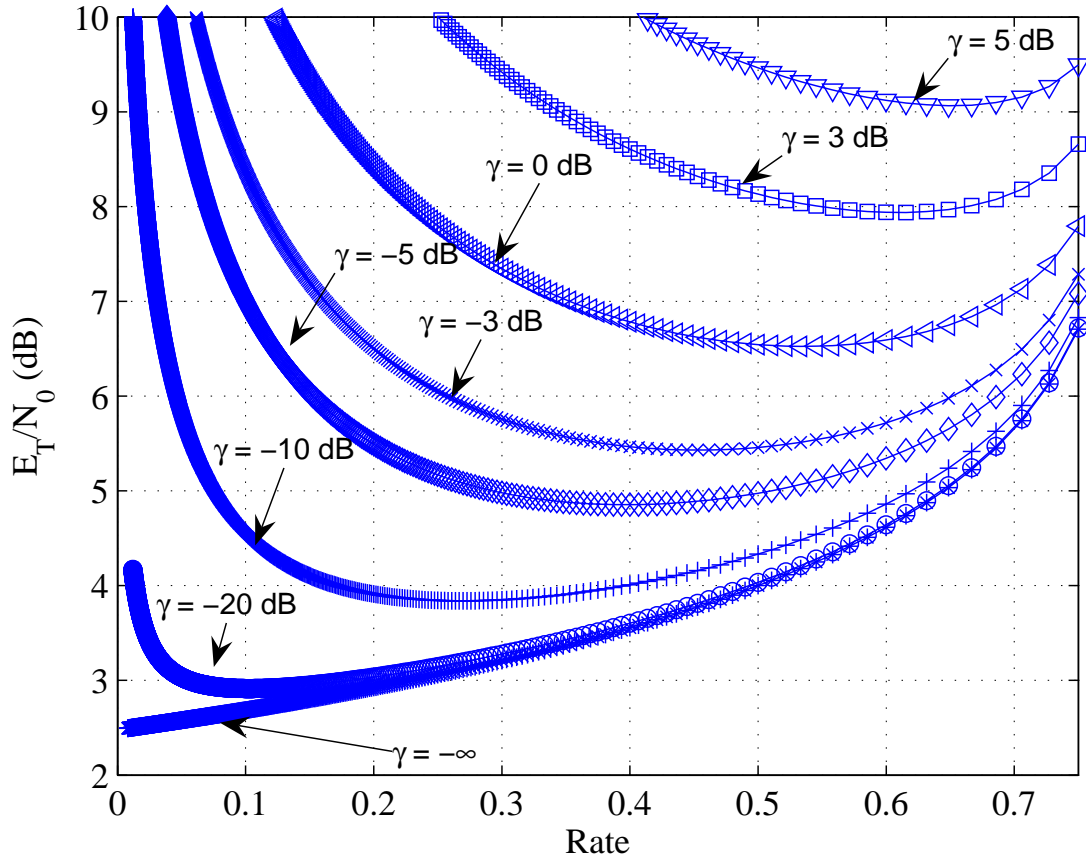


Figure 4.1: Variation of $\frac{E_T}{N_0}$ with R with various values of γ .

that for every γ , there exists a code rate R that achieves a minimum total energy consumed. This is because as the code rate decreases the error correction capability of the code increases at the expense of bandwidth efficiency. Thus, it reduces the required transmitted energy per transmitted bit to achieve the required bit error probability. However, as the code rate decreases, the receiver needs to process more coded bits and this increases the amount of processing energy required. As a result, more energy is consumed at the receiver. Hence, there is an optimal code rate that minimizes the

energy required per information bit. The variation of minimum energy required with

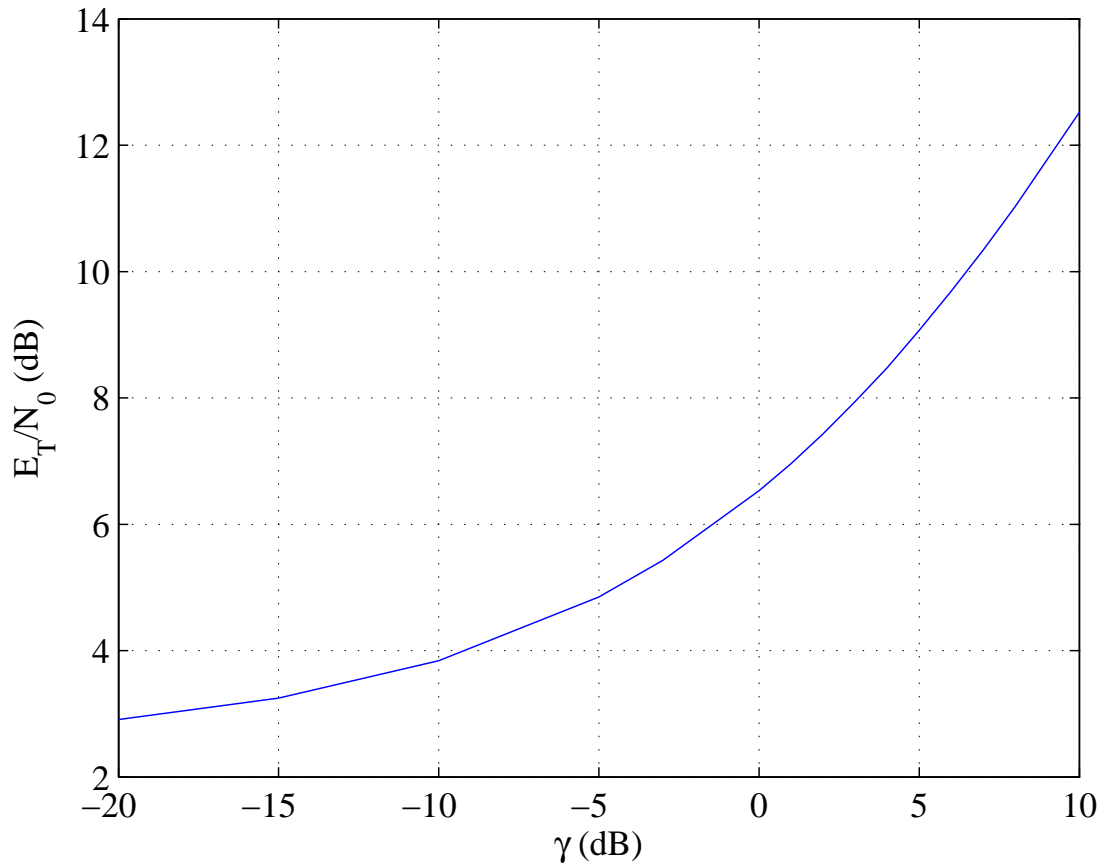


Figure 4.2: Variation of $\frac{E_T}{N_0}$ with γ when optimum R is used.

respect to γ is shown in Fig. 4.2. We note that when $\gamma > 0$ dB, the minimum energy varies approximately linear with γ . This is because from (4.8), we have

$$\left(\frac{E_b}{N_0}\right)_{\text{req}} = -\frac{1}{R} \ln \left(2^{1-R+\frac{1}{N} \log_2 P_e} - 1\right).$$

Hence, for finite $\left(\frac{E_b}{N_0}\right)_{req}$ and nonzero code rate R , the code rate R is upper bound as follows

$$\begin{aligned}
-\frac{1}{R} \ln \left(2^{1-R+\frac{1}{N} \log_2 P_e} - 1 \right) &> 0 \\
\ln \left(2^{1-R+\frac{1}{N} \log_2 P_e} - 1 \right) &< 0 \\
2^{1-R+\frac{1}{N} \log_2 P_e} &> 1 \\
1 - R \left(1 - \frac{\log_2 P_e}{K} \right) &> 0 \\
R &< \frac{1}{1 - \frac{\log_2 P_e}{K}}.
\end{aligned} \tag{4.10}$$

Therefore for a finite number of information bits and for packet error probability P_e the code rate must satisfy $R < R_M = \frac{1}{1 - \frac{\log_2 P_e}{K}}$.

From (4.9), when $\gamma \gg \left(\frac{E_b}{N_0}\right)_{req}$, we want R to be close to R_0 in order to minimize energy consumption. However, since $R < R_M$, when $\gamma \gg$ than $\left(\frac{E_b}{N_0}\right)_{req}$, the code rate required to achieve minimum energy consumption is R_M . This results in a linear expression of minimum energy required with respect to γ and is given below as

$$\left(\frac{E_T}{N_0}\right)_{min} \approx -\frac{\beta}{R_M} + \frac{\gamma}{R_M} \tag{4.11}$$

where the constant $\beta = \ln(2^\delta - 1)$.

4.2.3 Derivation of Optimum Code Rate

To find the required code rate R for minimum energy consumed, we differentiate (4.9) with respect to R and equate it to 0. We obtain the following condition for R :

$$0 = -\frac{\gamma}{R^2} + \frac{\ln(2^\delta - 1)}{R^2} + \frac{\alpha 2^\delta \ln 2}{R(2^\delta - 1)} \tag{4.12}$$

where $\alpha = 1 - \frac{1}{K} \log_2 P_e$. Simplifying (4.12), we have

$$(\alpha \ln 2)R - (1 - 2^{-\delta})\gamma + (1 - 2^{-\delta}) \ln(2^\delta - 1) = 0. \tag{4.13}$$

When $\gamma \ll \frac{E_b}{N_{0req}}$, we can use Taylor's series to express $(1 - 2^{-\delta})$ and $\ln(2^\delta - 1)$ as follow

$$\begin{aligned} (1 - 2^{-\delta}) &= 1 - 2^{-1+\alpha R} \\ &= 1 - \frac{1}{2}(1 + \alpha R \ln 2 + \frac{1}{2}(\alpha R \ln 2)^2 + \dots) \end{aligned} \quad (4.14)$$

$$\begin{aligned} \ln(2^\delta - 1) &= \ln(2^{1-\alpha R} - 1) \\ &= \ln(1 - 2R\alpha \ln 2 + (R\alpha \ln 2)^2 + \dots) \\ &= -2R\alpha \ln 2 + (R\alpha \ln 2)^2 \\ &\quad - \frac{1}{2}[2R\alpha \ln 2 - (R\alpha \ln 2)^2]^2 + \dots \end{aligned} \quad (4.15)$$

For the case when R is small, we can ignore the third order and above terms for R to obtain an approximation. Substituting (4.14) and (4.15) into (4.13), we have:

$$(\alpha \ln 2R)^2(1 + \frac{\gamma}{2}) + (\gamma\alpha \ln 2)R - \gamma \approx 0 \quad (4.16)$$

Therefore, we obtain an approximate closed form expression for R below

$$R \approx \frac{-\gamma + \sqrt{3\gamma^2 + 4\gamma}}{(\alpha \ln 2)(\gamma + 2)}. \quad (4.17)$$

From (4.17), when $\gamma = 0$, the approximate optimum code rate is 0. This agrees with the case when we do not consider the processing energy factor. Taking the limit as R approaches 0 in (4.17), we have

$$\begin{aligned} \lim_{R \rightarrow 0} \frac{E_T}{N_0} &= \lim_{R \rightarrow 0} -\frac{1}{R} \ln(2^\delta - 1) \\ &= \lim_{R \rightarrow 0} \frac{(2\alpha \ln 2)2^{-\alpha R}}{2^{1-\alpha R} - 1} \\ &= 2\alpha \ln 2. \end{aligned} \quad (4.18)$$

With information word length, $k = 24$ and codeword error probability, $P_e = 0.01$, from (4.10) we have $R_M = 0.783$. When $R = 0$, $\frac{E_T}{N_0} = 1.77$ dB. Table 1 shows the approximate optimum required R for minimum energy consumption, with respect to γ values and Fig. 4.3, 4.4 compares the actual and approximate energy consumed with respect to γ and code rate respectively.

From the table and figures, we observe that the approximation is very close to the exact value when γ or the code rate is small. However, when γ is greater than 0

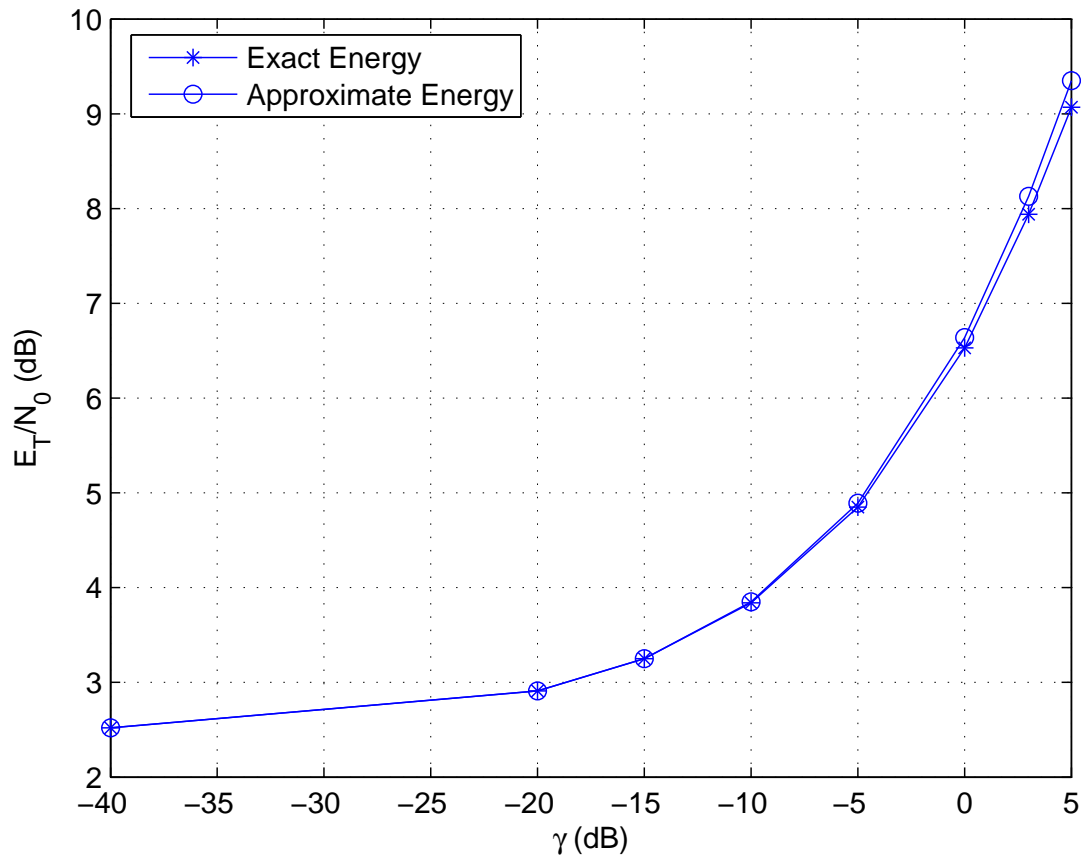


Figure 4.3: Comparison of actual and approximate energy consumed with respect to γ .

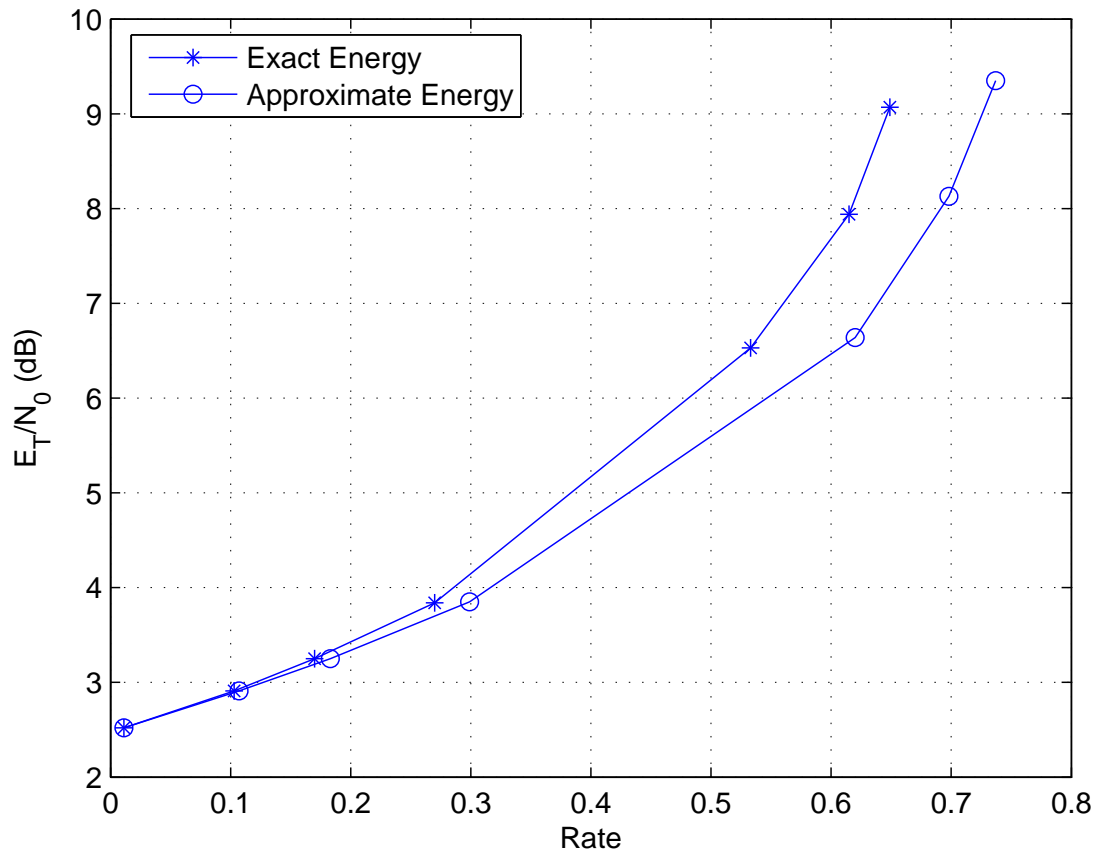


Figure 4.4: Comparison of actual and approximate energy consumed with respect to code rate.

γ (dB)	R_a	$(\frac{E_T}{N_0})_a$ (dB)	R	$\frac{E_T}{N_0}$ (dB)
$-\infty$	0	1.77	0	1.77
-40	0.0112	2.52	0.0112	2.52
-20	0.107	2.91	0.103	2.91
-15	0.183	3.25	0.170	3.25
-10	0.299	3.85	0.270	3.84
-5	0.456	4.89	0.400	4.85
0	0.620	6.64	0.533	6.53
3	0.698	8.13	0.615	7.94
5	0.737	9.35	0.649	9.07
10	0.795	-	0.73	12.5

Table 4.1: Approximate and exact value of required minimum energy and its respective rate.

dB or when code rate is greater than 0.3, the approximation begins to deteriorate. At $\gamma = 10$ dB, the approximate R exceeds the maximum allowable rate and at rate 0.6, the inaccuracy is about 1.5 dB. Therefore, we need a separate expression for the optimum rate when $\gamma > 0$.

The variation of R with respect to γ at when E_T/N_0 is minimum is shown in Fig. 4.5. The rate of change of R with respect to γ is quite large when γ is between -20 dB to 5 dB Hence, this explains the deterioration of the approximation of R about 0 when γ is high. When γ is large, we can derive an approximate linear function of R with respect to γ . Using linear least square approach, we have the following function for R

(4.19)

$$R(\gamma) = \begin{cases} 0.02271\gamma + 0.528 & 0.01 < \gamma < \frac{R_M - 0.528}{0.02271} \\ R_M & \gamma > \frac{\gamma - 0.528}{0.02271} \end{cases}$$

To get a better approximation, we use Taylor's series expansion about $R(\gamma)$ when $\gamma < -20$ dB. The approximate optimum rate and the corresponding energy consumed is shown in Table 2. This approximation agrees perfectly with the actual value for the

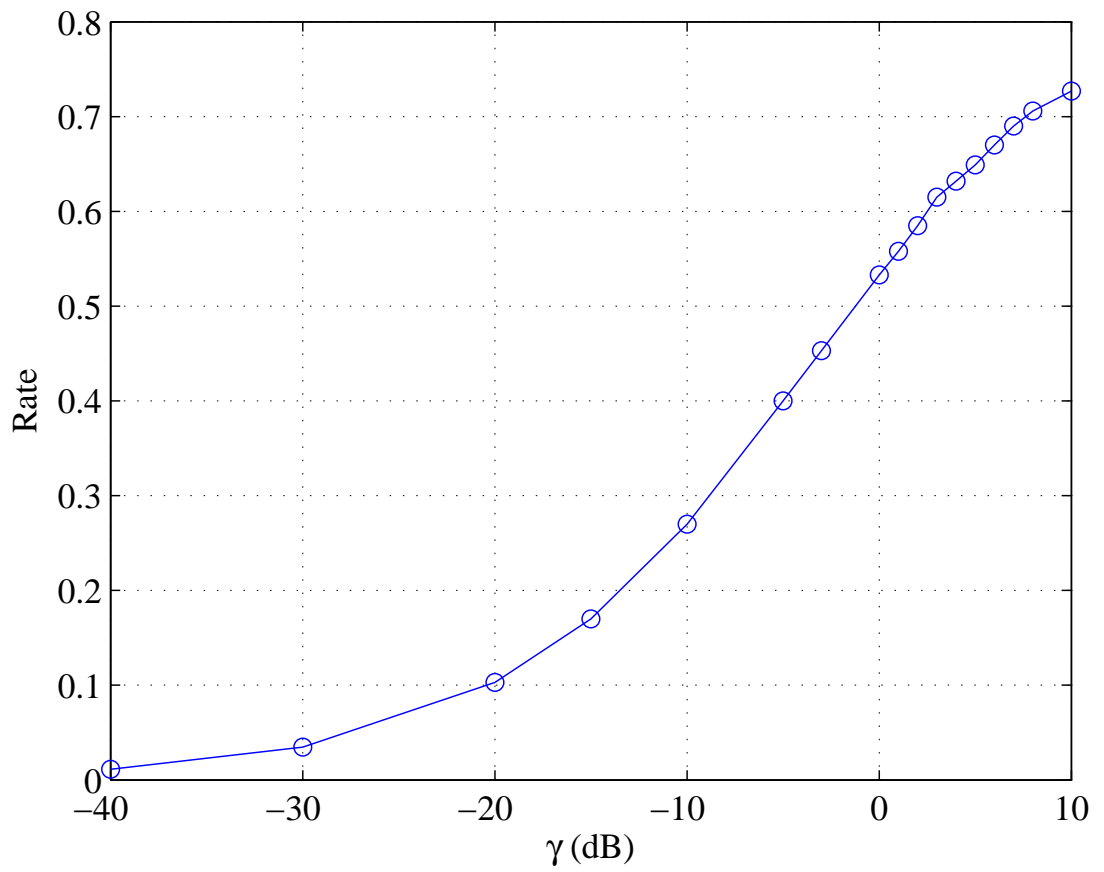


Figure 4.5: Variation of R with respect to γ at the required minimum energy.

γ (dB)	R_a	$(\frac{E_T}{N_0})_a$ (dB)	R	$\frac{E_T}{N_0}$ (dB)
-15	0.180	3.25	0.170	3.25
-10	0.276	3.84	0.270	3.84
-5	0.426	4.86	0.400	4.85
0	0.594	6.58	0.533	6.53
3	0.665	8.00	0.615	7.94
5	0.697	9.12	0.649	9.07
10	0.721	12.5	0.73	12.5

Table 4.2: Approximate and exact value of required minimum energy and its respective rate.

minimum energy required for any given γ value.

4.2.4 Optimum Code Rate for Large Information Packet

For $k = 240$ bits, the variation of $\frac{E_T}{N_0}$ with respect to R is shown in Fig. 4.6 and in Fig. 4.7, we show the required rate that achieves the minimum energy for different values of γ . We would like to understand the effect of different information packet lengths on the optimum code rate. Comparing Fig. 4.5 and Fig. 4.6 we observe that when the number of information bits increases, the optimum rate that achieve the minimum energy consumed also increases. This is because for a fixed value of γ , from (4.17), as the number of information bits k increases, α decreases and hence, the required code rate increases. Therefore, for long packet lengths, we should transmit at a high code rate in order to conserve energy. The result is shown in Fig. 4.8 for $\gamma = 0$ dB. We observe that the optimum code rate approaches asymptotically to a particular value when k approaches infinity.

The expression for optimum code rate (4.13) is reiterated below for convenience

$$(\alpha \ln 2)R - (1 - 2^{-\delta})\gamma + (1 - 2^{-\delta}) \ln(2^\delta - 1) = 0$$

where $\delta = 1 - (R - \frac{R}{K} \log_2 P_e)$. For a fixed packet error probability P_e , we take the

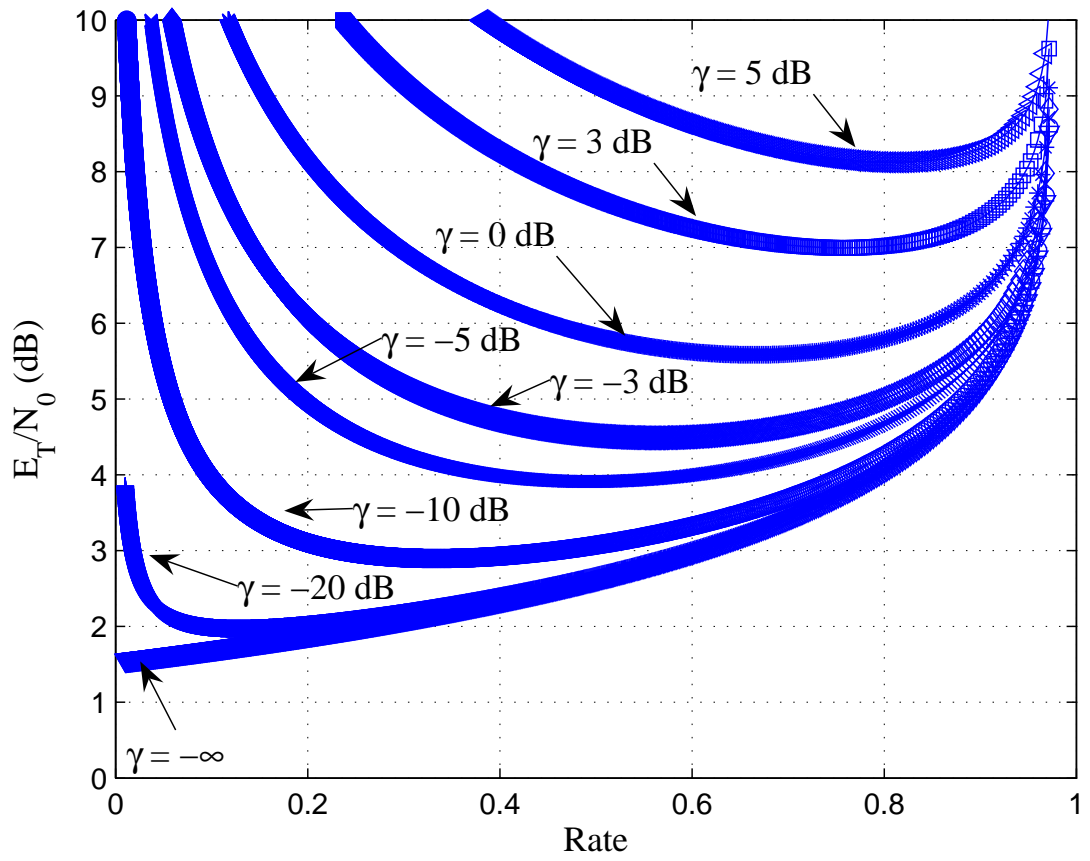


Figure 4.6: Variation of $\frac{E_T}{N_0}$ with respect to R ($k=240$).

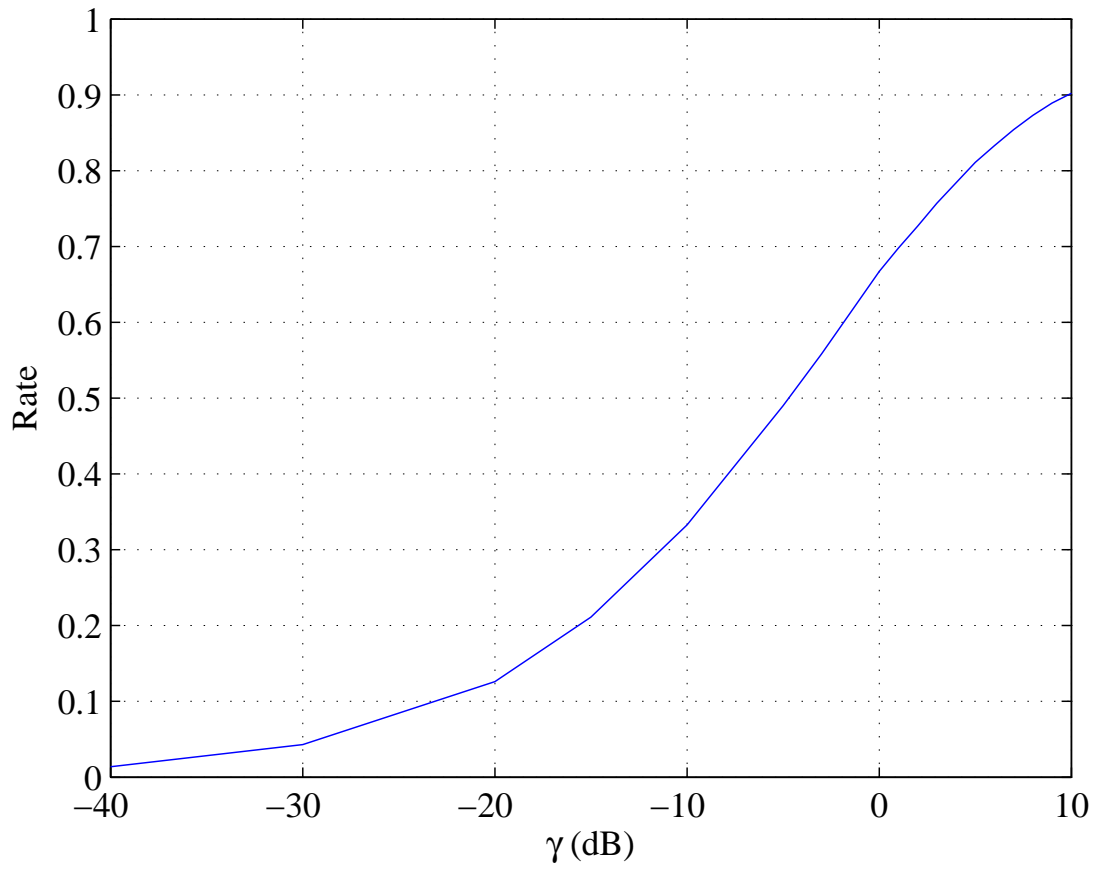


Figure 4.7: Variation of γ with respect to code rate at the required minimum energy ($k=240$).

limit as $k \rightarrow \infty$ for δ ,

$$\begin{aligned} \lim_{k \rightarrow \infty} \delta &= \lim_{k \rightarrow \infty} \left(1 - \left(R - \frac{R}{K} \log_2 P_e \right) \right) \\ &= 1 - R. \end{aligned} \quad (4.20)$$

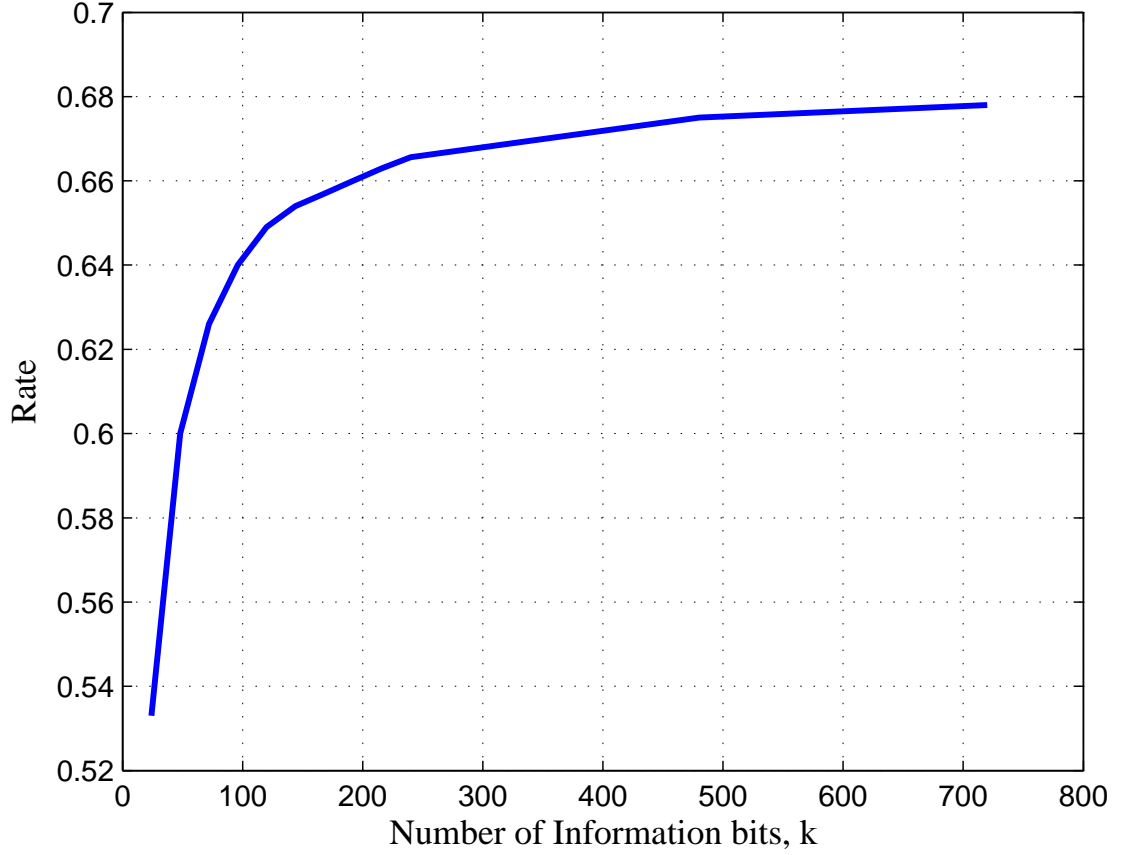


Figure 4.8: Optimum code rate with respect to number of information bits for $\gamma = 0$ dB.

Substituting (4.20) into (4.13), we have

$$R \ln 2 - (1 - 2^{R-1})\gamma + (1 - 2^{R-1}) \ln(2^{1-R} - 1) = 0 \quad (4.21)$$

Rearranging (4.20), we obtained a closed form relationship between normalized energy

γ and optimum code rate when k is infinite.

$$\gamma = \frac{R \ln 2}{1 - 2^{R-1}} + \ln(2^{1-R} - 1). \quad (4.22)$$

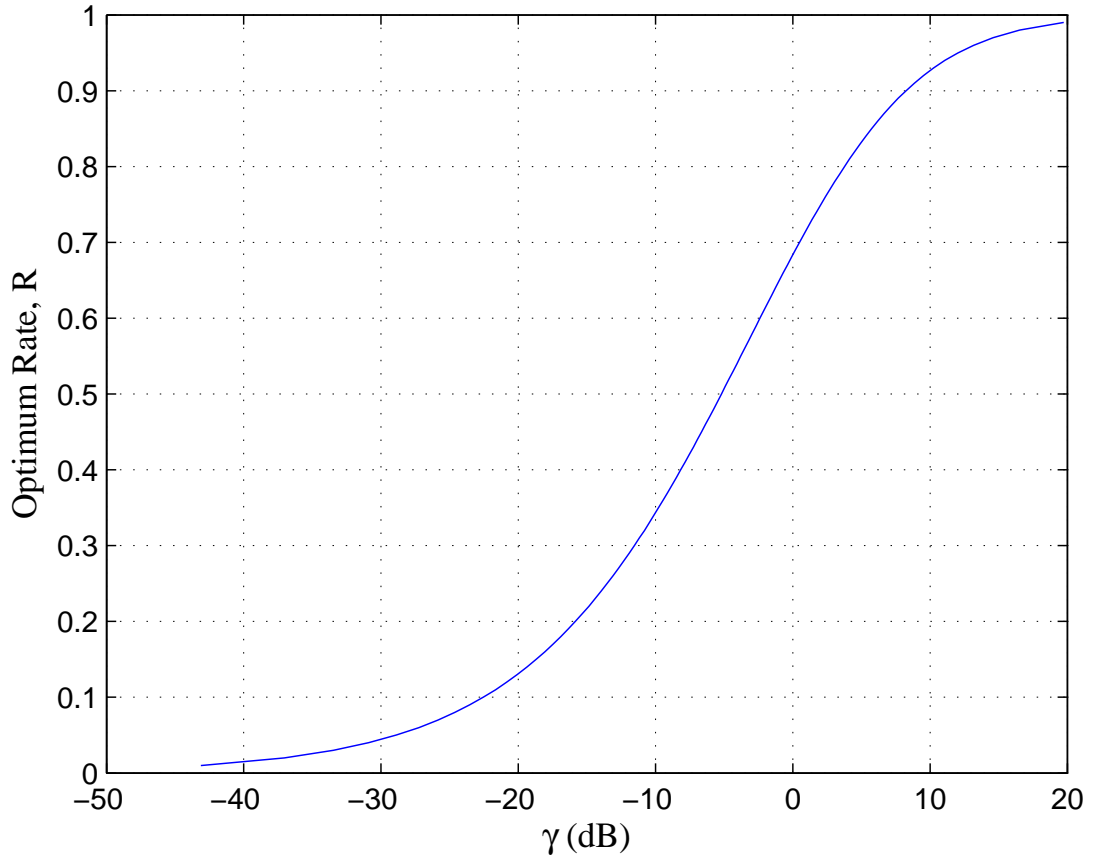


Figure 4.9: Optimum code rate for the normalized processing energy when $k \rightarrow \infty$.

The optimum code rate required for the normalized processing energy is shown in Fig. 4.9. When the contribution of the normalized processing energy is negligible ($\gamma < -30$ dB), the optimum code rate is less than 0.1. However, when the normalized processing energy is very large (> 20 dB), the optimum code rate is close to 1. This is due to the fact that the contribution of the normalized processing energy is inversely proportional to code rate. The information in Fig. 4.9 allows us to choose an optimum code rate for the channel code that can achieve minimum energy consumption over an

AWGN channel when the packet length is relatively large if we know the value of the normalized processing energy. For example, if the normalized processing energy is 0 dB, then the optimum cutoff rate is 0.68 and from Fig. 4.8 when $k > 600$ bits, the optimum code rate is close to 0.68.

4.2.5 Variation of Optimum Code Rate With Packet Error Probability

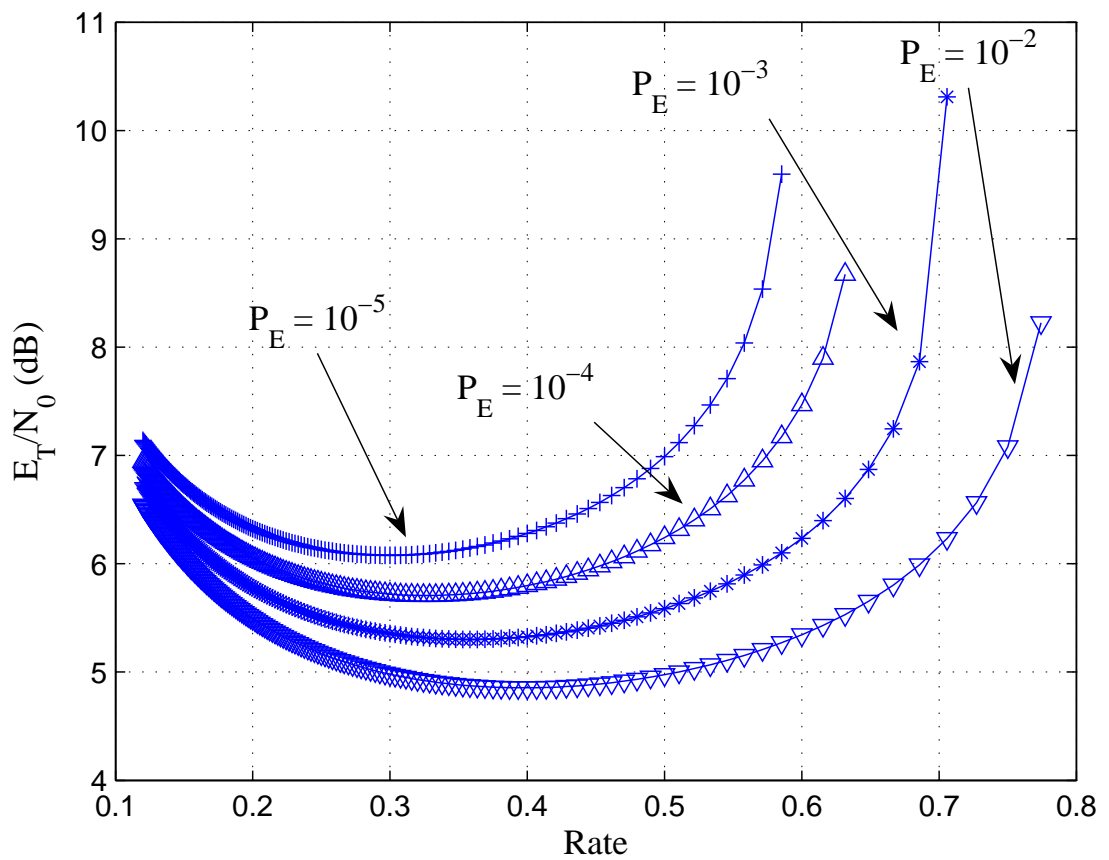


Figure 4.10: Total energy vs different code rate for various packet error probabilities (for $\gamma = -5$ dB).

We reiterate. The average codeword error probability (4.7) as follow

$$\log_2 P_e \leq -\frac{K}{R}(R_0 - R). \quad (4.23)$$

For given value of K , to have a lower packet error probability requires a lower rate (i.e. a larger value of N). Using $K = k = 24$ bits, we show the variation of total energy consumed with different code rates for various packet error probabilities, P_E in Fig. 4.10, Fig. 4.11, Fig. 4.12 for $\gamma = -5, 0, 5$ dB respectively. From the figures, as the packet error probability P_E decreases from 10^{-2} to 10^{-5} , the optimum code rates decreases from 0.4 to 0.3 for $\gamma = -5$ dB, from 0.533 to 0.4 for $\gamma = 0$ dB and from 0.649 to 0.5 for $\gamma = 5$ dB.

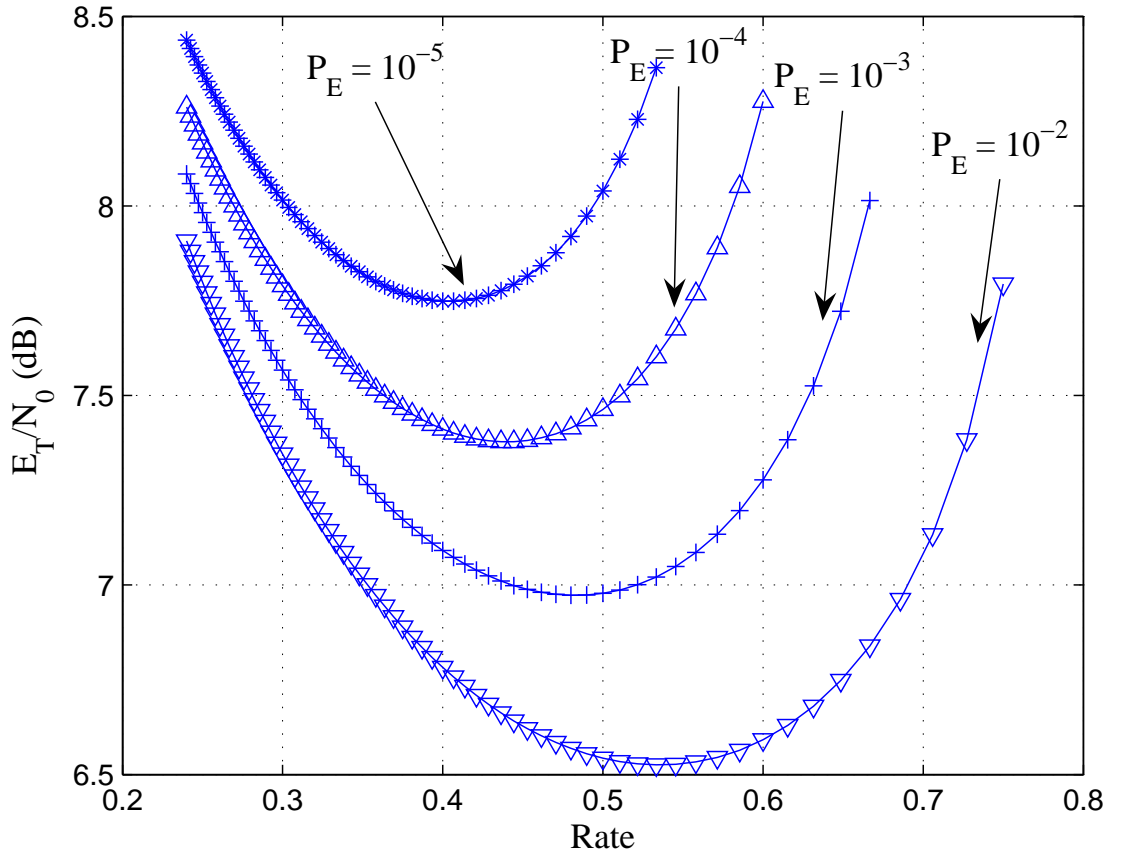


Figure 4.11: Total energy consumed vs code rate for various packet error probabilities (for $\gamma = 0$ dB).

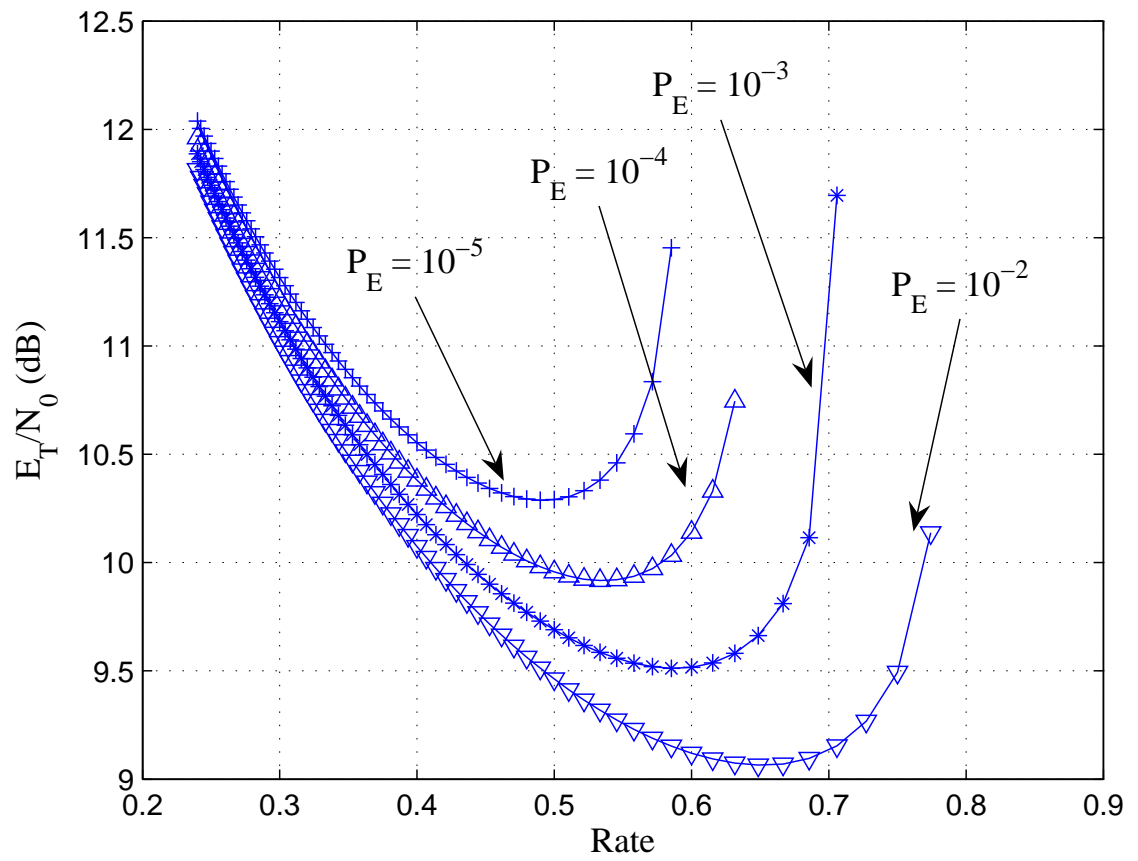


Figure 4.12: Total energy consumed vs code rate for various packet error probabilities (for $\gamma = 5$ dB).

4.2.6 Throughput With Optimum Energy Consumption

In this section, we investigate the throughput of our system model for $k=240$ bits. We define the throughput of a communication system, λ , as the ratio of successful received information bits to transmitted bits. Let P_s be the probability of a packet success. Then

$$\begin{aligned}\lambda &= \frac{k}{n}P_s \\ &= R(1 - P_E)\end{aligned}\tag{4.24}$$

Using the optimum code rate obtained for $k = 240$ information bits, we plot the throughput with respect to total energy consumed, $\frac{E_T}{N_0}$ in Fig. 4.13, 4.14 and 4.15 for $\gamma = -5, 0, 5$ dB respectively. The curves are not smooth as we fix k at 240 and increase n discretely. Thus, the code rate is not continuous. We see from the figures there is an optimal energy that maximizes the throughput. When γ is -5 dB, from Fig. 4.13, the optimum rate is close to 0.49, with packet error probability of 5×10^{-3} and $\frac{E_T}{N_0} = 3.93$ dB. For $\gamma = 0$ dB, from Fig. 4.14 the optimum throughput is close to 0.66, with packet error probability of 5×10^{-3} and $\frac{E_T}{N_0} = 5.6$ dB. From Fig. 4.10, Fig. 4.11 and Fig. 4.12, we observe that both the optimum code rate and packet error probability decreases as $\frac{E_T}{N_0}$ increases. From (4.24), a low P_E results in high throughput. However, a low code rate R causes a low throughput. When $\frac{E_T}{N_0}$ increases beyond the optimum throughput point, the effect of low code rate is greater than the effect of P_E on the throughput. This causes the throughput to decrease with high $\frac{E_T}{N_0}$ as shown in Fig. 4.13, 4.14 and 4.15 for $\gamma = -5, 0, 5$ dB respectively.

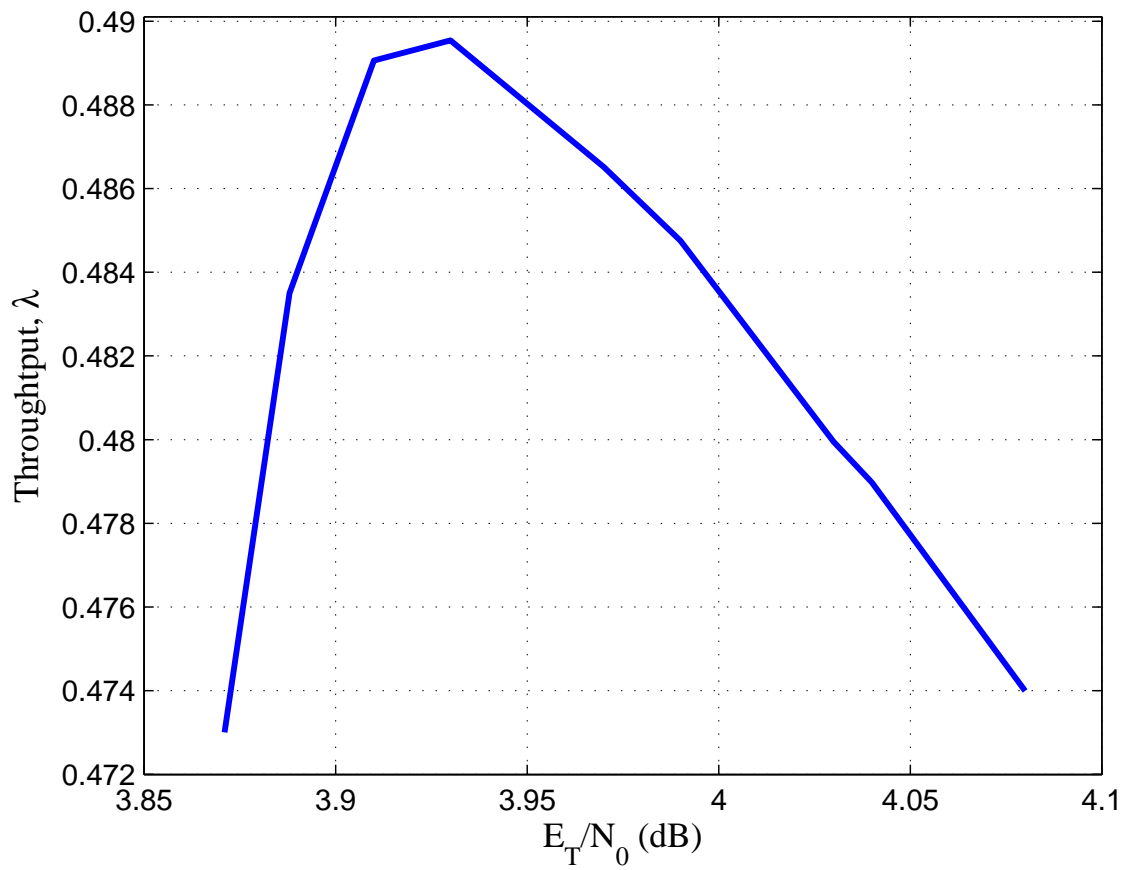


Figure 4.13: Throughput using optimum code rate (for $\gamma = -5$ dB).

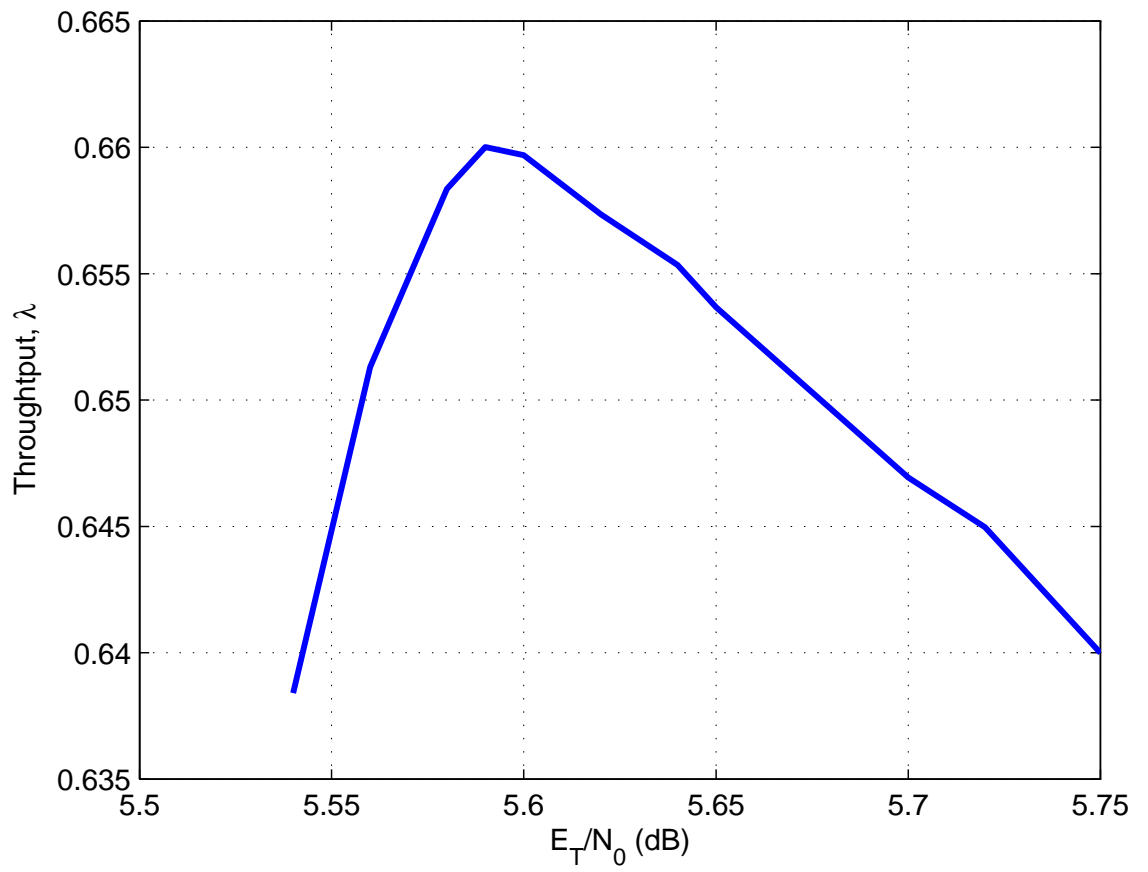


Figure 4.14: Throughput using optimum code rate (for $\gamma = 0$ dB).

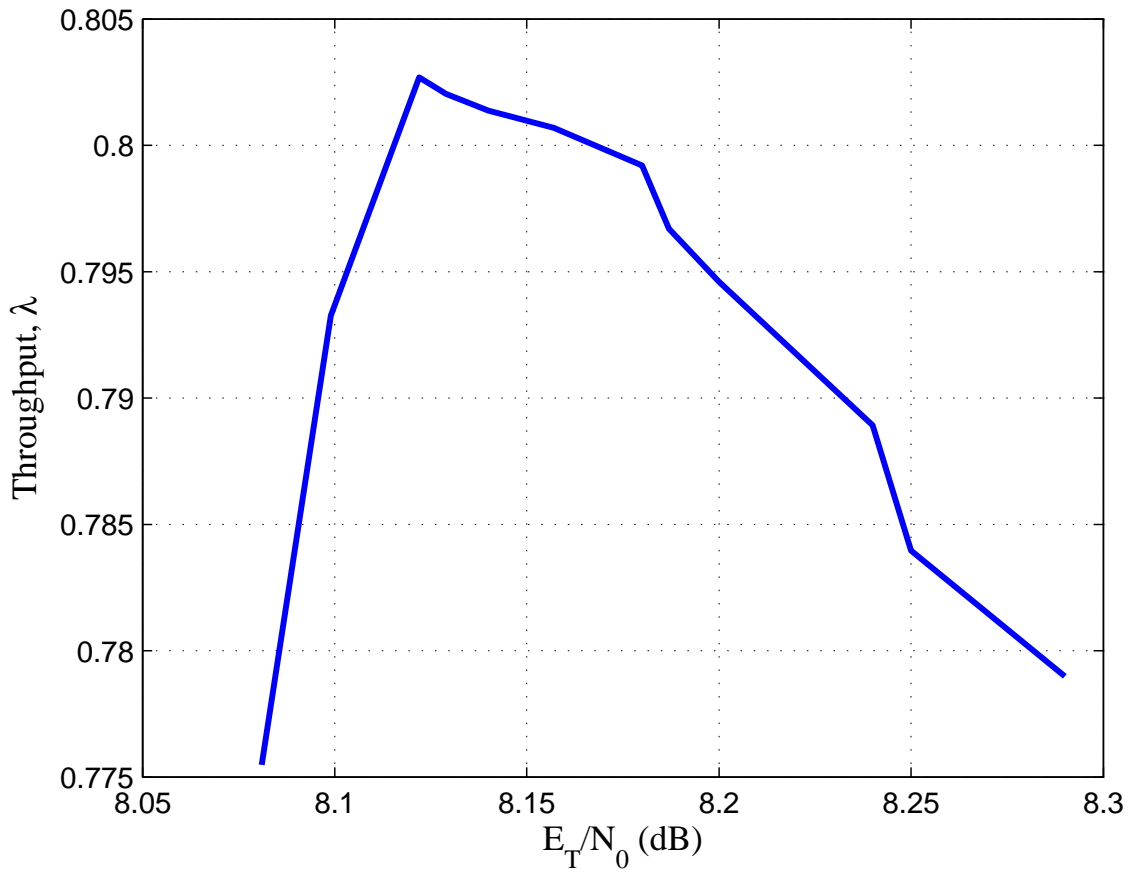


Figure 4.15: Throughput using optimum code rate (for $\gamma = 5$ dB).

4.3 Analysis of Total Energy Consumption Over an AWGN Channel Using Capacity

In this section, we investigate the optimum code rate of our model using the capacity theorem. This optimum code rate is compared with the one obtained from the cutoff rate theorem.

For binary antipodal signalling over an AWGN channel, the channel capacity is

$$\begin{aligned}
C &= \max_{p(x)} (I(X; Y)) \\
&= \max_{p(x)} \left(\sum_x \int_{y=-\infty}^{\infty} p(x, y) \log_2 \left(\frac{p(x, y)}{p(y)p(x)} \right) dy \right) \\
&= \max_{p(x)} \left(\sum_x \int_{y=-\infty}^{\infty} p(y|x)p(x) \log_2 \left(\frac{p(y|x)}{p(y)} \right) dy \right) \\
&= \max_{p(x)} \left(\int_{y=-\infty}^{\infty} p(y|x = -\sqrt{E_c})p(x = -\sqrt{E_c}) \log_2 \left(\frac{p(y|x = -\sqrt{E_c})}{p(y)} \right) dy \right. \\
&\quad \left. + \int_{y=-\infty}^{\infty} p(y|x = \sqrt{E_c})p(x = \sqrt{E_c}) \log_2 \left(\frac{p(y|x = \sqrt{E_c})}{p(y)} \right) dy \right). \tag{4.25}
\end{aligned}$$

The average mutual information in (4.25) is maximized when the input probabilities $p(x = \sqrt{E_c}) = p(x = -\sqrt{E_c}) = \frac{1}{2}$ [10]. Therefore, the channel capacity of the AWGN channel is given by

$$\begin{aligned}
C(E_b) &= \frac{1}{2} \int_{y=-\infty}^{\infty} p(y|x = -\sqrt{E_c}) \log_2 \left(\frac{p(y|x = -\sqrt{E_c})}{p(y)} \right) dy \\
&\quad + \frac{1}{2} \int_{y=-\infty}^{\infty} p(y|x = \sqrt{E_c}) \log_2 \left(\frac{p(y|x = \sqrt{E_c})}{p(y)} \right) dy \\
&= \int_{y=-\infty}^{\infty} p(y|x) \log_2 \left(\frac{p(y|x)}{p(y)} \right) dy \\
&= \int_{y=-\infty}^{\infty} p(y|x) \log_2 \left(\frac{p(y|x = -\sqrt{E_c})}{p(y|x = -\sqrt{E_c})p(x = -\sqrt{E_c}) + p(y|x = \sqrt{E_c})p(x = \sqrt{E_c})} \right) dy \\
&= \int_{y=-\infty}^{\infty} p(y|x) \log_2 \left(\frac{p(y|x = -\sqrt{E_c})}{\frac{1}{2}p(y|x = -\sqrt{E_c}) + \frac{1}{2}p(y|x = \sqrt{E_c})} \right) dy \\
&= \int_{y=-\infty}^{\infty} p(y|x) \log_2 \left(\frac{2p(y|x = -\sqrt{E_c})}{p(y|x = -\sqrt{E_c}) + p(y|x = \sqrt{E_c})} \right) dy
\end{aligned}$$

$$\begin{aligned}
&= \int_{y=-\infty}^{\infty} p(y|x)dy + \int_{y=-\infty}^{\infty} p(y|x) \log_2 \left(\frac{p(y|x = -\sqrt{E_c})}{p(y|x = -\sqrt{E_c}) + p(y|x = \sqrt{E_c})} \right) dy \\
&= 1 - \int_{y=-\infty}^{\infty} p(y|x) \log_2 \left(\frac{p(y|x = -\sqrt{E_c}) + p(y|x = \sqrt{E_c})}{p(y|x = -\sqrt{E_c})} \right) dy \\
&= 1 - \int_{y=-\infty}^{\infty} p(y|x) \log_2 \left(1 + \frac{p(y|x = \sqrt{E_c})}{p(y|x = -\sqrt{E_c})} \right) dy \\
&= 1 - \int_{y=-\infty}^{\infty} \frac{1}{\sqrt{2\pi}} \exp \left\{ -\frac{(y - \sqrt{\frac{2E_c}{N_0}})^2}{2} \right\} \log_2 [1 + \exp \{ -2y\sqrt{\frac{2E_c}{N_0}} \}] dy \\
&= 1 - \int_{y=-\infty}^{\infty} \frac{1}{\sqrt{2\pi}} \exp \left\{ -\frac{(y - \sqrt{\frac{2RE_b}{N_0}})^2}{2} \right\} \log_2 [1 + \exp \{ -2y\sqrt{\frac{2RE_b}{N_0}} \}] dy. \quad (4.26)
\end{aligned}$$

The above expression allows us to compute the capacity $C(E_b)$ at a given bit energy E_b . We can equate code rate R with capacity C . That is, for every E_b , we have an optimum code rate R . Hence, we define $R(E_b)$ to be the optimum code rate function. This allows us to obtain an inverse function of $R(E_b)$. We define $E_b(R)$ to be the inverse function of $R(E_b)$. This function, $E_b(R)$, relates the minimum energy required for the system to transmit a packet at a code rate R over an AWGN channel. Using (4.26), we are able to numerically evaluate the function $E_b(R)$. Therefore, the total energy consumed in a single hop communication system is

$$\frac{E_T}{N_0} = \frac{E_b(R)}{N_0} + \frac{\gamma}{R} \quad (4.27)$$

The variation of total energy consumed with code rate is shown in Fig. 4.16 for $\gamma = -\infty, -20$ dB, -10 dB, -5 dB, -3 dB, 0 dB, 3 dB and 5 dB. From the figure, there exist an optimal code rate when γ is nonzero.

The comparison of the variation of processing energy γ and optimum code rate R using the cutoff rate when $N = \infty$ and capacity is shown in Fig. 4.17 and 4.18 for -20 dB $\leq \gamma \leq -2$ dB and -2 dB $\leq \gamma \leq 20$ dB respectively. We observe that the two curves are very close to one another, especially at the range where $\gamma < -8$ dB and $\gamma > 5$ dB. For the case when -8 dB $< \gamma < 5$ dB, the capacity curve is able to achieve a slightly higher rate as compare to the cutoff rate curve.

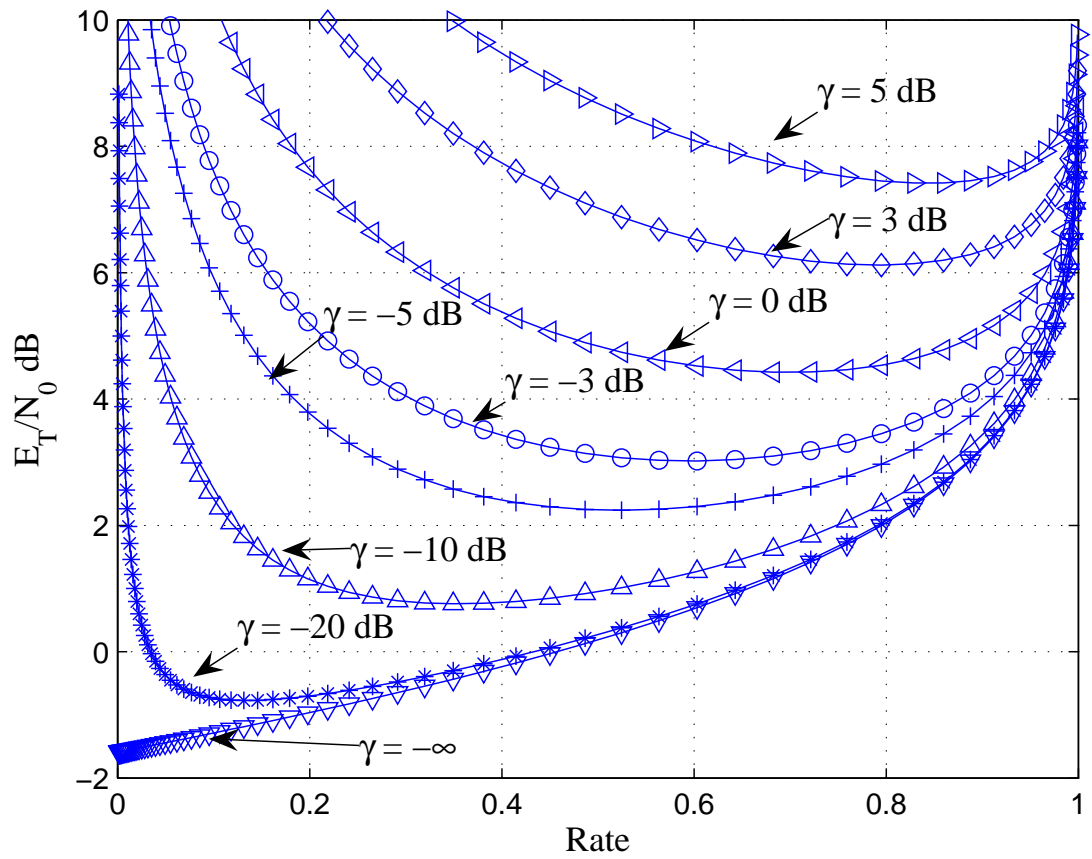


Figure 4.16: Variation of $\frac{E_T}{N_0}$ with R with various values of γ using the capacity for antipodal signalling over an AWGN channel.

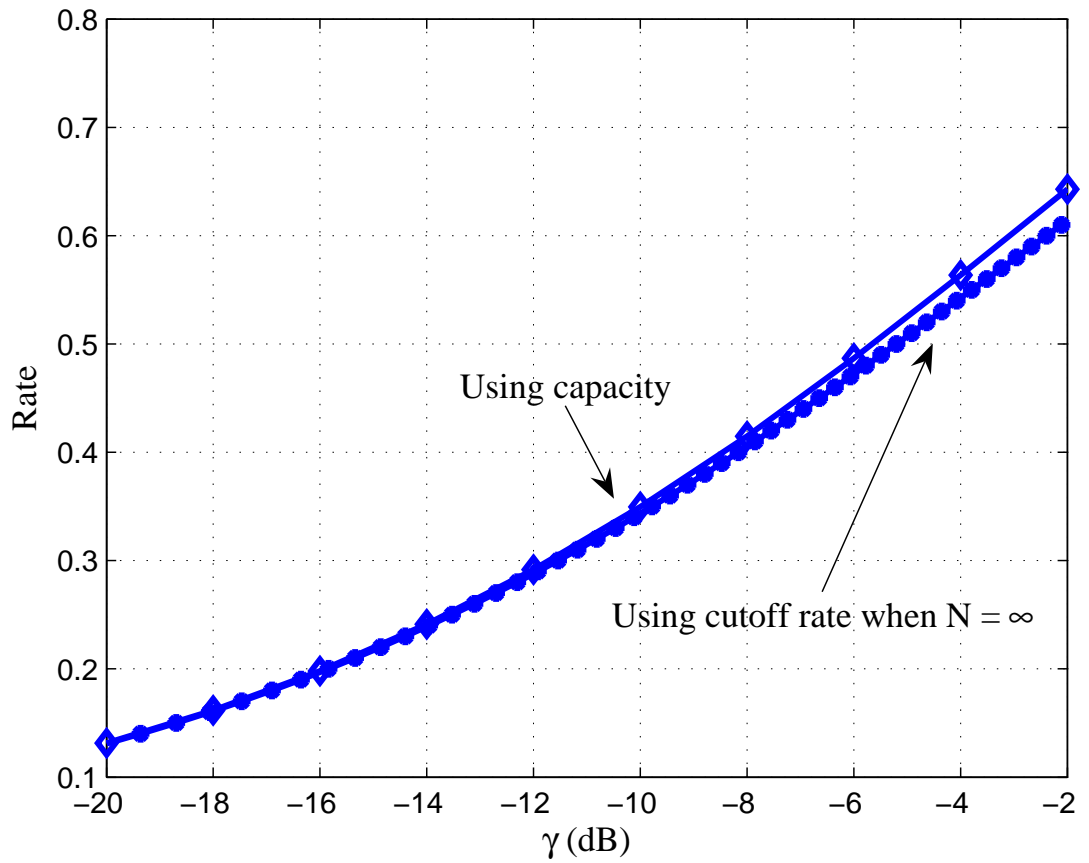


Figure 4.17: Variation of optimum code rate R with γ using the cutoff rate and capacity (for antipodal signalling over an AWGN channel).

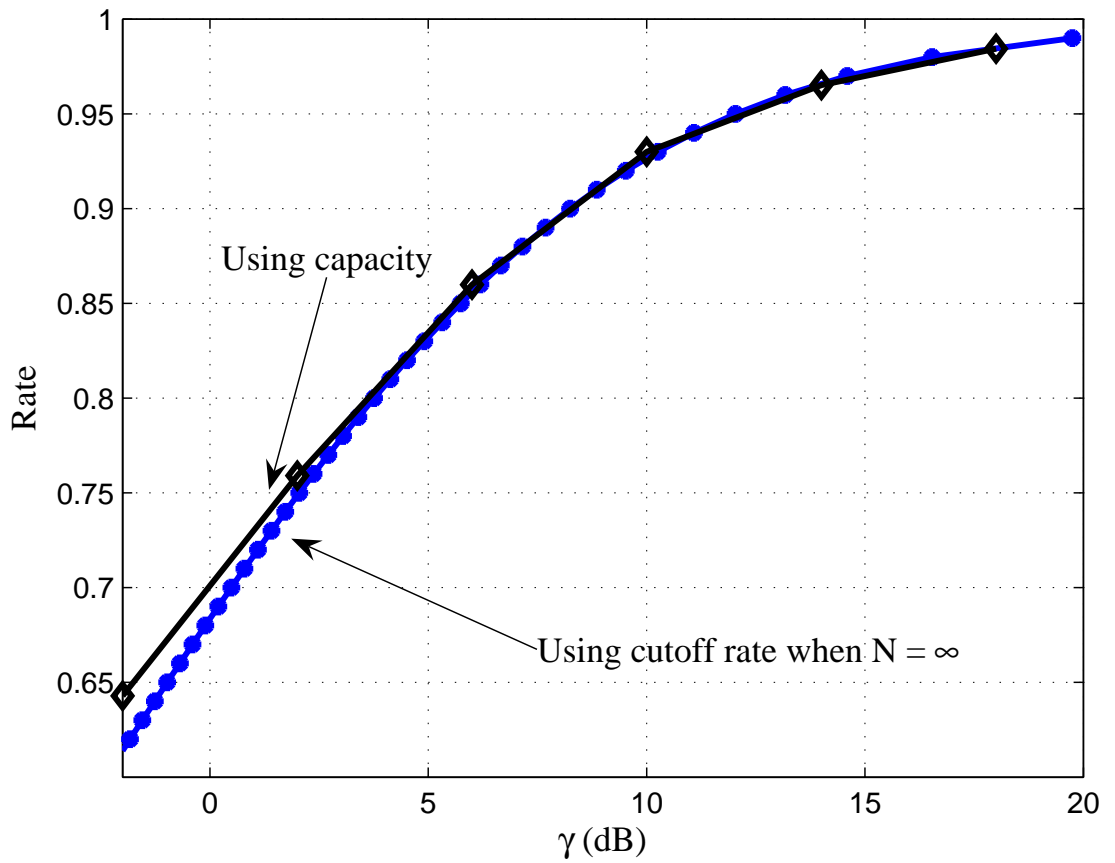


Figure 4.18: Variation of optimum code rate R with γ using the cutoff rate and capacity (for antipodal signalling over an AWGN channel).

4.4 Analysis Using Cutoff Rate for Noncoherent Detection Over Rayleigh Fading Channel

In this section, we compute the total energy consumed using a Rayleigh fading channel. Here, we use BFSK modulation with noncoherent detection. We assumed that transmitted bit experience independent fading and the receiver uses soft-decision decoding without side information.

4.4.1 Derivation of Total Energy Consumed

From (4.7), the codeword error is bounded by

$$P_e \leq 2^{-N(R_0-R)}. \quad (4.28)$$

For BFSK modulation with noncoherent demodulation over a Rayleigh fading channel, the bit error probability is $p = \frac{1}{2+RE_b/N_0}$ and the cutoff rate R_0 is [46]

$$R_0 = 1 - \log_2\{1 + 4p(1-p)\}. \quad (4.29)$$

Substituting (4.29) into(4.28), we have

$$4p(1-p) = 2^\delta - 1. \quad (4.30)$$

Solving (4.30), we obtain

$$\left(\frac{E_b}{N_0}\right)_{\text{req}} = \frac{1}{R} \left\{ \frac{\sqrt{2-2^\delta}}{1-\sqrt{2-2^\delta}} \right\}. \quad (4.31)$$

Therefore, from (4.9), we have

$$\frac{E_T}{N_0} = \frac{1}{R} \left\{ \frac{\sqrt{2-2^\delta}}{1-\sqrt{2-2^\delta}} \right\} + \frac{\gamma}{R}. \quad (4.32)$$

4.4.2 Performance for a Fixed Information Packet Length

The variation of total energy consumed with code rate R for $\gamma = -\infty$ to $\gamma = -5$ dB and $\gamma = -5$ dB to $\gamma = 10$ dB is shown in Fig. 4.19 and 4.20 respectively. We notice that when γ is very low, the processing energy does not contribute much to the total

energy consumed and therefore, the energy-rate curve for $\gamma = -\infty$ is very close to the energy-rate curve for $\gamma = -20$ dB. That is, when γ is low, the optimum code rate does not change much.

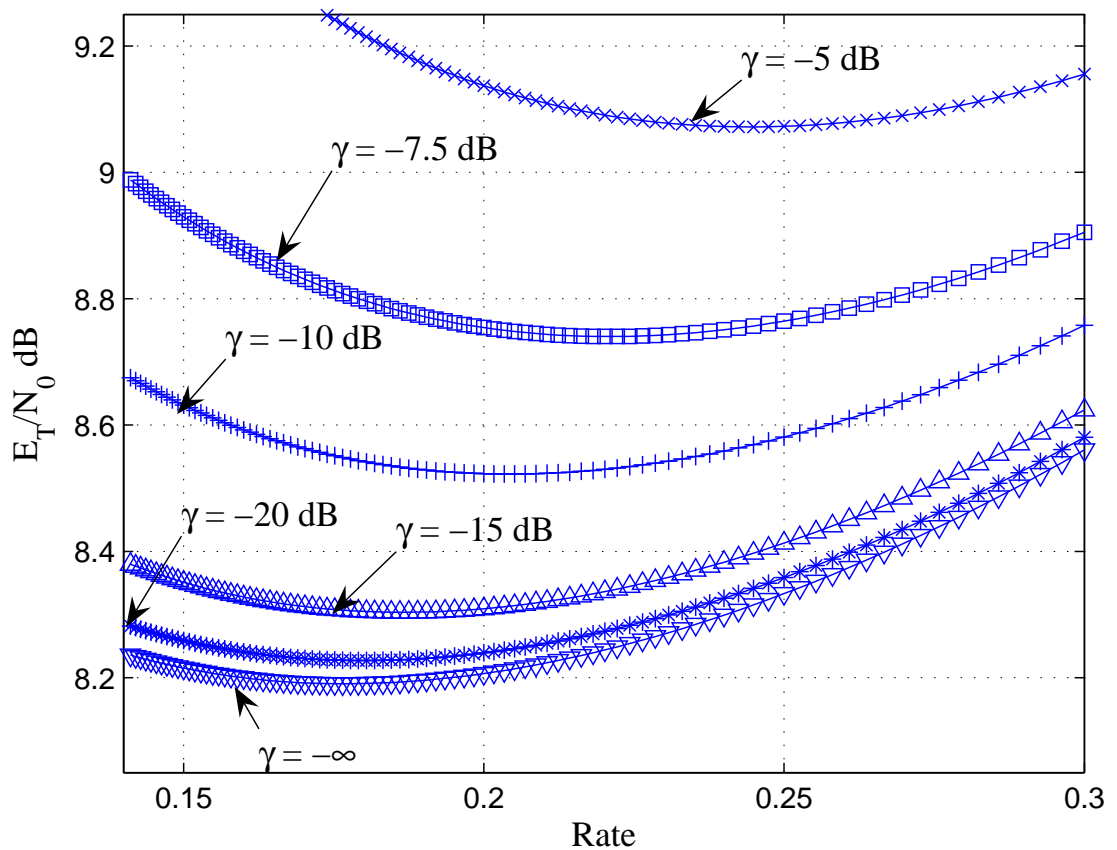


Figure 4.19: Variation of $\frac{E_T}{N_0}$ with R with various values of γ from $-\infty$ to -5 dB using the cutoff rate for noncoherent detection over a Rayleigh fading channel.

We show the variation of optimum code rate with γ for $k = 24$ in Fig. 4.21. From the figure, we observe that when the contribution of γ to the total energy consumed is less than -10 dB, the optimum code rate remains around 0.18 .

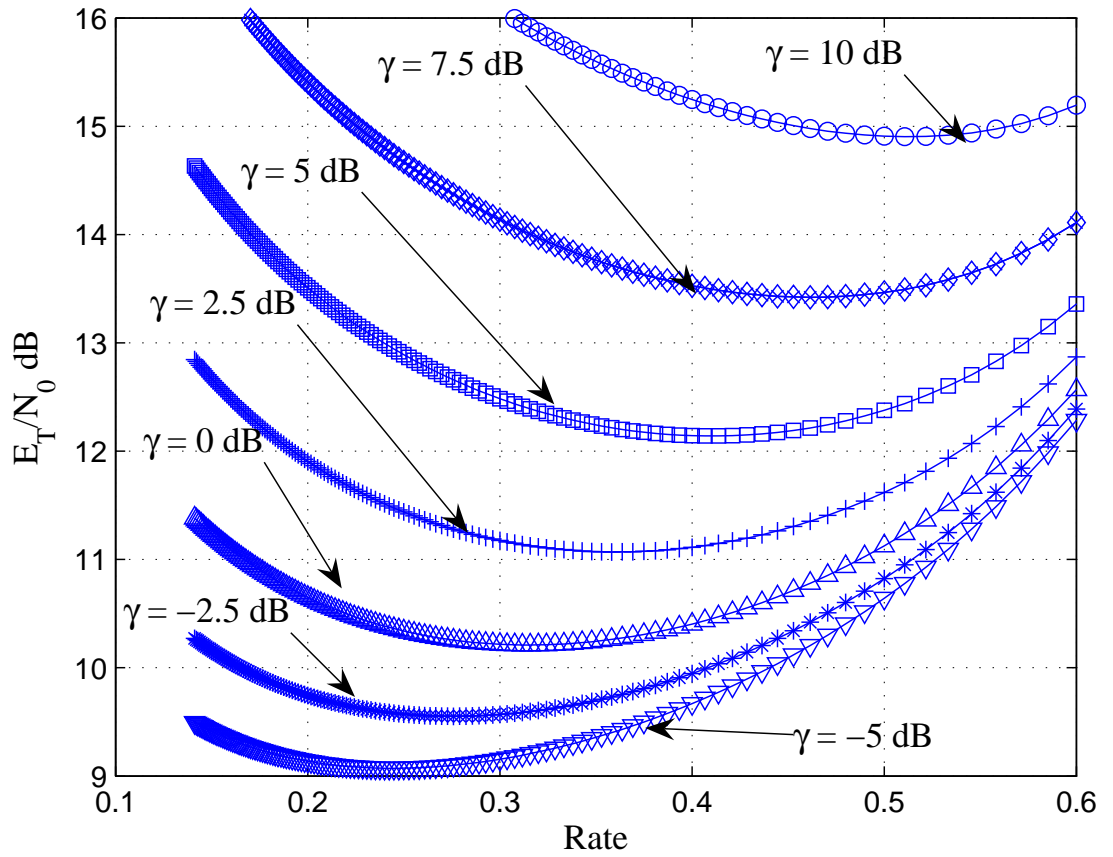


Figure 4.20: Variation of $\frac{E_T}{N_0}$ with R with various values of γ from -5 to 10 dB using the cutoff rate for noncoherent detection over a Rayleigh fading channel.

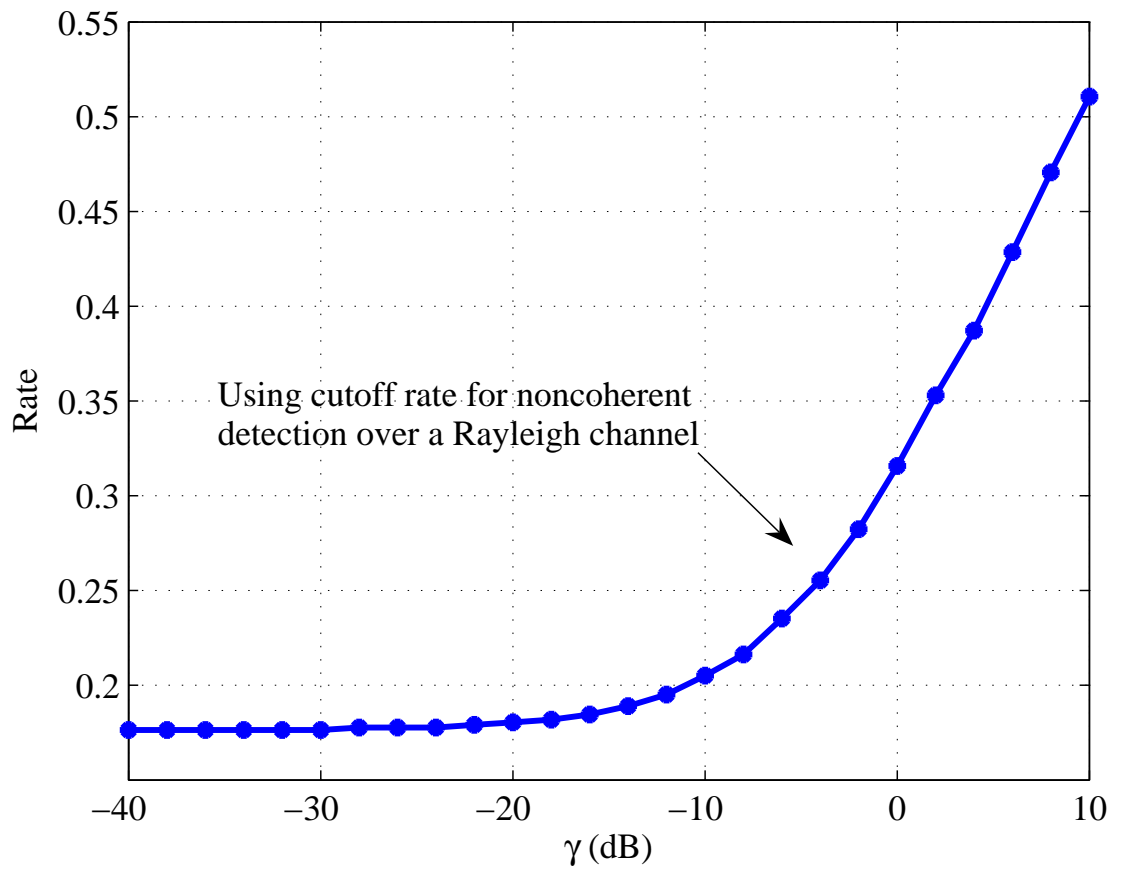


Figure 4.21: Optimum code rate using cutoff rate for noncoherent detection over a Rayleigh fading channel.

4.4.3 Derivation of Optimum Code Rate

To find an expression for the optimum code rate, we differentiate (4.32) with respect to R and equating it to 0. We obtain the following expression:

$$\begin{aligned} 0 &= -\frac{\gamma}{R^2} + \frac{2^{-\alpha R} \alpha \ln 2}{R(1 - \sqrt{2 - 2^\delta})\sqrt{2 - 2^\delta}} - \frac{\sqrt{2 - 2^\delta}}{R^2(1 - \sqrt{2 - 2^\delta})} + \frac{2^{-\alpha R} \alpha \ln 2}{R(1 - \sqrt{2 - 2^\delta})^2} \\ &= (4\gamma - 2) + 2^{-\alpha R}(R\alpha \ln 2 + 2 - 4\gamma) + \sqrt{2 - 2^\delta}[(2 - 2^\delta)(1 - \gamma) - \gamma]. \end{aligned} \quad (4.33)$$

It was shown in [46] that if we ignore processing energy, the required code rate for minimum energy consumption is 0.23 for arbitrarily small P_E and $N \rightarrow \infty$. When γ is low, the optimum code rate does not vary much. Therefore, when $\gamma \ll 1$, we use Taylor's series expansion for $2^{-R\alpha}$ and $\sqrt{1 - 2^{-R\alpha}}$ about $R = 0.2$.

$$\begin{aligned} \sqrt{1 - 2^{-R\alpha}} &\approx f(0.2) + f'(0.2)(R - 0.2) \\ &\quad + \frac{1}{2}f''(0.2)(R - 0.2)^2 \end{aligned} \quad (4.34)$$

$$\begin{aligned} 2^{-R\alpha} &\approx g(0.2) + g'(0.2)(R - 0.2) \\ &\quad + \frac{1}{2}g''(0.2)(R - 0.2)^2 \end{aligned} \quad (4.35)$$

$$\begin{aligned} f(0.2) &= \sqrt{1 - 2^{-0.2\alpha}} \\ f'(0.2) &= \frac{2^{-0.2\alpha} \alpha \ln 2}{2f(0.2)} \\ f''(0.2) &= f'(0.2) \left(-1 - \frac{2^{-0.2\alpha}}{2(1 - 2^{-0.2\alpha})} \right) \alpha \ln 2 \\ g(0.2) &= 2^{-0.2\alpha} \\ g'(0.2) &= -g(0.2) \alpha \ln 2 \\ g''(0.2) &= -g'(0.2) \alpha \ln 2. \end{aligned}$$

Using the above expression, we have an approximate value for R as follow

$$R = \frac{-b + \sqrt{b^2 - 4ac}}{2a} \quad (4.36)$$

where

$$\begin{aligned}
a = & \frac{1}{\sqrt{2}}f''(0.2)(2 - 3\gamma) + \frac{1}{2}g''(0.2)\{2 - 4\gamma - (1 - \gamma)2\sqrt{2}[f(0.2) - 0.2f'(0.2) + 0.02f''(0.2)]\} \\
& + [g(0.2) - 0.2g'(0.2) + 0.02g''(0.2)][-\sqrt{2}(1 - \gamma)f''(0.2)] + [g'(0.2) - 0.2g''(0.2)]\{\alpha \ln 2 \\
& - (1 - \gamma)2\sqrt{2}[f'(0.2) - 0.2f''(0.2)]\}, \tag{4.37}
\end{aligned}$$

$$\begin{aligned}
b = & \sqrt{2}(2 - 3\gamma)\{f'(0.2) - 0.2f''(0.2)\} + \{g(0.2) - 0.2g'(0.2) + 0.02g''(0.2)\}\{\alpha \ln 2 - 2\sqrt{2}(1 \\
& - \gamma)[f'(0.2) - 0.2f''(0.2)]\} + \{g'(0.2) - 0.2g''(0.2)\}\{2 - 4\gamma - 2\sqrt{2}(1 - \gamma)[f(0.2) \\
& - 0.2f'(0.2) + 0.02f''(0.2)]\} \tag{4.38}
\end{aligned}$$

and

$$\begin{aligned}
c = & 4\gamma - 2 + \sqrt{2}(2 - 3\gamma)\{f(0.2) - 0.2f'(0.2) + 0.02f''(0.2)\} + \{g(0.2) - 0.2g'(0.2) \\
& + 0.02g''(0.2)\}\{2 - 4\gamma - (1 - \gamma)2\sqrt{2}[f(0.2) - 0.2f'(0.2) + 0.02f''(0.2)]\}. \tag{4.39}
\end{aligned}$$

Table 4.4.3 shows the approximate optimum required R_a for minimum energy consumption with respect to γ values. Similar to the case of using the cutoff rate over an AWGN channel, the approximation is only good when γ is low. The comparison on the actual energy consumed and the approximation is shown in Fig. 4.22.

4.4.4 Optimum Code Rate for Large Information Packet

For $k = 240$ information bits, the variation of $\frac{E_T}{N_0}$ with respect to R is shown in Fig. 4.23 and 4.24. In comparing these figures with Fig. 4.19 and 4.20, the optimum rates are higher and the energy consumption is lower. This is because with larger k , there are more independent realization and we can achieve a particular packet error probability at a higher code rate and lower energy.

For $\gamma = 0$ dB, we show the variation of code rate R with information bits k in Fig. 4.25. The optimum code rate approaches 0.4 when k approaches infinity.

For the limiting case when $k \rightarrow \infty$, we substitute (4.20) into (4.33) and obtain a closed form relationship between normalized energy γ and optimum code rate R as

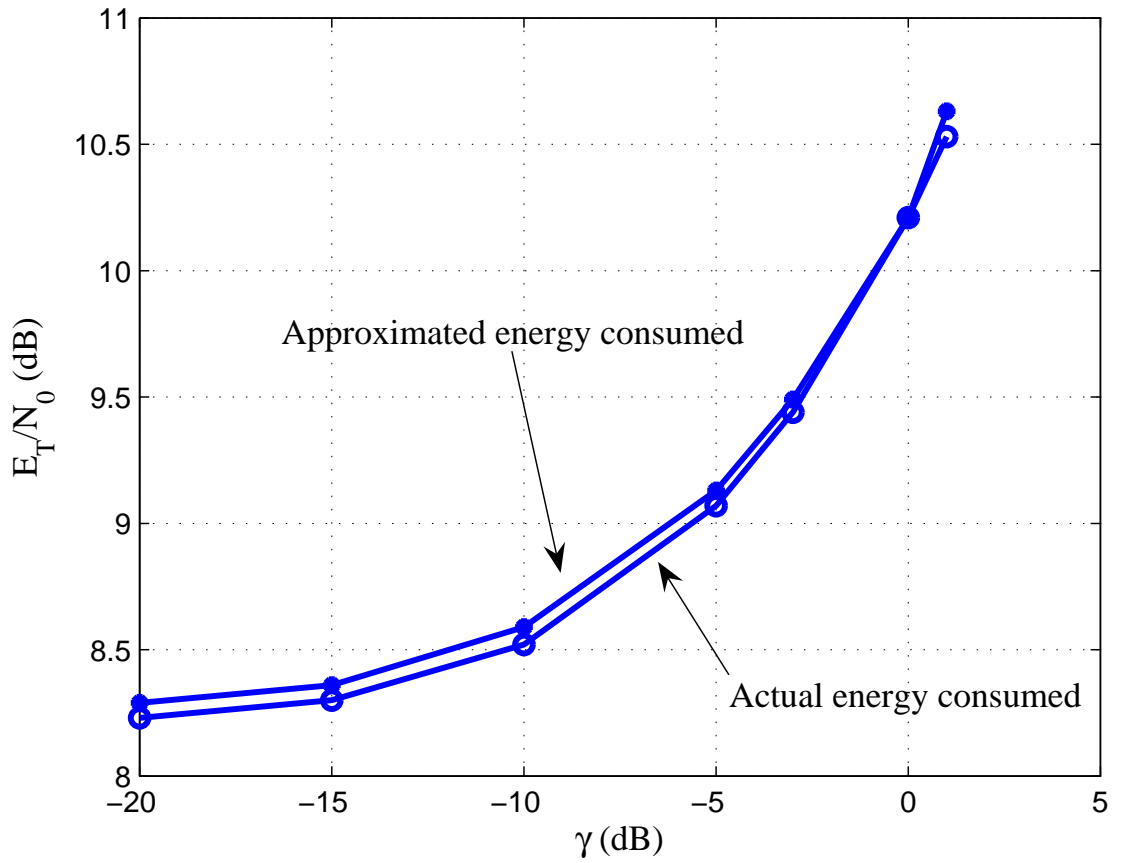


Figure 4.22: Comparison of actual energy consumed and the approximation for various γ values using cutoff rate for noncoherent detection over a Rayleigh fading channel.

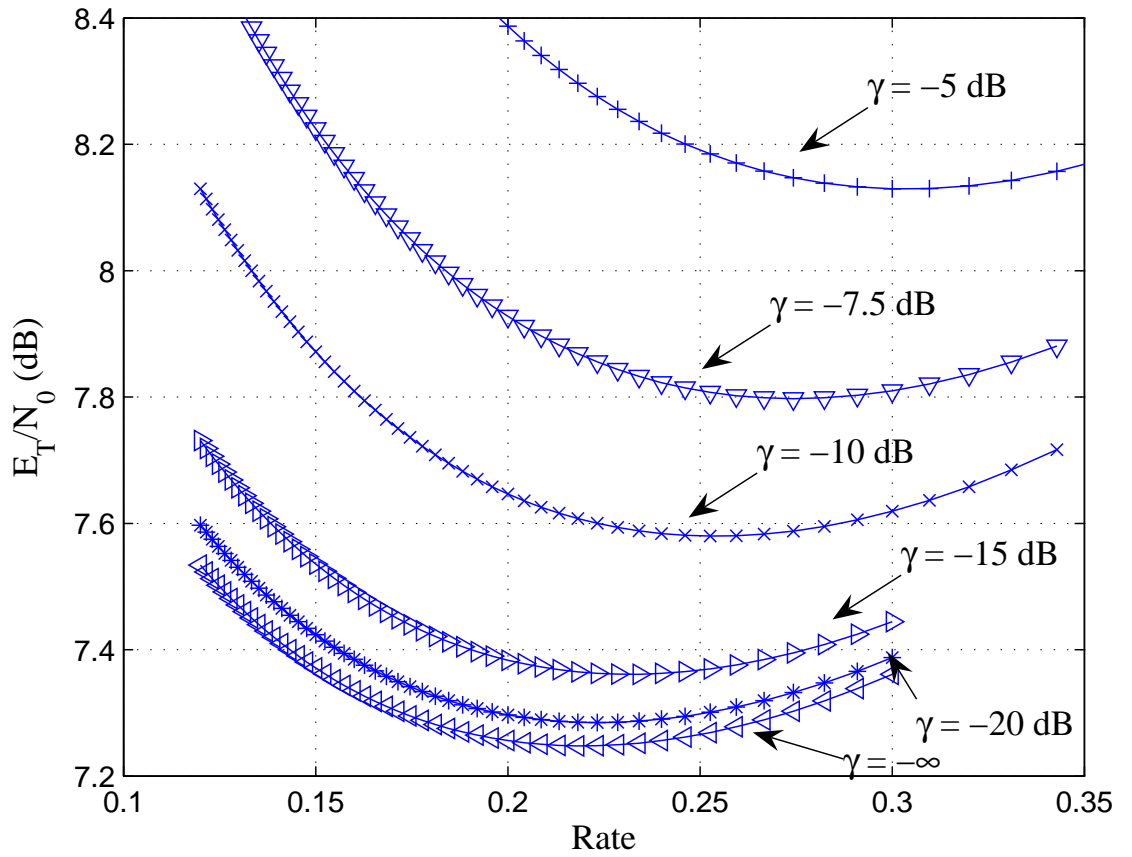


Figure 4.23: Variation of $\frac{E_T}{N_0}$ with respect to R for $\gamma = -\infty$ dB to $\gamma = -5$ dB when $k = 240$, using cutoff rate for noncoherent detection over a Rayleigh fading channel.

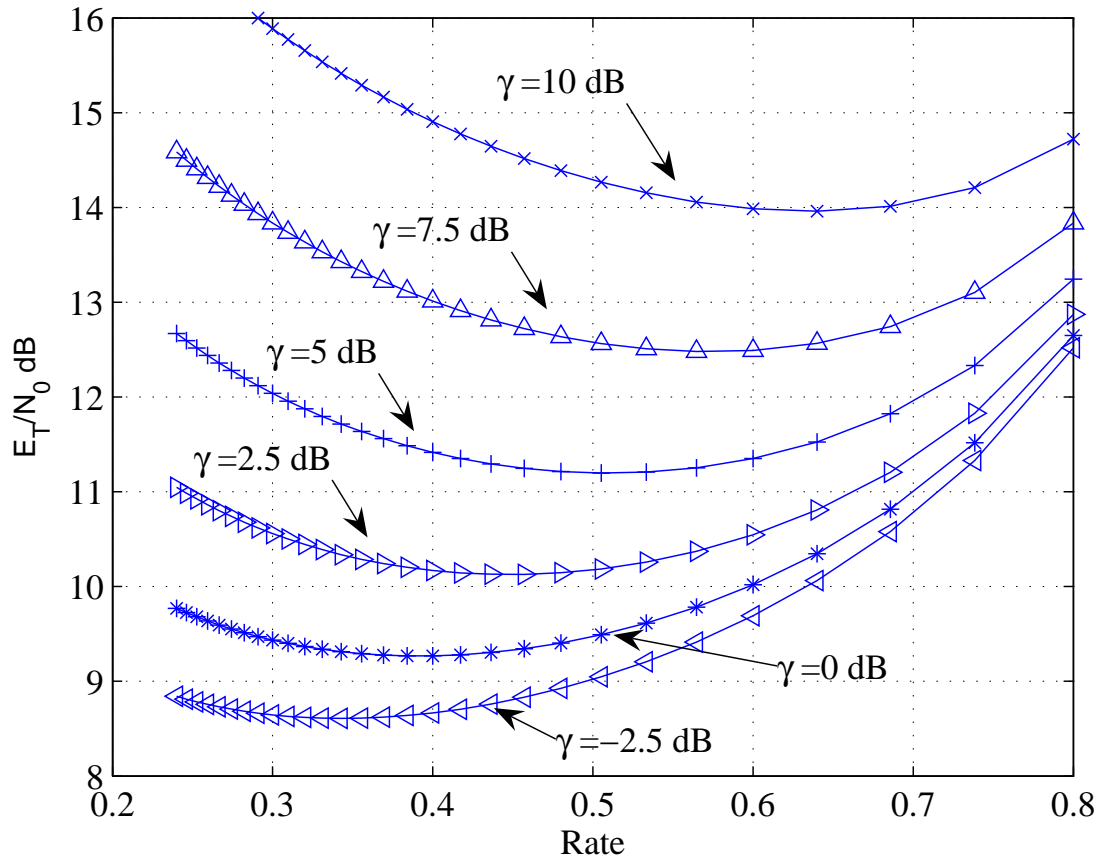


Figure 4.24: Variation of $\frac{E_T}{N_0}$ with respect to R for $\gamma = -2.5$ dB to $\gamma = 10$ dB when $k = 240$, using cutoff rate for noncoherent detection over a Rayleigh fading channel.

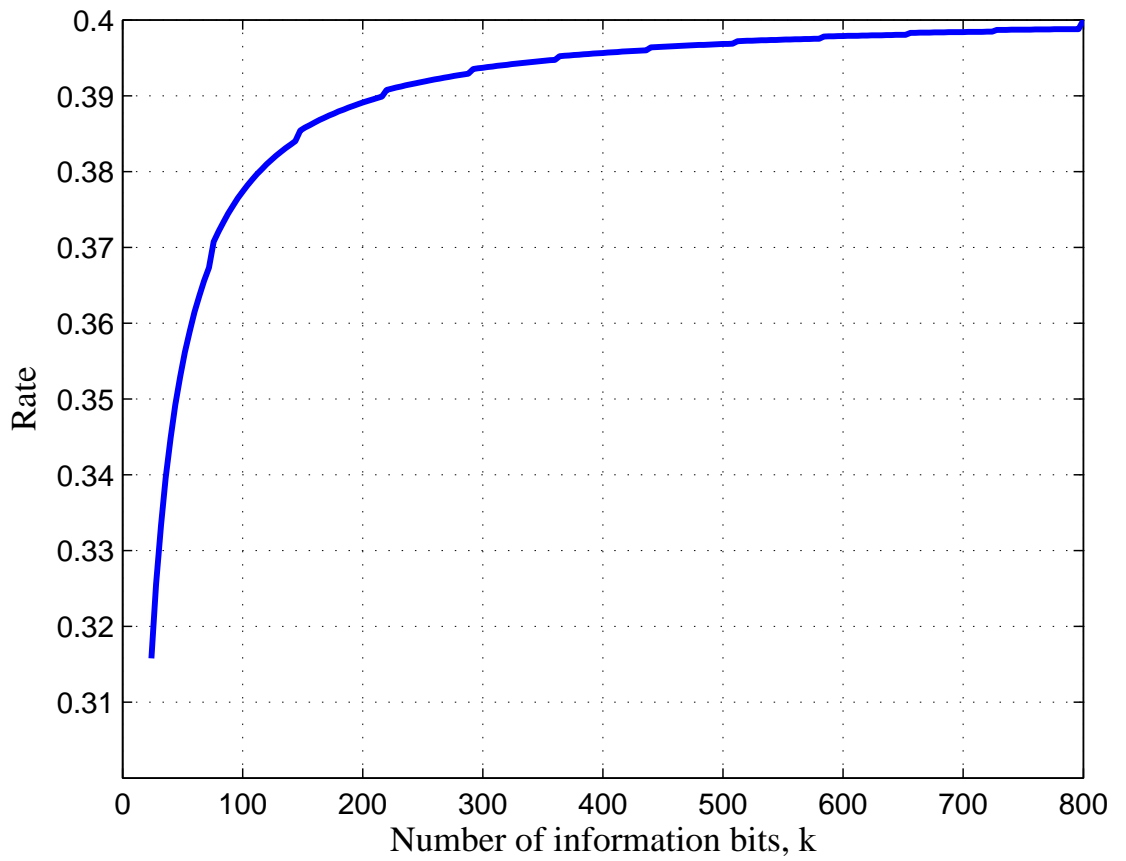


Figure 4.25: Optimum code rate with respect to number of information bits k for $\gamma = 0$ dB, using cutoff rate for noncoherent detection over a Rayleigh fading channel.

γ (dB)	R_a	$(\frac{E_T}{N_0})_a$ (dB)	R	$\frac{E_T}{N_0}$ (dB)
$-\infty$	0.137	8.25	0.176	8.19
-20	0.140	8.29	0.180	8.23
-15	0.146	8.36	0.186	8.30
-10	0.162	8.59	0.205	8.52
-5	0.201	9.13	0.245	9.07
-3	0.231	9.49	0.270	9.44
0	0.320	10.21	0.316	10.21
1	0.395	10.63	0.333	10.53

Table 4.3: Approximate and exact values of required minimum energy and its respective code rate for different values of γ , using cutoff rate for noncoherent detection over a Rayleigh fading channel.

follow

$$\gamma = \frac{2^{-R}R \ln 2}{(1 - \sqrt{2 - 2^{1-R}})\sqrt{2 - 2^{1-R}}} - \frac{\sqrt{2 - 2^{1-R}}}{(1 - \sqrt{2 - 2^{1-R}})} + \frac{2^{-R}R \ln 2}{(1 - \sqrt{2 - 2^{1-R}})^2}. \quad (4.40)$$

The variation of normalized processing energy and optimum code rate is shown in Fig. 4.26. When $\gamma \rightarrow -\infty$ dB, the optimum code rate approaches 0.23, as in [46]. We note that when γ is low, the optimum code rate is less than 0.3. When the contribution of the processing energy is significant, the optimum code rate is closed to 1. The information in Fig. 4.26 allows engineers to select an optimum code rate for the channel code that can achieve the optimum energy consumption for communications over a Rayleigh fading channel for known values of γ .

4.4.5 Throughput With Optimum Energy Consumption

The throughput of a communication system is defined in (4.24). Using the optimum code rate for $k = 240$ information bits, the throughput is shown in Fig. 4.27 and 4.28 for $\gamma = -5$ dB and 0 dB respectively. Similar to the case of coherent detection over an AWGN channel, the curve is not smooth as we only consider discrete n values and this

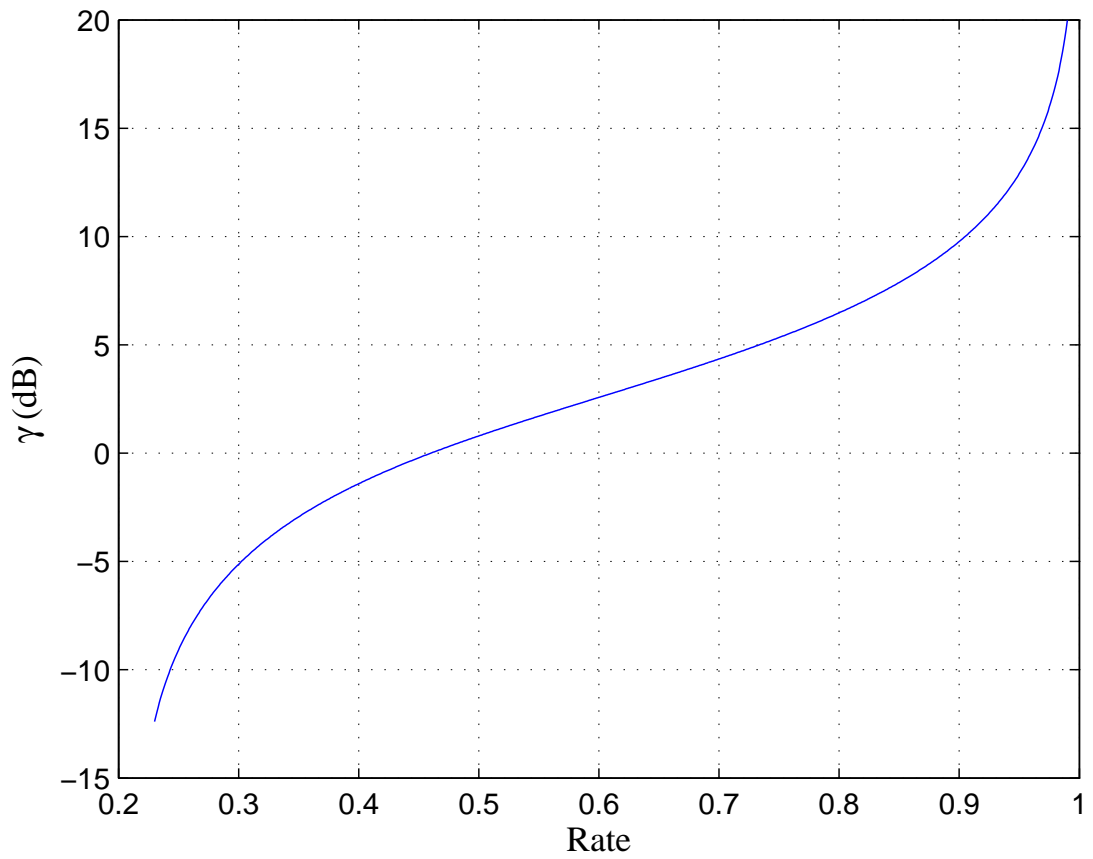


Figure 4.26: Optimum code rate for the normalized processing energy when $k \rightarrow \infty$, using cutoff rate for noncoherent detection over a Rayleigh fading channel.

causes the code rate to be non continuous. We observe that there exists an optimum throughput. When $\gamma = -5$ dB, the optimum throughput is around 0.301 with code rate about 0.302, at a packet probability error close to 5×10^{-3} and the total energy required is about 8.145 dB. When $\gamma = 0$ dB, we are able to achieve a higher throughput of 0.388 at the expense of higher energy consumption of 9.275dB.

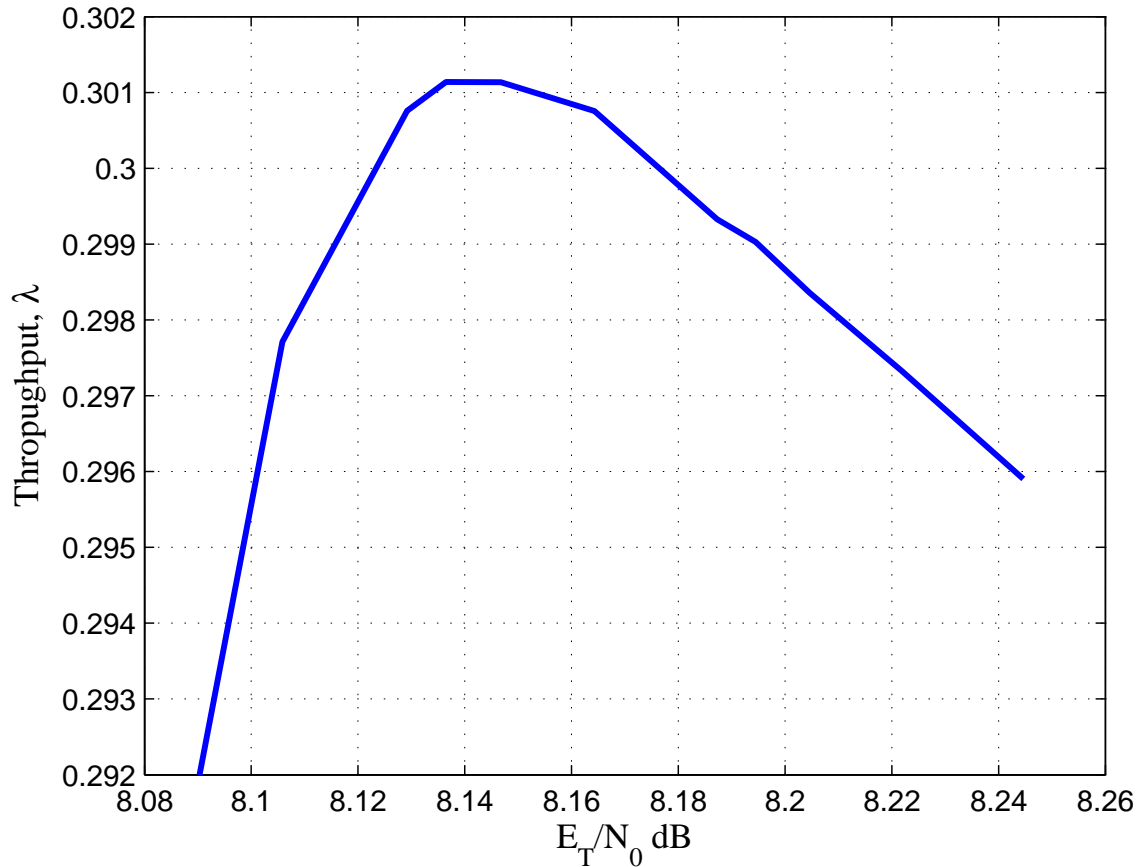


Figure 4.27: Performance of Throughput Using Optimum Code Rate (for $\gamma = -5$ dB).

4.5 Energy Performance Using Practical Codes

In this section, we investigate the energy needed for using RS codes and convolutional codes in order to achieve a given packet error probability. We compare the performance of these codes with the one that uses the cutoff rate.

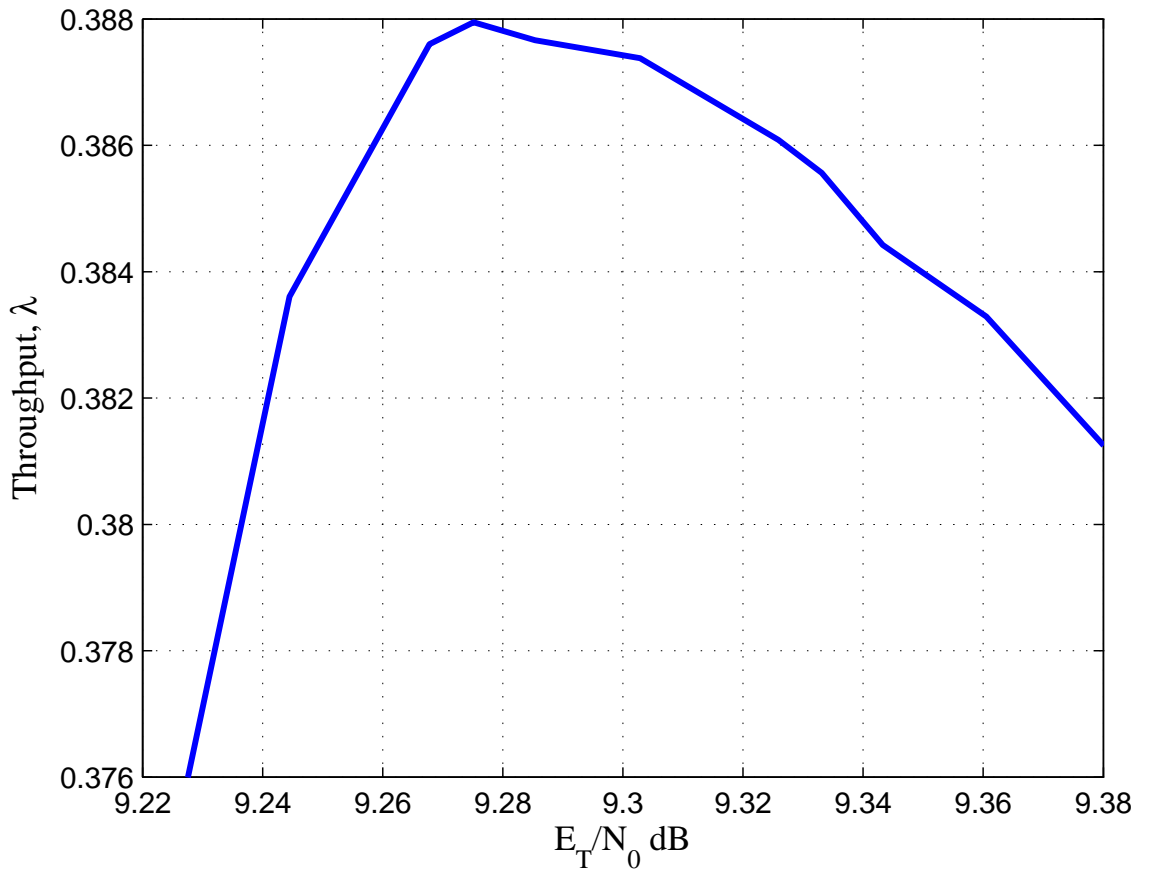


Figure 4.28: Performance of Throughput Using Optimum Code Rate (for $\gamma = 0$ dB).

4.5.1 Using RS codes over an AWGN channel

For an (N, K) RS code over $GF(2^m)$, a symbol is represented by m data bits and the maximum codeword length is $2^m + 1$ bits. The packet (codeword) error probability is determined by the number of errors, t , it can correct. This value depends on the value of N chosen for the RS code and is given by $t = \lfloor \frac{N-K}{2} \rfloor$. For a given required codeword error probability, there exist an optimum code rate that achieves this error probability at the minimum signal-to-noise ratio $\frac{E_b}{N_0}$. However, this “optimum” code rate may not result in minimum total energy consumed in a communication system.

For antipodal signalling with coherent detection over an AWGN channel, the bit error probability is $p = Q(\sqrt{\frac{2E}{N_0}})$. In our investigation, we consider binary hard decision inputs to the RS decoder. Therefore, we assume a memoryless binary symmetric channel (BSC) in our study with transition probability p . The packet error probability for a RS code is

$$P_E = \sum_{j=t+1}^N \binom{N}{j} P_B^j (1 - P_B)^{N-j} \quad (4.41)$$

where $P_B = 1 - (1 - p)^m$ is the symbol error probability and p is bit error probability. Given a required packet error probability P_E , we can determined the signal-to-noise ratio $\frac{E_b}{N_0}_{RS}$ required by using (4.41). The total energy required is

$$\frac{E_T}{N_0} = \frac{E_b}{N_0}_{RS} + \frac{\gamma}{R}. \quad (4.42)$$

The energy required to achieve a packet error rate of 0.01 and 0.001 for various code rates is shown in Fig. 4.29 and Fig. 4.30 respectively. We observe in both Fig. 4.29 and Fig. 4.30 that as the processing energy, γ , increases, the optimum rate to achieve the minimum energy consumed increases, similar to the previous cases.

4.5.2 Using Convolutional Codes

Convolutional codes are widely used in many practical applications of communications system design. A convolutional code is generated by passing the information sequence to be transmitted through a linear finite-state shift register. In general, the

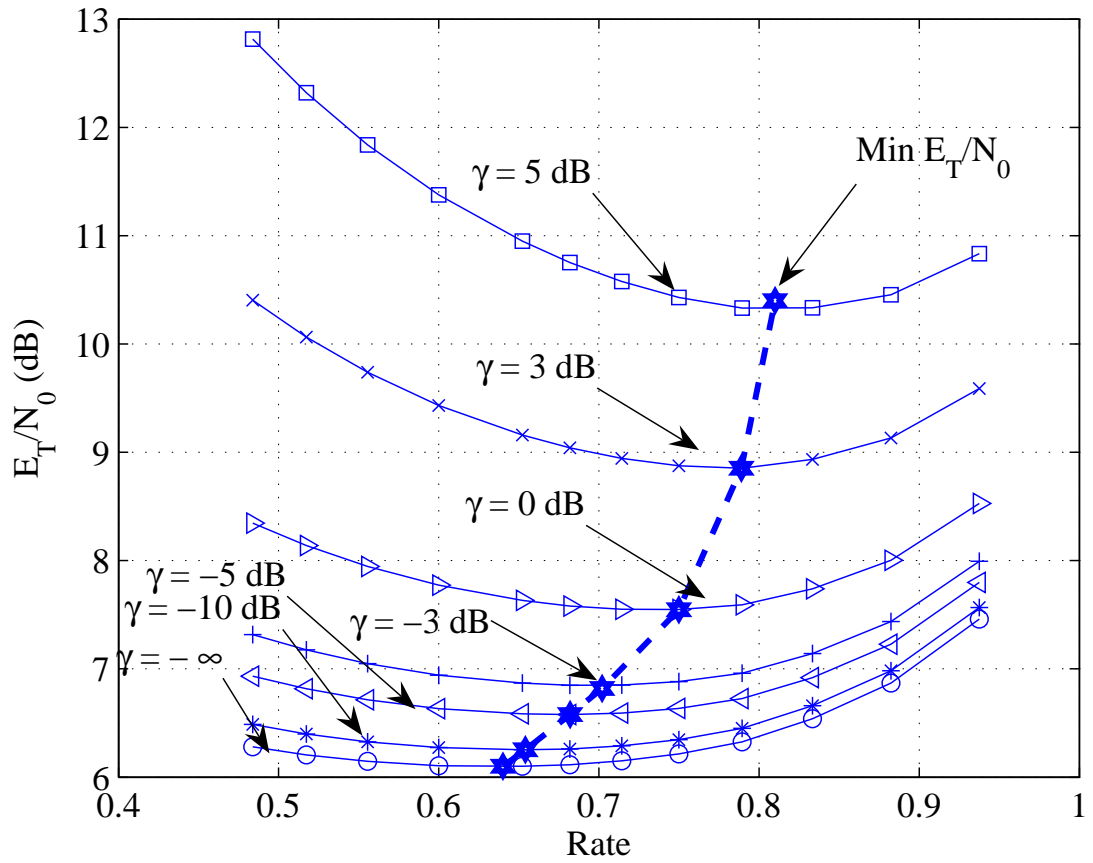


Figure 4.29: Total energy consumption for a communication system using RS codes over $GF(2^8)$ with $K = 30$ and packet error rate of 0.01 .

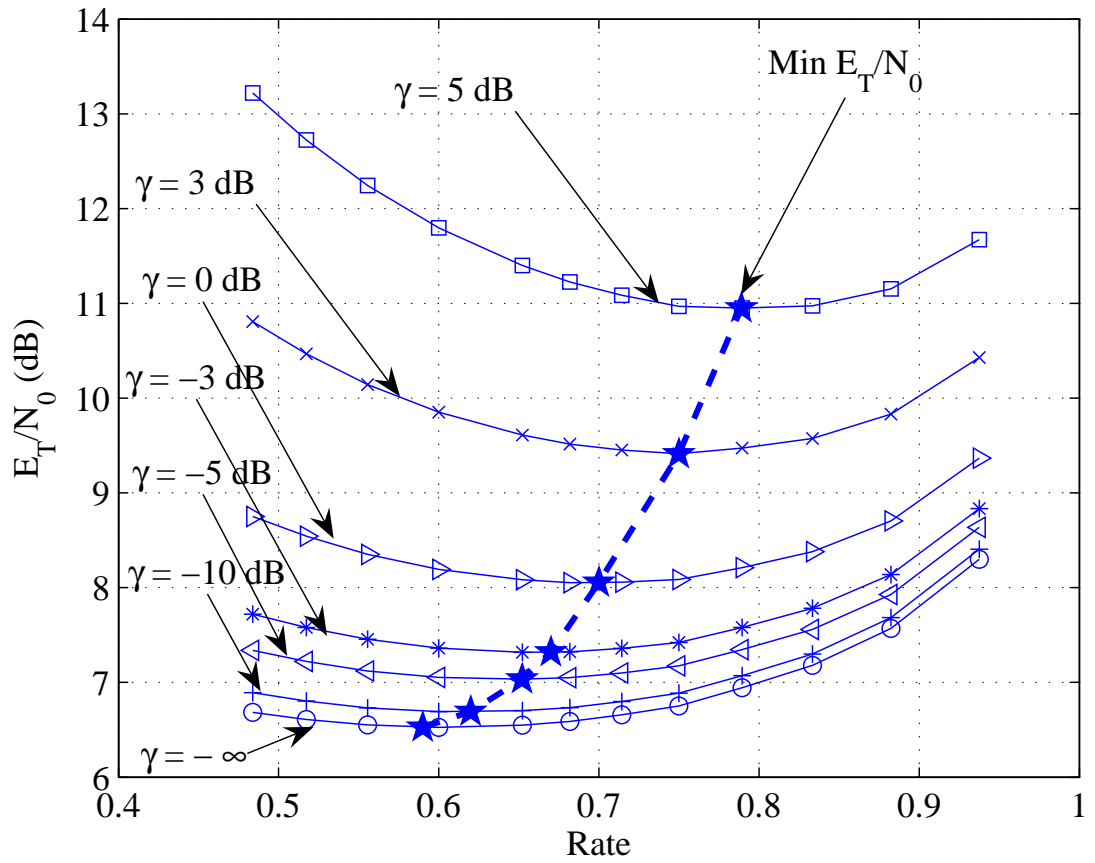


Figure 4.30: Total energy consumption for a communication system using RS codes over $GF(2^8)$ with $K = 30$ and packet error rate of 0.001 .

shift register consists of L stages and m linear algebraic function generators. The parameter L is called the constraint length of the convolutional code. For short constraint length convolutional codes, Viterbi decoding is predominately used. For long constraint length, sequential decoding is preferred as the complexity of Viterbi decoding becomes prohibitive. The choice of constraint length is dictated by the desired coding gain.

We use rate $\frac{1}{2}$, $\frac{1}{3}$ and $\frac{1}{2}$ convolutional codes of constraint length 7 with generators [133] and [171]. In addition, by puncturing the codes, we obtain rate $\frac{2}{3}$, $\frac{3}{4}$, $\frac{7}{8}$ and $\frac{15}{16}$ convolutional codes. The rate 1 convolutional code is actually the uncoded case. The information packet size is 128 bits with packet error probability of 0.01. The optimum code rate for an error probability of 0.01 using various convolutional codes is simulated over an AWGN channel. The results are compared with the cutoff rate over an AWGN channel for normalized processing energy -10.10 dB and 1.938 dB in Fig. (4.31) and (4.32) respectively.

From the figures, we observed that the performance of convolutional codes is very close to the cutoff rate over an AWGN channel when $k = 128$ bits. In addition, it is seen that convolutional codes perform better than that predicted by the cutoff rate when the code rate is very high. This is not really true since when code rate =1, there is no coding done on the information packet. That is, we are not using convolutional code at rate=1. As the cutoff rate is only good at predicting performance with coding, it is not surprise that the uncoded case is better. The performance comparison between the convolutional codes and cutoff rate over a Rayleigh fading channel with noncoherent detection is shown in Fig. 4.33. Similar to the case of AWGN channel, the performance of convolutional codes is only slightly inferior to the cutoff rate at low rate.

4.6 Conclusion

In this chapter, we studied the relationship between total energy consumed and channel code rate using the cutoff rate. We derived a closed form expression for the optimal code rate over an AWGN channel. The performance using the cutoff rate was compared with the one using the capacity over an AWGN channel. For Rayleigh fading

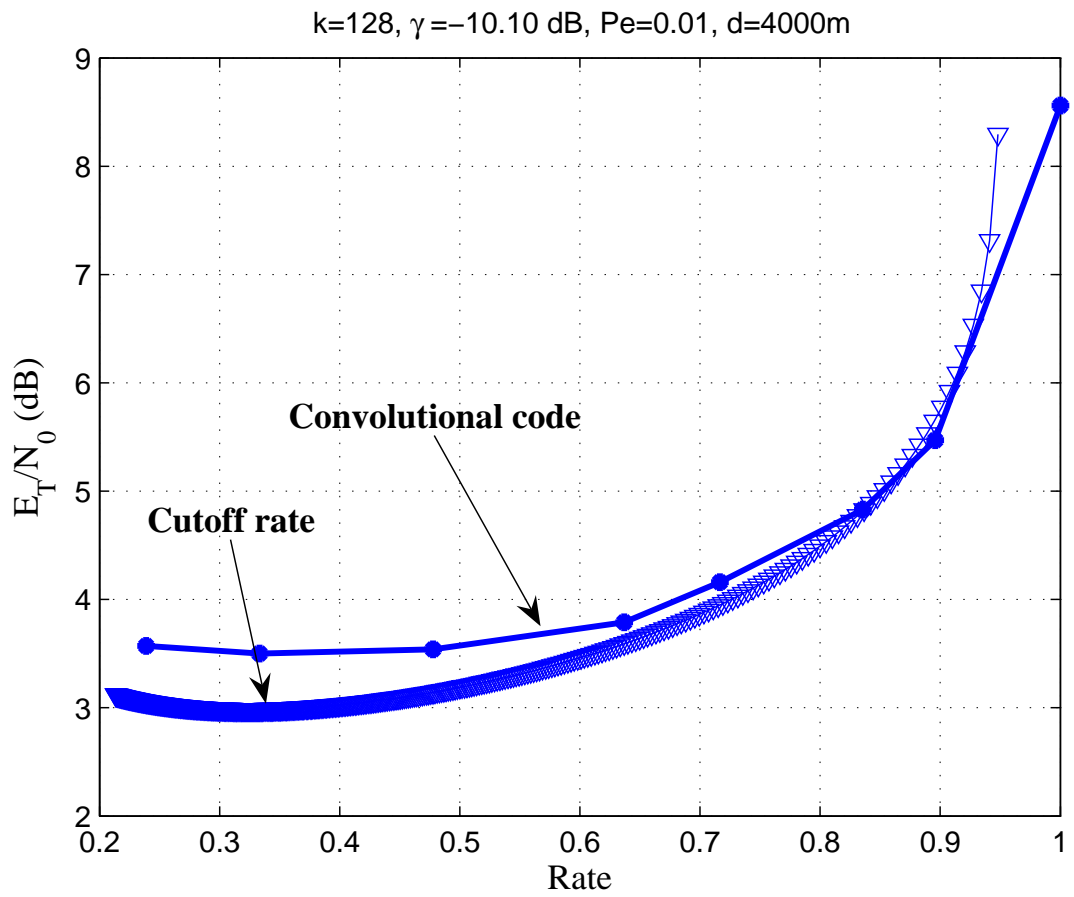


Figure 4.31: Performance comparison using cutoff rate and convolutional code over an AWGN channel for $\gamma = -10.10$ dB.

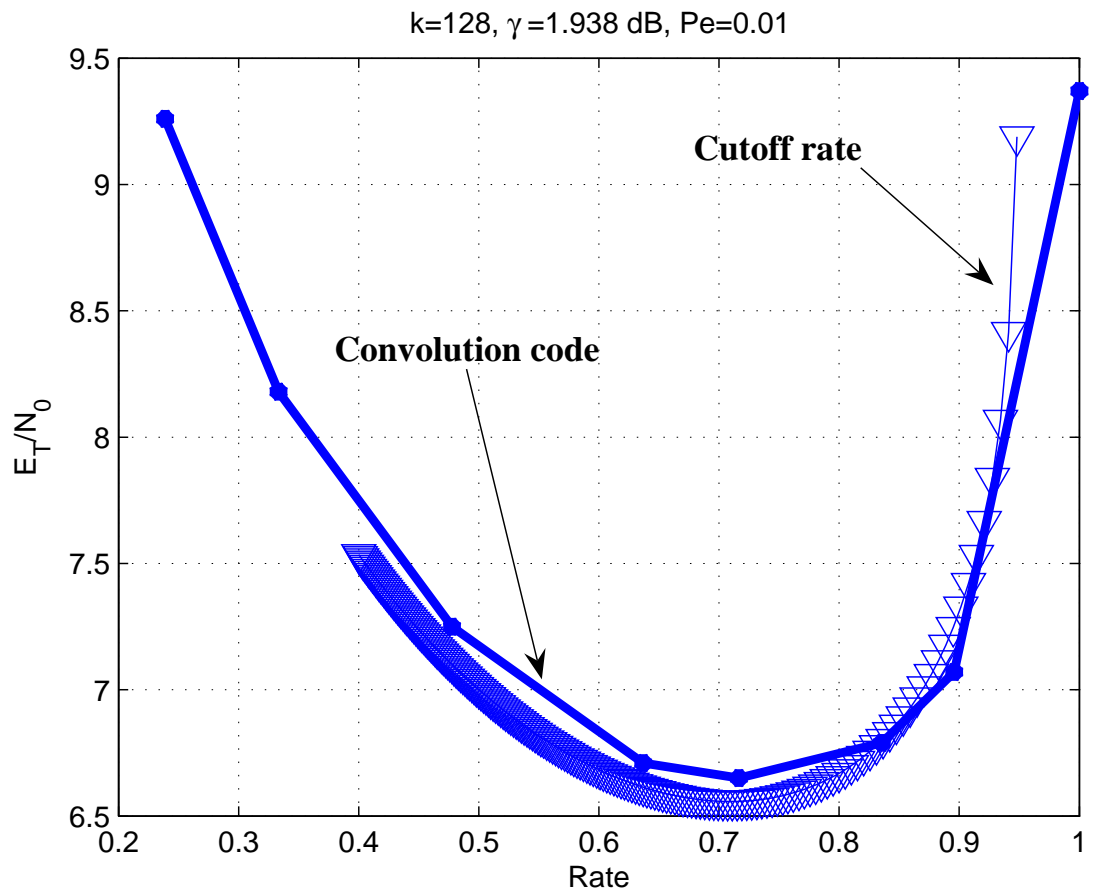


Figure 4.32: Performance comparison using cutoff rate and convolutional code over an AWGN channel for $\gamma = 1.938$ dB.

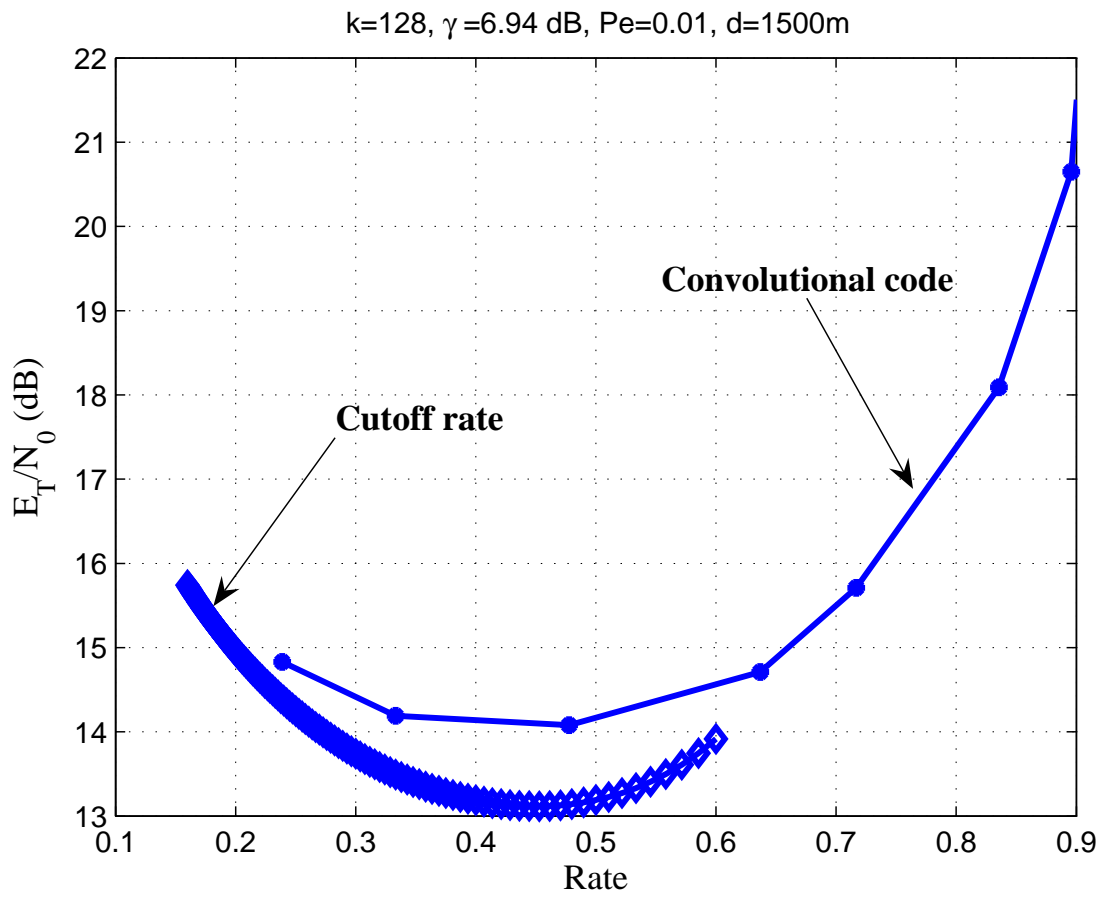


Figure 4.33: Performance comparison using cutoff rate and convolutional code over a Rayleigh channel for $\gamma = 6.94$ dB.

channel, the cutoff rate for noncoherent detection was used in the study. Both the energy consumption over an AWGN and a Rayleigh channel show that a high code rate is desired when the contribution of processing energy is large. For practical coding, we present the result using RS codes and convolutional codes. The result also show that to achieve minimum energy consumed, high code rate is required when processing energy is not insignificant. The performance of convolutional codes is slightly inferior to the cutoff rate for both an AWGN channel and a Rayleigh channel.

CHAPTER 5

Performance Comparison of Product Codes and Reed-Solomon Codes

In this chapter, we compare the performance of turbo product codes and RS codes over a binary symmetric channel (BSC), an additive white Gaussian noise channel (AWGN) and a bursty channel using binary phase shift keying (BPSK) modulation. While turbo product codes are shown to be effective in reducing the signal-to-noise ratio required to achieve given performance requirements, the iterative MAP decoding algorithm requires considerable computational cost. Whereas for the RS code, they can be configured with long block lengths (in bits) with less decoding time than other codes of similar lengths. This is because the decoder logic works with symbol-based rather than bit-based arithmetic [15]. This lead to our motivation in comparing the performance of RS and turbo product codes under different situations and hope to understand situations where the RS decoder's performance is comparable to turbo decoder. In situations where the bit error performance is comparable, we can replace the turbo decoder with the widely used RS decoder.

In Section 5.1, we give an overview of the structure of a product code and follow by a description on the construction of a rate $\frac{1}{2}$ product code and its decoding algorithm in Section 5.2 and 5.3 respectively. In Section 5.4, we present the system models under considerations for the various channels that we investigated. A discussion on the performance comparison over the BSC and AWGN channel is presented in Section

5.5 and 5.6 respectively. In Section 5.7, we look at their performance over the erasure channel. Finally, the chapter concludes with an investigation of performance on bursty channel in Section 5.8.

5.1 Structure of Product Codes

Product codes are powerful error correcting block codes first described by Elias in 1954 [22]. The concept of product codes is very simple. These codes are relatively efficient for building very long block codes by using two or more short block codes. By the early 1980s, at least one paper and textbook had been published describing the advantages of the iterative decoding of product codes [15], [47]. In this section, we describe the construction of a product code.

A linear systematic block code C is parameterized by (n, k, d_{min}) , where n, k and d_{min} stand for the number of bits in a codeword, the number of information bits and the minimum Hamming distance respectively. The minimum distance d_{min} is defined as the smallest distance between all pairs of codewords. For MDS codes, $d_{min} = n - k + 1$. A code with minimum distance d_{min} is capable of correcting any combination of t or fewer errors, provided [7]

$$t \leq \left\lfloor \frac{d_{min} - 1}{2} \right\rfloor = \left\lfloor \frac{n - k}{2} \right\rfloor \quad (5.1)$$

where $\lfloor x \rfloor$ means the largest integer not to exceed x .

Consider two linear systematic codes C^1 and C^2 with parameters $(n_1, K_1, d_{min,1})$ and $(n_2, k_2, d_{min,2})$. From Fig. 5.1, the product code $\mathcal{P} = C^1 \otimes C^2$ is constructed by:

- 1) placing $(k_1 \times k_2)$ information bits in an array of k_1 rows and k_2 columns;
- 2) encoding each of the k_1 rows using code C^2 and as a result, we have a total of n_2 columns;
- 3) encoding each of the n_2 columns using code C^1 .

The parameters of the product code \mathcal{P} are $n = n_1 \times n_2, k = k_1 \times k_2, d_{min} = d_{min,1} \times d_{min,2}$. Its code rate is $R = R_1 \times R_2$ where code rate is defined as ratio of the number of

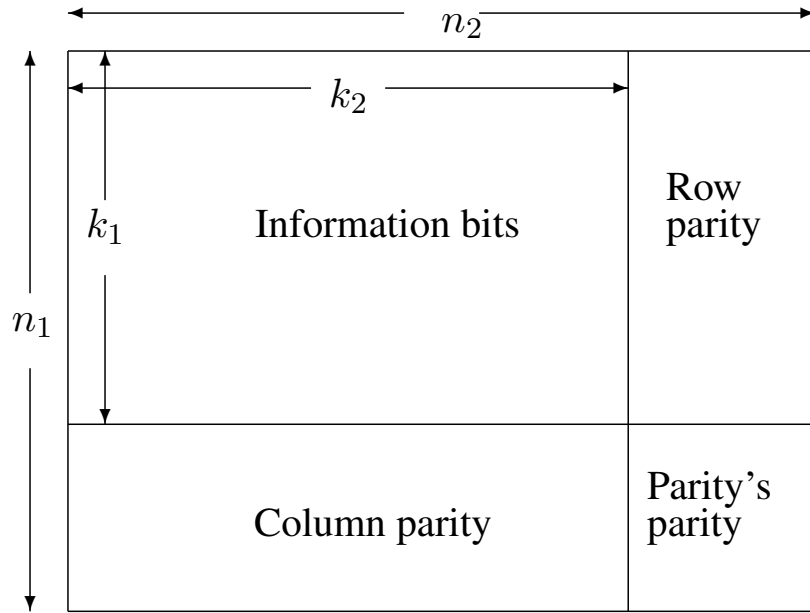


Figure 5.1: Construction of product code $\mathcal{P} = C_1 \times C_2$.

information bits (k) over the total number of bits transmitted (n). Therefore, $R_1 = k_1/n_1$ and $R_2 = k_2/n_2$. Hence, it is possible to construct very long block codes with large minimum Hamming distance by combining short codes with small minimum Hamming distance. From the way the product code is constructed, it is obvious that the $(n_2 - k_2)$ last columns of the matrix \mathcal{P} belongs to the codeword of C^2 and the $(n_1 - k_1)$ last rows of matrix \mathcal{P} are codewords of C^1 . Therefore, all rows of matrix \mathcal{P} are codewords of C^2 and all columns of matrix \mathcal{P} are codewords of C^1 .

Decoding is performed iteratively by decoding first the row code followed by column code. This decoding process is iterated several times, feeding the decoder output back to the input, to maximize performance of the decoder. Because of the parallels with a turbocharger on an engine (where the exhaust drives the inlet) this type of error correcting scheme has been given the name turbo coding.

5.2 Construction of Rate 1/2 Product Codes

This section is devoted to the construction of rate $\frac{1}{2}$ product code using the well known Hamming code. These codes were discovered independently by Marcel Golay in 1949 and Richard Hamming in 1950 [3]. They are perfect, linear, and very easy to decode. Consider a (15,11) Hamming code which has the following generator matrix:

$$G = \begin{bmatrix} 1 & 0 & 0 & 0 & 0 & 0 & 0 & 0 & 0 & 0 & 0 & 0 & 1 & 0 & 1 \\ 0 & 1 & 0 & 0 & 0 & 0 & 0 & 0 & 0 & 0 & 0 & 0 & 0 & 1 & 1 & 0 \\ 0 & 0 & 1 & 0 & 0 & 0 & 0 & 0 & 0 & 0 & 0 & 0 & 0 & 1 & 1 & 1 \\ 0 & 0 & 0 & 1 & 0 & 0 & 0 & 0 & 0 & 0 & 0 & 0 & 0 & 0 & 1 & 1 \\ 0 & 0 & 0 & 0 & 1 & 0 & 0 & 0 & 0 & 0 & 0 & 0 & 1 & 0 & 0 & 1 \\ 0 & 0 & 0 & 0 & 0 & 1 & 0 & 0 & 0 & 0 & 0 & 0 & 1 & 0 & 1 & 0 \\ 0 & 0 & 0 & 0 & 0 & 0 & 1 & 0 & 0 & 0 & 0 & 0 & 1 & 0 & 1 & 1 \\ 0 & 0 & 0 & 0 & 0 & 0 & 0 & 1 & 0 & 0 & 0 & 0 & 1 & 1 & 0 & 0 \\ 0 & 0 & 0 & 0 & 0 & 0 & 0 & 0 & 1 & 0 & 0 & 0 & 1 & 1 & 0 & 1 \\ 0 & 0 & 0 & 0 & 0 & 0 & 0 & 0 & 0 & 1 & 0 & 1 & 1 & 1 & 1 & 0 \\ 0 & 0 & 0 & 0 & 0 & 0 & 0 & 0 & 0 & 0 & 1 & 1 & 1 & 1 & 1 & 1 \end{bmatrix}$$

and parity check matrix

$$H = \begin{bmatrix} 0 & 0 & 0 & 0 & 1 & 1 & 1 & 1 & 1 & 1 & 1 & 1 & 0 & 0 & 0 \\ 1 & 1 & 1 & 0 & 0 & 0 & 0 & 1 & 1 & 1 & 1 & 0 & 1 & 0 & 0 \\ 0 & 1 & 1 & 1 & 0 & 1 & 1 & 0 & 0 & 1 & 1 & 0 & 0 & 1 & 0 \\ 1 & 0 & 1 & 1 & 1 & 0 & 1 & 0 & 1 & 0 & 1 & 0 & 0 & 0 & 1 \end{bmatrix}$$

Shortening a code means reducing the number of information bits, keeping the number of parity checks the same. The length n and the dimension k are thus reduced by the

same amount [48]. Therefore, by code shortening, we are able to transform the (15,11) code to (12,8) code by reducing 3 information bits. The resulting generator matrix is of dimension 8×12

$$G = \begin{bmatrix} 1 & 0 & 0 & 0 & 0 & 0 & 0 & 0 & 0 & 0 & 1 & 1 \\ 0 & 1 & 0 & 0 & 0 & 0 & 0 & 0 & 1 & 0 & 0 & 1 \\ 0 & 0 & 1 & 0 & 0 & 0 & 0 & 0 & 1 & 0 & 1 & 0 \\ 0 & 0 & 0 & 1 & 0 & 0 & 0 & 0 & 1 & 0 & 1 & 1 \\ 0 & 0 & 0 & 0 & 1 & 0 & 0 & 0 & 1 & 1 & 0 & 0 \\ 0 & 0 & 0 & 0 & 0 & 1 & 0 & 0 & 1 & 1 & 0 & 1 \\ 0 & 0 & 0 & 0 & 0 & 0 & 1 & 0 & 1 & 1 & 1 & 0 \\ 0 & 0 & 0 & 0 & 0 & 0 & 0 & 1 & 1 & 1 & 1 & 1 \end{bmatrix}$$

and correspond parity check matrix

$$H = \begin{bmatrix} 0 & 1 & 1 & 1 & 1 & 1 & 1 & 1 & 1 & 0 & 0 & 0 \\ 0 & 0 & 0 & 0 & 1 & 1 & 1 & 1 & 0 & 1 & 0 & 0 \\ 1 & 0 & 1 & 1 & 0 & 0 & 1 & 1 & 0 & 0 & 1 & 0 \\ 1 & 1 & 0 & 1 & 0 & 1 & 0 & 1 & 0 & 0 & 0 & 1 \end{bmatrix}$$

By removing the parity's parity bits, the product code is reduced from (144,64) to (128,64). The (128,64) product code has 64 information bits arranged in a 8 by 8 array. Each row and column are protected by the (12,8) shortened Hamming code with the above generator matrix and parity check matrix. The code is describe by the following figure.

b_1	b_2	b_3	b_4	b_5	b_6	b_7	b_8	$p_{1,1}$	$p_{1,2}$	$p_{1,3}$	$p_{1,4}$
b_9	b_{10}	b_{11}	b_{12}	b_{13}	b_{14}	b_{15}	b_{16}	$p_{2,1}$	$p_{2,2}$	$p_{2,3}$	$p_{2,4}$
b_{17}	b_{18}	b_{19}	b_{20}	b_{21}	b_{22}	b_{23}	b_{24}	$p_{3,1}$	$p_{3,2}$	$p_{3,3}$	$p_{3,4}$
b_{25}	b_{26}	b_{27}	b_{28}	b_{29}	b_{30}	b_{31}	b_{32}	$p_{4,1}$	$p_{4,2}$	$p_{4,3}$	$p_{4,4}$
b_{33}	b_{34}	b_{35}	b_{36}	b_{37}	b_{38}	b_{39}	b_{40}	$p_{5,1}$	$p_{5,2}$	$p_{5,3}$	$p_{5,4}$
b_{41}	b_{42}	b_{43}	b_{44}	b_{45}	b_{46}	b_{47}	b_{48}	$p_{6,1}$	$p_{6,2}$	$p_{6,3}$	$p_{6,4}$
b_{49}	b_{50}	b_{51}	b_{52}	b_{53}	b_{54}	b_{55}	b_{56}	$p_{7,1}$	$p_{7,2}$	$p_{7,3}$	$p_{7,4}$
b_{57}	b_{58}	b_{59}	b_{60}	b_{61}	b_{62}	b_{63}	b_{64}	$p_{8,1}$	$p_{8,2}$	$p_{8,3}$	$p_{8,4}$
$p_{9,1}$	$p_{10,1}$	$p_{11,1}$	$p_{12,1}$	$p_{13,1}$	$p_{14,1}$	$p_{15,1}$	$p_{16,1}$				
$p_{9,2}$	$p_{10,2}$	$p_{11,2}$	$p_{12,2}$	$p_{13,2}$	$p_{14,2}$	$p_{15,2}$	$p_{16,2}$				
$p_{9,3}$	$p_{10,3}$	$p_{11,3}$	$p_{12,3}$	$p_{13,3}$	$p_{14,3}$	$p_{15,3}$	$p_{16,3}$				
$p_{9,4}$	$p_{10,4}$	$p_{11,4}$	$p_{12,4}$	$p_{13,4}$	$p_{14,4}$	$p_{15,4}$	$p_{16,4}$				

5.3 Turbo Decoding of Rate 1/2 Product Codes

The received signal of a (128,64) product code can be written as written as

r_1	r_2	r_3	r_4	r_5	r_6	r_7	r_8	r_{65}	r_{66}	r_{67}	r_{68}
r_9	r_{10}	r_{11}	r_{12}	r_{13}	r_{14}	r_{15}	r_{16}	r_{69}	r_{70}	r_{71}	r_{72}
r_{17}	r_{18}	r_{19}	r_{20}	r_{21}	r_{22}	r_{23}	r_{24}	r_{73}	r_{74}	r_{75}	r_{76}
r_{25}	r_{26}	r_{27}	r_{28}	r_{29}	r_{30}	r_{31}	r_{32}	r_{77}	r_{78}	r_{79}	r_{80}
r_{33}	r_{34}	r_{35}	r_{36}	r_{37}	r_{38}	r_{39}	r_{40}	r_{81}	r_{82}	r_{83}	r_{84}
r_{41}	r_{42}	r_{43}	r_{44}	r_{45}	r_{46}	r_{47}	r_{48}	r_{85}	r_{86}	r_{87}	r_{88}
r_{49}	r_{50}	r_{51}	r_{52}	r_{53}	r_{54}	r_{55}	r_{56}	r_{89}	r_{90}	r_{91}	r_{92}
r_{57}	r_{58}	r_{59}	r_{60}	r_{61}	r_{62}	r_{63}	r_{64}	r_{93}	r_{94}	r_{95}	r_{96}
r_{97}	r_{98}	r_{99}	r_{100}	r_{101}	r_{102}	r_{103}	r_{104}				
r_{105}	r_{106}	r_{107}	r_{108}	r_{109}	r_{110}	r_{111}	r_{112}				
r_{113}	r_{114}	r_{115}	r_{116}	r_{117}	r_{118}	r_{119}	r_{120}				
r_{121}	r_{122}	r_{123}	r_{124}	r_{125}	r_{126}	r_{127}	r_{128}				

We use iterative decoding to approximate the minimize the probability of choosing the wrong information bit for each of the 64 information bits. To do this, we need to

start with the optimal bit decision rule. For the first bit, b_1 , the minimum bit error probability rule is to compute the maximum a posteriori probability. Consider the likelihood for b_1 based solely on the received values corresponding to the first row of the product code, \mathbf{r}). For AWGN channel, the log-likelihood for this bit can be written as:

$$\begin{aligned}
\Lambda_{h,1} &= \log \left[\frac{P(b_1 = +1|\mathbf{r})}{P(b_1 = -1|\mathbf{r})} \right] \\
&= \log \left[\frac{P(\mathbf{r}|b_1 = +1)P(b_1 = +1)/P(\mathbf{r})}{P(\mathbf{r}|b_1 = -1)P(b_1 = -1)/P(\mathbf{r})} \right] \\
&= \log \left[\frac{P(\mathbf{r}|b_1 = +1)P(b_1 = +1)}{P(\mathbf{r}|b_1 = -1)P(b_1 = -1)} \right] \\
&= \log \left\{ \left[\frac{P(b_1 = +1)}{P(b_1 = -1)} \right] \left[\frac{P(r_1, \dots, r_8, r_{65}, r_{66}, r_{67}, r_{68}|b_1 = +1)}{P(r_1, \dots, r_8, r_{65}, r_{66}, r_{67}, r_{68}|b_1 = -1)} \right] \right\} \\
&= \log \left[\frac{P(b_1 = +1)}{P(b_1 = -1)} \right] + \log \left[\frac{P(r_1, \dots, r_8, r_{65}, r_{66}, r_{67}, r_{68}|b_1 = +1)}{P(r_1, \dots, r_8, r_{65}, r_{66}, r_{67}, r_{68}|b_1 = -1)} \right] \\
&= \log \left[\frac{P(b_1 = +1)}{P(b_1 = -1)} \right] + \log \left[\frac{P(r_1|b_1 = +1)}{P(r_1|b_1 = -1)} \right] \\
&+ \log \left[\frac{P(r_2, \dots, r_8, r_{65}, r_{66}, r_{67}, r_{68}|b_1 = +1)}{P(r_2, \dots, r_8, r_{65}, r_{66}, r_{67}, r_{68}|b_1 = -1)} \right]. \tag{5.2}
\end{aligned}$$

The first term is the a priori information about b_1 without any observation, the second term is the intrinsic information about b_1 given the observation r_1 . The last term is the extrinsic information about b_1 based on observing just $r_2, r_3, r_4, r_5, r_6, r_7, r_8, r_{65}, r_{66}, r_{67}, r_{68}$. Let

$$L_i = \log \left[\frac{P(b_i = +1)}{P(b_i = -1)} \right]. \tag{5.3}$$

$$\begin{aligned}
L(r_i) &= \log \left[\frac{P(r_i|b_i = +1)}{P(r_i|b_i = -1)} \right] \\
&= \log \left[\frac{\frac{1}{\sqrt{\pi N_0}} \exp\{-(r_i - \sqrt{E})^2/N_0\}}{\frac{1}{\sqrt{\pi N_0}} \exp\{-(r_i + \sqrt{E})^2/N_0\}} \right] \\
&= \frac{4r_i\sqrt{E}}{N_0} \quad i = 1, 2, \dots, 64. \tag{5.4}
\end{aligned}$$

$$L_{h,1} = \log \left[\frac{P(r_2, \dots, r_8, r_{65}, r_{66}, r_{67}, r_{68} | b_1 = +1)}{P(r_2, \dots, r_8, r_{65}, r_{66}, r_{67}, r_{68} | b_1 = -1)} \right]. \quad (5.5)$$

Therefore, we have

$$\Lambda_{h,1} = L_1 + L(r_1) + L_{h,1}. \quad (5.6)$$

In order to calculate the extrinsic information, we average out the “nuisance parameters” $b_2, b_3, b_4, b_5, b_6, b_7, b_8$.

$$\begin{aligned} & P(r_2, \dots, r_8, r_{65}, r_{66}, r_{67}, r_{68} | b_1 = +1) \\ = & \sum_{b_2, \dots, b_8} P(r_2, \dots, r_8, r_{65}, r_{66}, r_{67}, r_{68} | b_1 = +1, b_2, b_3, \dots, b_7, b_8) P\{b_2\} P\{b_3\} \dots P\{b_7\} P\{b_8\}. \end{aligned} \quad (5.7)$$

$$\begin{aligned} & P(r_2, \dots, r_8, r_{65}, r_{66}, r_{67}, r_{68} | b_1 = -1) \\ = & \sum_{b_2, \dots, b_8} P(r_2, \dots, r_8, r_{65}, r_{66}, r_{67}, r_{68} | b_1 = -1, b_2, b_3, \dots, b_7, b_8) P\{b_2\} P\{b_3\} \dots P\{b_7\} P\{b_8\}. \end{aligned} \quad (5.8)$$

The likelihoods for $b_2, b_3, b_4, b_5, b_6, b_7, b_8$ are initially set to $1/2$ for data bits $+1$ and -1 . After computing the extrinsic information of the likelihood for b_1 , we proceed with bits b_2, b_3, \dots, b_{64} based on their corresponding horizontal parity checks.

Once we complete an iteration of all the rows, we continue to compute the extrinsic information for the likelihood of the b_i 's based on their corresponding vertical parity checks, using the extrinsic information from the previous row computation. After a full iteration of both the column and the rows, the likelihoods for these bits will be obtained from the extrinsic information from the vertical parity checks. After several iterations, we compute the decisions for the bits based on (assuming equally likely a priori probabilities)

$$\Lambda_i = L(r_i) + L_{h,i} + L_{v,i}. \quad (5.9)$$

If $\Lambda_i \geq 0$ we decide $b_i = 1$, else $b_i = 0$. For the BSC, $b_i \in \{0,1\}$ and $r_i \in \{0,1\}$, we have

$$\begin{aligned} \Lambda_1 &= \log \left[\frac{P(b_1 = 1)}{P(b_1 = 0)} \right] + \log \left[\frac{P(r_1|b_1 = 1)}{P(r_1|b_1 = 0)} \right] \\ &+ \log \left[\frac{P(r_2, \dots, r_8, r_{65}, r_{66}, r_{67}, r_{68}|b_1 = 1)}{P(r_2, \dots, r_8, r_{65}, r_{66}, r_{67}, r_{68}|b_1 = 0)} \right]. \end{aligned} \quad (5.10)$$

$$L_i = \log \left[\frac{P(b_i = 1)}{P(b_i = 0)} \right]. \quad (5.11)$$

$$\begin{aligned} L(r_i) &= \log \left[\frac{P(r_i|b_i = 1)}{P(r_i|b_i = 0)} \right] \\ &= \log \left[\frac{(1-p)^{r_i} p^{1-r_i}}{(1-p)^{1-r_i} p^{r_i}} \right] \\ &= \log \left(\frac{p}{1-p} \right)^{1-2r_i} \\ &= (1-2r_i) \log \left(\frac{p}{1-p} \right). \end{aligned} \quad (5.12)$$

$$L_{h,1} = \log \left[\frac{P(r_2, \dots, r_8, r_{65}, r_{66}, r_{67}, r_{68}|b_1 = 1)}{P(r_2, \dots, r_8, r_{65}, r_{66}, r_{67}, r_{68}|b_1 = 0)} \right]. \quad (5.13)$$

5.4 System Models

In our study, we investigate 3 different channels. They are the BSC, AWGN channel and a bursty channel. The BSC shown in Fig. 5.2 is a discrete memoryless channel model which captures the behavior of a communications system with binary modulation and hard decisions on each symbol. The input x has alphabet 0,1 and the demodulator output y has alphabet 0,1. For a BSC, for either input value of x , and independent

of the transmitted or received values of any previous bits, x is received in error with probability p and received correctly with probability $1 - p$. In terms of conditional probability, we write this as

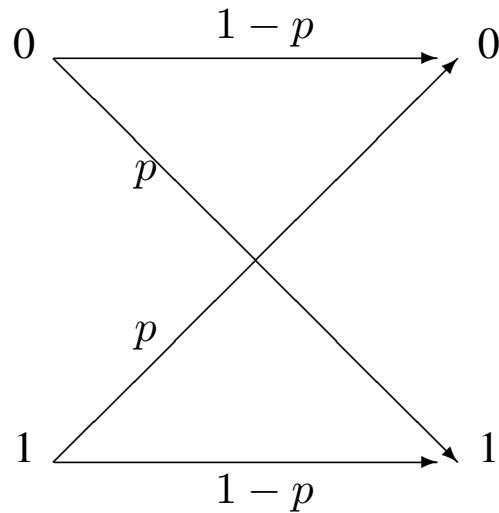


Figure 5.2: BSC model for communication channel.

$$P(y = 1|x = 0) = P(y = 0|x = 1) = p;$$

$$P(y = 0|x = 0) = P(y = 1|x = 1) = 1 - p;$$

The system model for the BSC which use the RS codes is shown in Fig. 5.3 We define t to be the number of symbol errors that is correctable by the RS codes and assume that the decoding error of RS codes is negligible. In this setup, when the number of error symbols is greater than t , the RS decoder will not be able to decode the received symbols and the selecting switch will switch to accept the bits directly from the output of the demodulator. The system model on the BSC using the TP codes is shown in Fig. 5.4

In the AWGN channel, the received signal r is modelled as follow:

$$r = s + n,$$

where s is the transmitted signal and n is the AWGN, which is a Gaussian random variable. The system models for the RS codes and TP codes are shown in Fig. 5.5

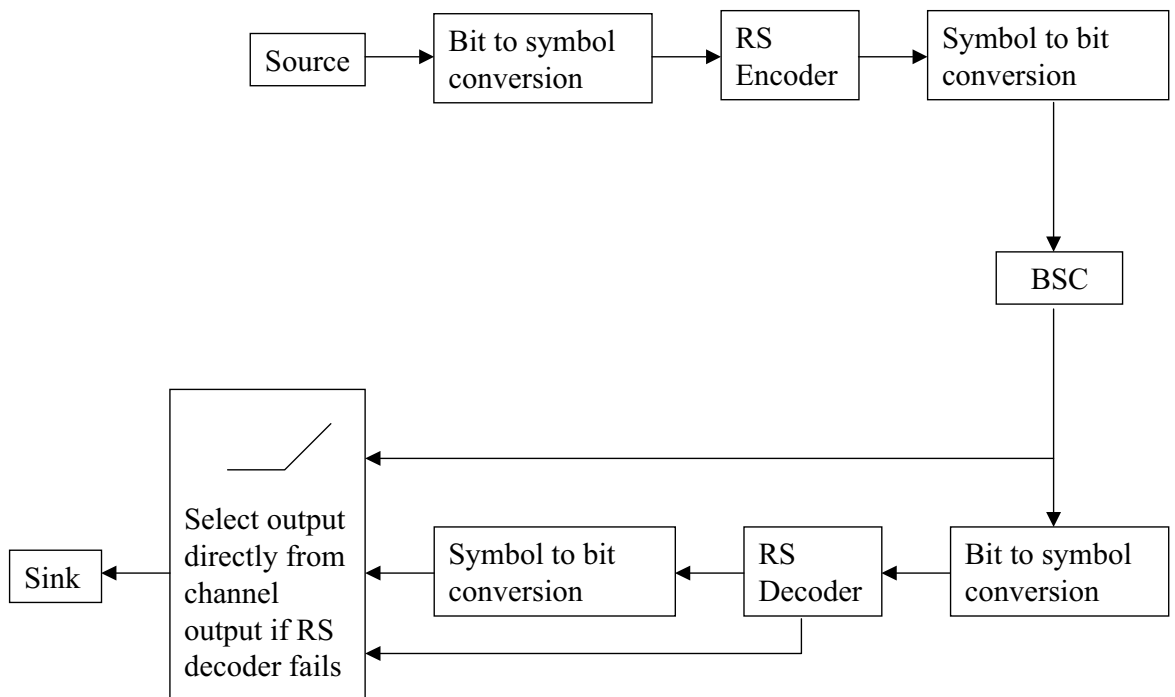


Figure 5.3: System model with BSC and RS codes.

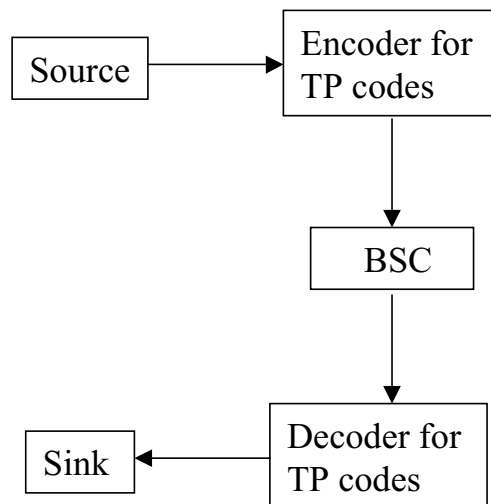


Figure 5.4: System model with BSC and TP codes.

and Fig. 5.6 respectively. Again, if the RS decoder is unable to decode the received symbols, the selecting switch will choose the received bits from the quantizer directly.

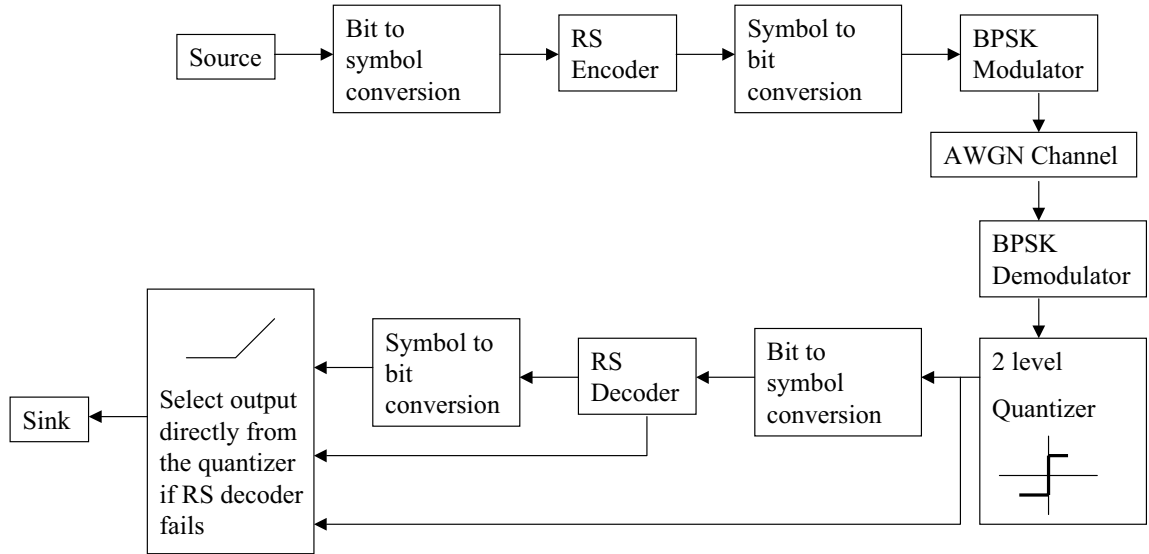


Figure 5.5: System model with AWGN channel and RS codes.

As RS codes have the capability of correcting erasures, we study the performance of RS codes for the erasure channel. In modeling the erasure channel, we use a three level quantizer to quantize the received bits from the AWGN channel as $\{-1, 0, 1\}$. From Fig. 5.7, the relationship between the received bits and the output of the quantizer, Q , is:

$$Q = \begin{cases} -1 & r \leq -\beta\sqrt{E}, \\ 0 & -\beta\sqrt{E} < r < \beta\sqrt{E}, \\ +1 & r \geq \beta\sqrt{E}, \end{cases}$$

where E is the energy of the coded bits transmitted.

When the output of the quantizer is 0, this indicates a bit erasure. We will give our definition of symbol error and erasure in Section IV. If the total number of symbol errors and erasures is greater than the maximum number of errors and erasures that the RS decoder can correct, the selecting switch will choose the received bits from the 2 level quantizer directly. The system model for the RS codes for the erasure channel is shown in Fig. 5.8.

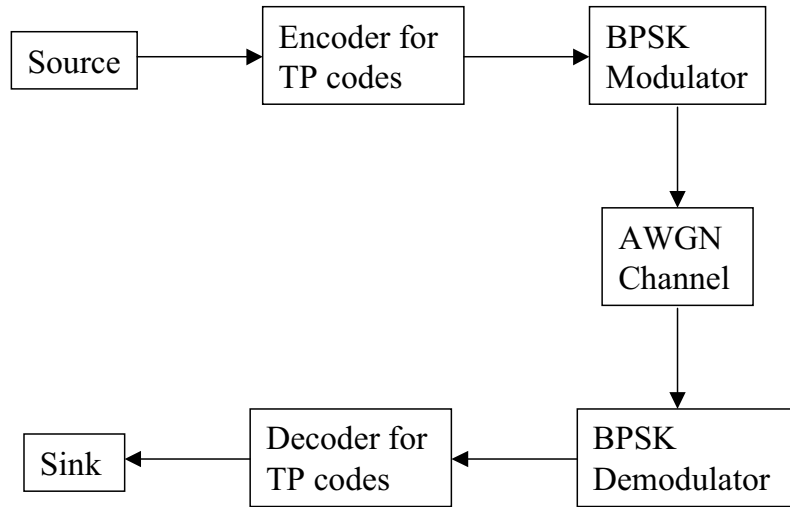


Figure 5.6: System configurations on the AWGN channel using TP codes.

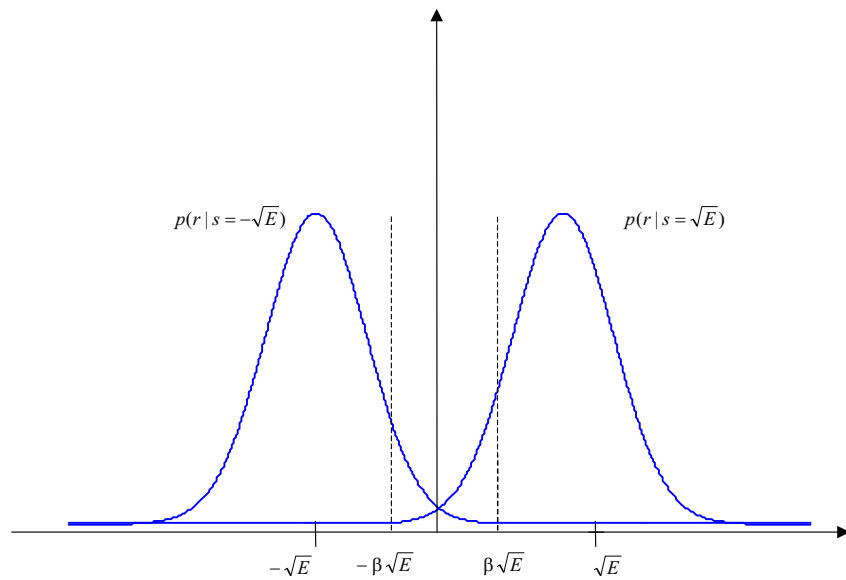


Figure 5.7: Probability density function of r with given transmitted bits. $|\beta\sqrt{E}|$ is the threshold for determine the receive bit as an erasure.

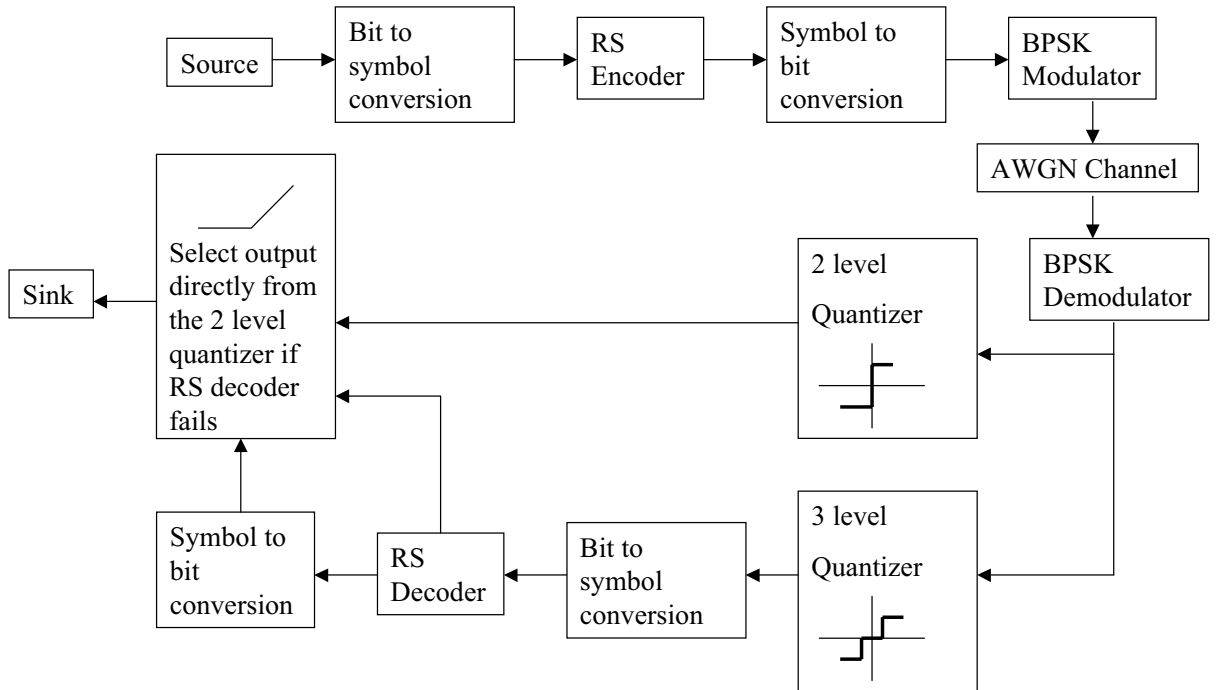


Figure 5.8: System configurations on the erasure channel using RS codes.

In the analysis of the the performance over a bursty channel, we study the case when the burst of noise last for a duration of 8 bits. The system model which uses RS codes over the bursty channel is similar to Fig. 5.5 and detailed analysis of its performance is discussed in Section 5.5. For the TP codes, we interleave the coded bits before transmission and at the receiver side, we deinterleave the coded bits before performing the turbo decoding. The system model is shown in Fig. 5.9 and its analysis is done in Section 5.5.

5.5 Performance Comparison over BSC

From the previous section, we know that the RS(16,8) over GF(256) code is able to correct up to $t=4$ byte errors. For a crossover probability p of the BSC, the 8-bit byte error, P_B is

$$P_B = 1 - (1 - p)^8. \quad (5.14)$$

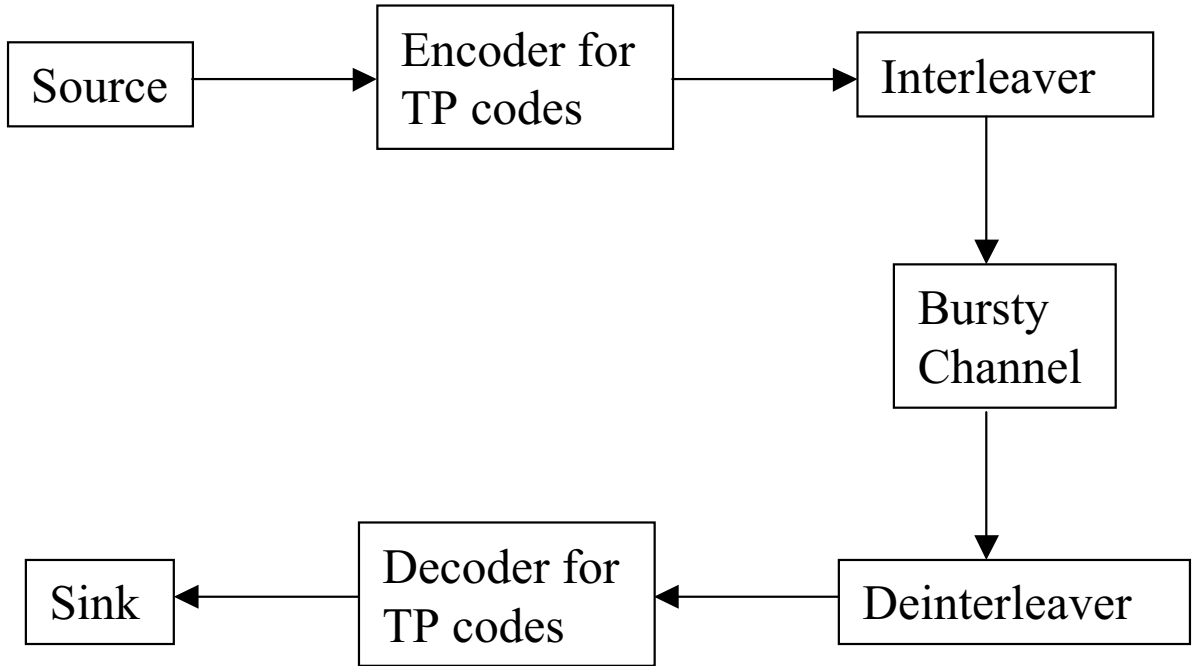


Figure 5.9: System configurations on the bursty channel using TP codes.

There are three possible decoding events for a RS decoder. They are:

1. ξ_{CD} : the RS decoder decodes the received bytes correctly.
2. ξ_{ICD} : the RS decoder decodes the received bytes incorrectly.
3. ξ_{ED} : the RS decoder detect the existence of symbol errors but fails to decode it, i.e. decoding failure.

An exact analysis of the probabilities of incorrect decoding requires a weight enumerator that lists the number of times each nonzero symbols (bytes) appears in the codeword of a given weight. Such information is much harder to obtain than the simple weight distribution. This has been studied in [7], [16], [49] and [50] extensively over the q -ary channel, with the assumption that all incorrect channel symbols occur with equal probability. This is not true in our model as each incorrect 8-bit byte occurs with different probability. Since the probability of a byte error decreases with the number of incorrect bits, by assuming that each symbol occur with equal probability, we arrive at

an upper bound for $Pr\{\xi_{ICD}\}$. In our analysis, we assume that $Pr\{\xi_{ICD}\}$ is negligible. Thus, this would give a lower bound performance that our system can achieve over the BSC. Let ξ_d, ξ_b, ξ_4 be the events that first bit is in error after decoding, first bit is in error, 4 or more of the last 15 bytes in error, respectively. From Fig. 5.3, we assume that if more than 4 byte errors occur, the decoder is able to determine an uncorrectable situation occurred (i.e. the event ξ_{ED}) and puts out the raw data. Then, since the RS decoder is able to correct a maximum of 4 byte errors, ξ_d occurs if the first received bit is in error and there are at least 4 out of the last 15 bytes are in errors. Also, event ξ_b and ξ_4 are independent. Therefore, we have

$$Pr\{\xi_d\} = Pr\{\xi_b \cap \xi_4\} = Pr\{\xi_b\}Pr\{\xi_4\} = p \sum_{l=4}^{15} \binom{15}{l} P_B^l (1 - P_B)^{15-l}. \quad (5.15)$$

A comparison of the performance of the RS code and TP code over BSC is shown in Fig. 5.10. The vertical axis is the bit error rate (BER) and horizontal axis is converted from p to signal-to-noise (SNR) ratio, E_b/N_0 , of the AWGN channel by comparing its equivalent with BPSK detection. Since it is a rate $\frac{1}{2}$ code, we have, $E_b = 2E$ and $p = Q(\sqrt{\frac{2E}{N_0}})$. Where E and E_b denotes the energy of the coded and uncoded bit respectively. From the figure, we observed that the TP code is about 2 dB better than the RS code.

Note that from (5.11), when implementing the decoder for the TP codes, we have used the actual value of p in our iterative decoding of the received codewords whereas the RS decoder does not need to know the value of p . However, in real situation, most of the time the TP decoder would not know the channel condition (i.e. the value of p). If the decoder uses a value that is different than the actual, we have a mismatch between the channel and the decoder. To investigate how the incorrect value of p affect the performance of the TP decoder, a simulation was done by fixing the value of p for the TP decoder while the channel experiences various different p values. If we fixed p at the corresponding E_b/N_0 of 3dB and 6dB, it can be seen from Fig. 5.11 that the TP decoder is very close to the performance of a decoder that uses the actual value of p . Hence, if we are unable to obtain the actual value of p , we can arbitrarily fixed it at one of these 2 values without a noticeable performance degradation.

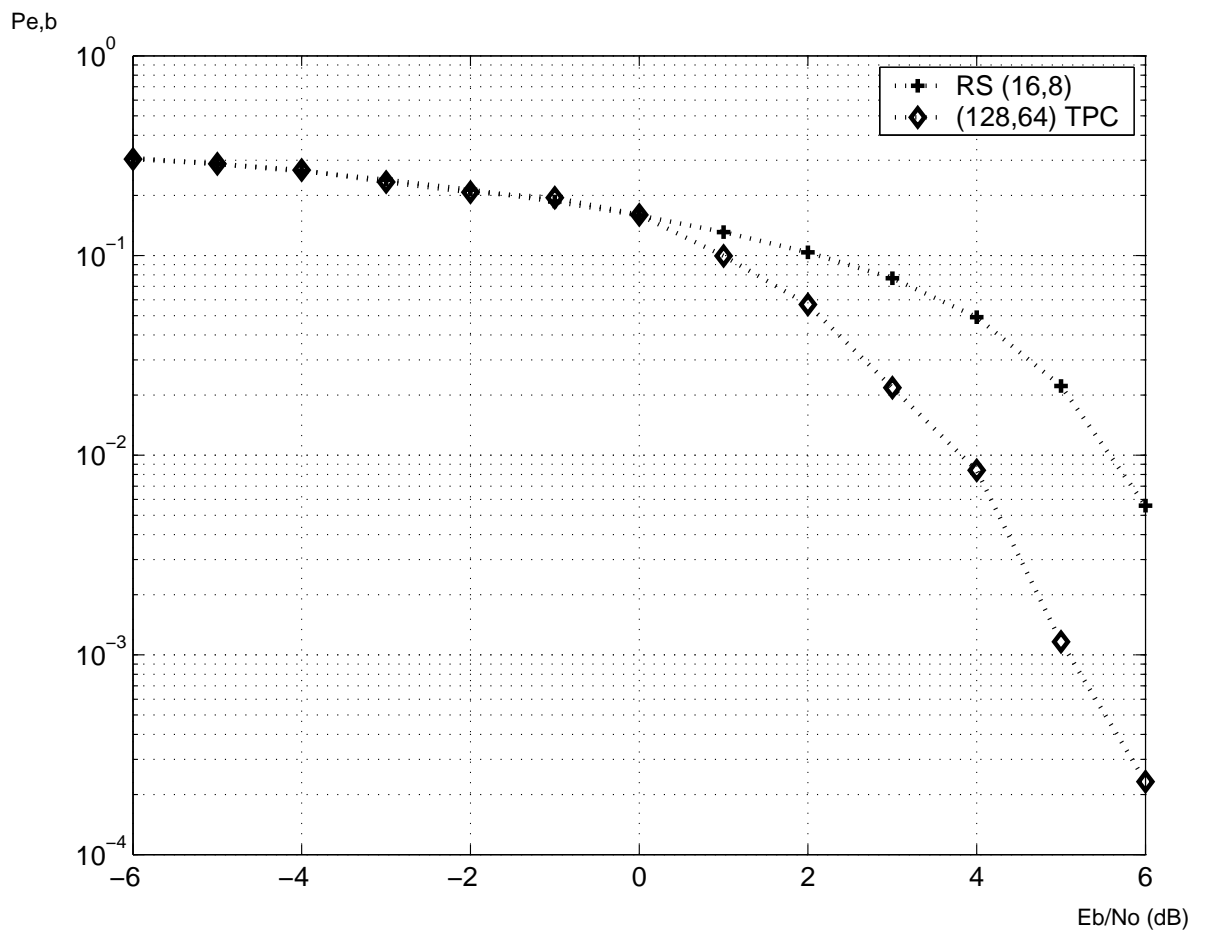


Figure 5.10: Comparison of performance between (128,64) TP codes and RS codes over BSC.

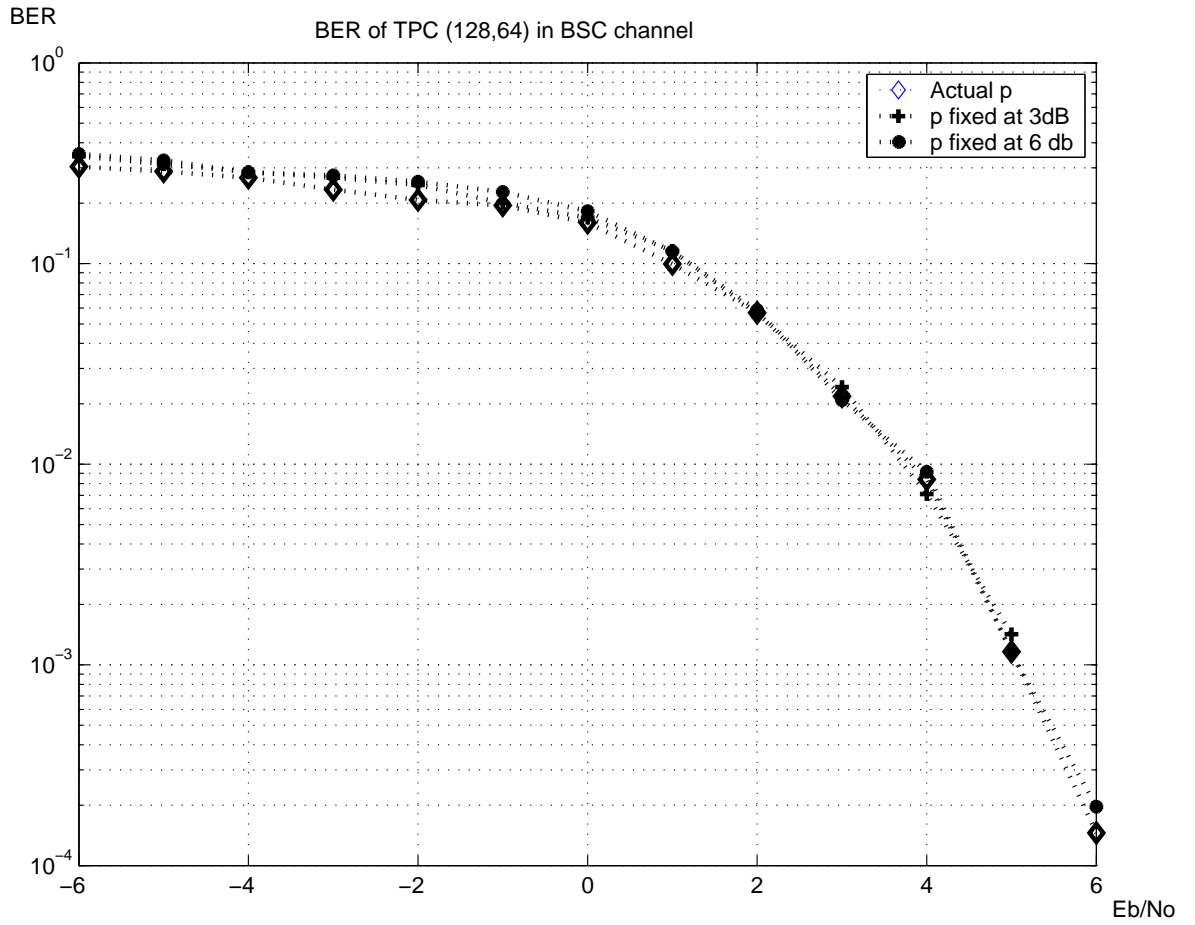


Figure 5.11: Comparison on the performance of the product code with a single fixed value of p code

5.6 Performance Comparison over AWGN Channel

The performance of the system using RS decoder in AWGN channel is the same as the BSC case since the RS decoder uses hard decision decoding. However, the TP decoder is able to perform soft decision decoding and we expect its performance to be better than the case of BSC. As seen from (5.4), the TP decoder needs to know the actual E_b/N_0 in order to decode the received bits. We perform a simulation similar to Fig. 5.11 by fixing the value of E_b/N_0 used by the TP decoder at 3dB or 8dB while the channel experience different level of noise power. Again from Fig. 5.12, by fixing E_b/N_0 used by the TP decoder at 3dB or 8dB, its performance is very closely to one that uses the actual value. Therefore, in situation where E_b/N_0 is not known by the receiver, we can fixed it at one of those 2 values.

In Fig. 5.13, a comparison is made between the RS codes and the TP codes over BSC (which is equivalent to hard decision decoding) and over in AWGN channel (which is equivalent to soft decision decoding). Indeed, the soft decision TP codes has the best performance among the 3 of them. It is about 2dB and 4dB better than the hard decision TP codes and RS codes respectively.

Suppose a genie told the RS decoder on which of the symbols that actually was in error and the RS decoder erased those symbols. This would be the best performance that any erasure scheme could achieve. We would like to know how it's performance compares to the performance of TP codes. Let ξ_8 be the event that {8 or more of the last 15 bytes in error}. Since the RS decoder is able to correct a maximum of 8 erasures, with the help of genie, it is able to know the location of the error bytes and erase them. In this case, it is able to correct up to 8 bytes of error. Following the same argument in previous paragraph, the probability of bit error is computed as follow

$$Pr\{\xi_d\} = Pr\{\xi_b \cap \xi_8\} = Pr\{\xi_b\}Pr\{\xi_8\} = p \sum_{l=8}^{15} \binom{15}{l} P_B^l (1 - P_B)^{15-l}. \quad (5.16)$$

From Fig. 5.14, we observe that with the help of the genie, the RS decoder performs better than the TP codes over BSC after 5dB. In situation where the channel is modelled as BSC, if we are able to locate all the symbol errors, we can replace the TP decoder with a simple RS decoder when $E_b/N_0 \geq 5$ dB.

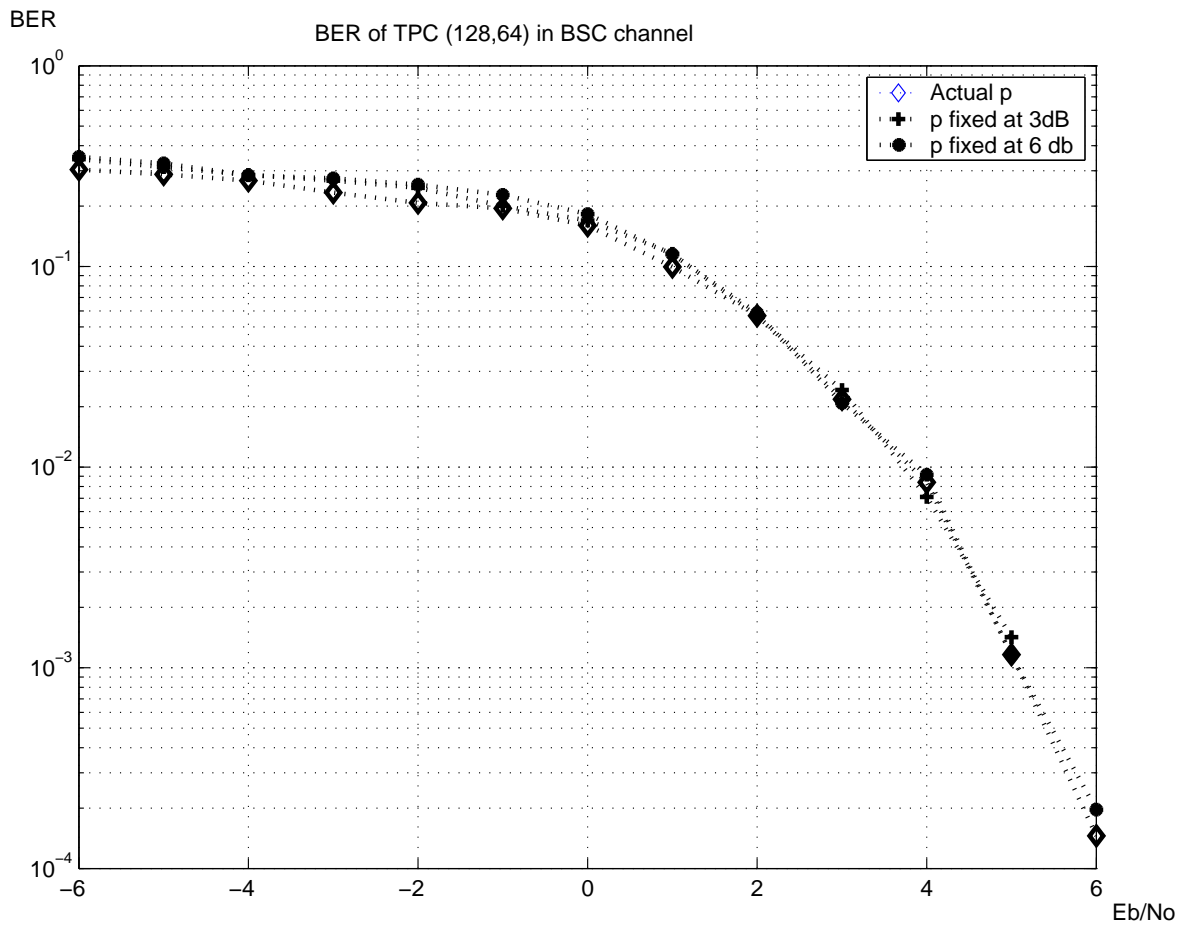


Figure 5.12: Comparison on the performance of the TP codes with a single fixed value of E_b/N_0 code.

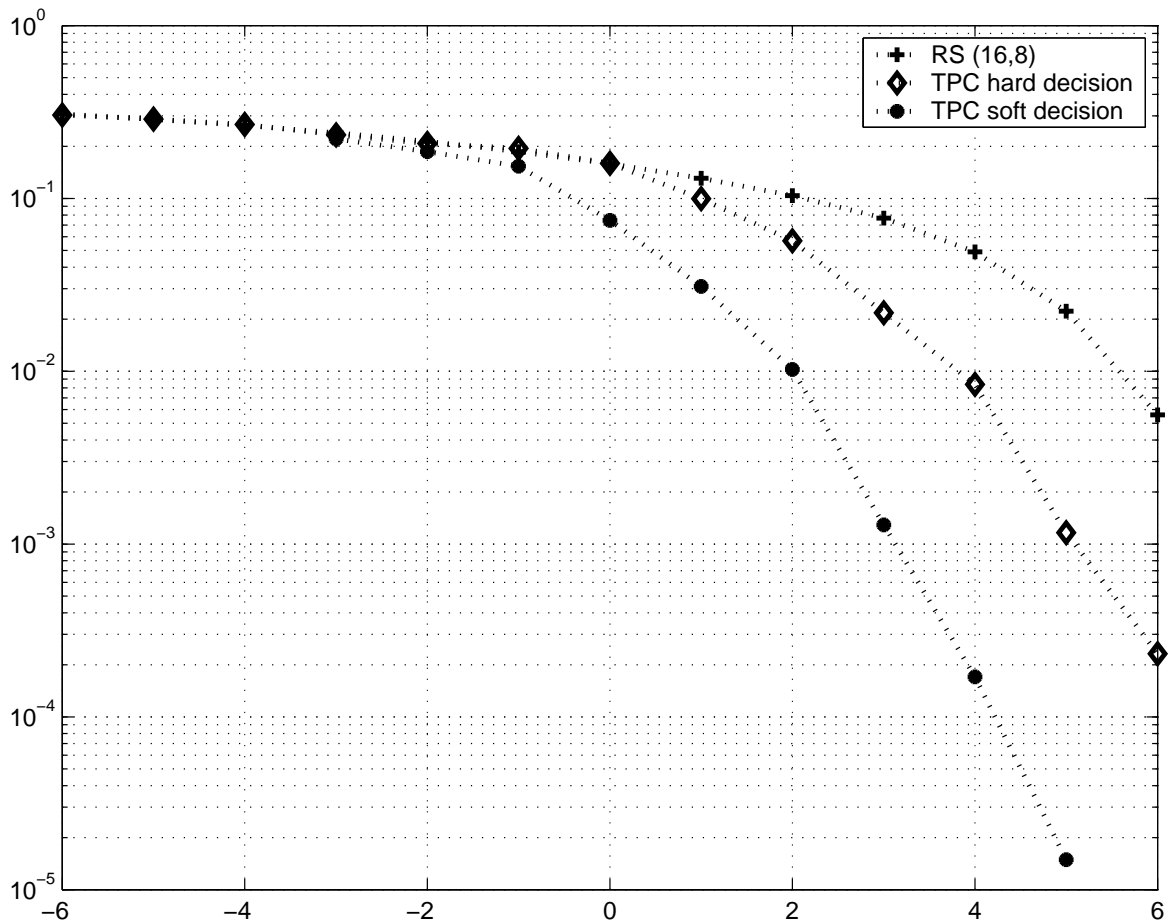


Figure 5.13: Comparison on the performance of the RS codes, hard and soft decision TP codes over AWGN channel.

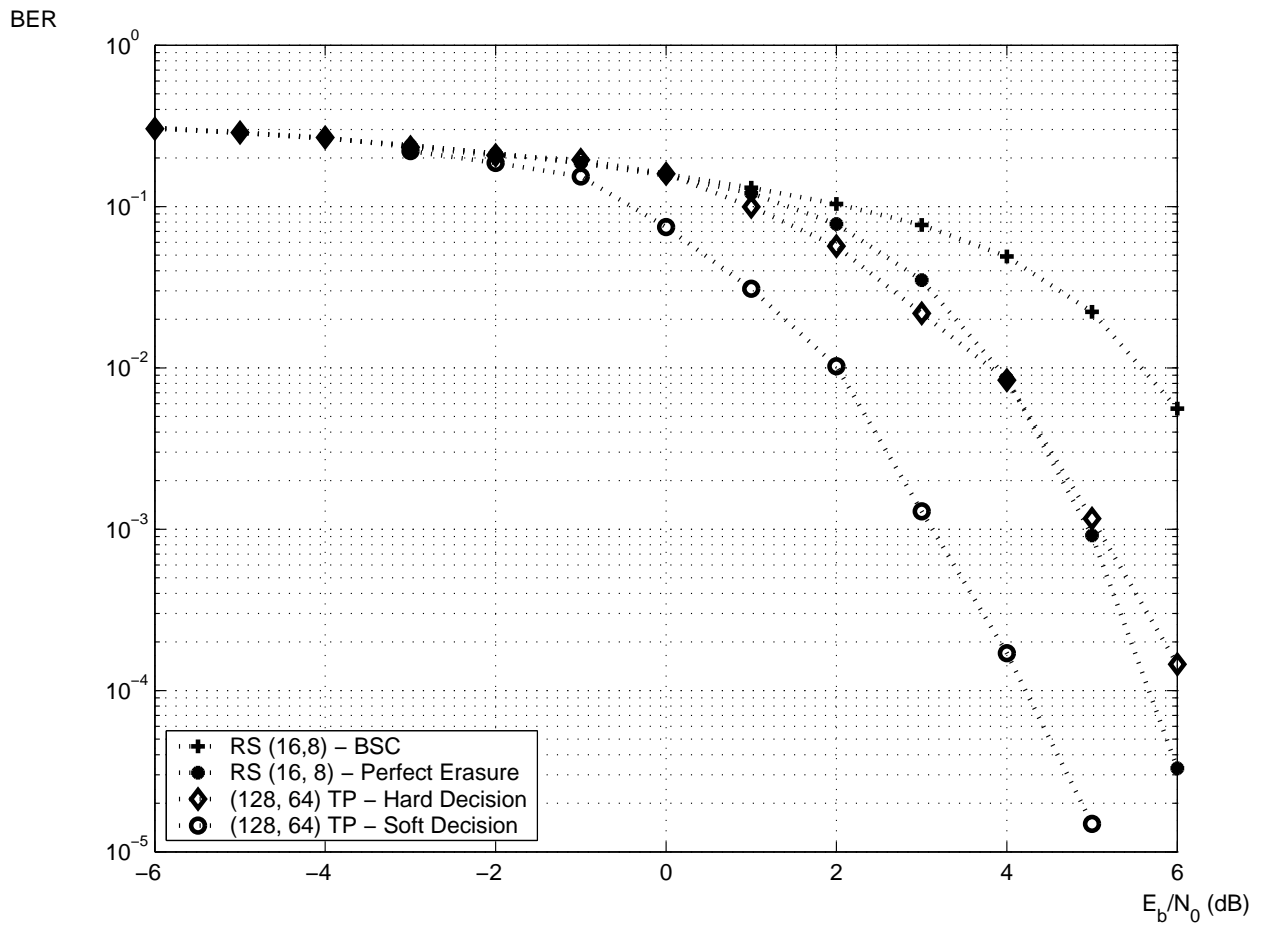


Figure 5.14: Comparison on the performance of the RS codes (with and without genie's help), TP codes over BSC and over AWGN channel.

5.7 Performance of RS Codes Over an Erasure Channel

As the RS code is able to correct up to 8 symbol erasures or 4 symbol errors. We consider the case when the decoder is able to identify the least reliable bits and erase them. From Fig. 5.7, if $|r|$ is less than $|\beta\sqrt{E}|$, the received bit is treated as an “erasure”. The challenge here is to decide the optimal value of β that will give the lowest $Pr\{\xi_d\}$. The analysis of the error probability is as follow.

Each bit received by the RS decoder can either be correct, in error or erased. Denote by $P_{b,correct}$, $P_{b,error}$ and $P_{b,erase}$ the probabilities that a bit is correct, in error and erased respectively. Also, denote by $P_{B,correct}$, $P_{B,error}$ and $P_{B,erase}$ the probabilities that the 8-bit byte is correct, in error and erased respectively. Thus, we have

$$P_{b,correct} + P_{b,error} + P_{b,erase} = 1. \quad (5.17)$$

$$P_{b,erase} = Q\left(\sqrt{\frac{2E}{N_o}}(1 - \beta)\right) - Q\left(\sqrt{\frac{2E}{N_o}}(1 + \beta)\right). \quad (5.18)$$

$$P_{b,error} = Q\left(\sqrt{\frac{2E}{N_o}}(1 + \beta)\right). \quad (5.19)$$

$$P_{B,correct} = P_{b,correct}^8. \quad (5.20)$$

$$P_{B,error} = 1 - (1 - P_{b,error})^8. \quad (5.21)$$

since a 8-bit byte is in error when at least one of the 8 bits is in error. Therefore,

$$\{\text{Received byte is an erasure byte}\} = \left(\left\{\bigcup_{i=1}^8 \text{Bit } i \text{ is in error}\right\} \cup \left\{\bigcap_{i=1}^8 \text{Bit } i \text{ is correct}\right\}\right)^c$$

Hence, we have

$$P_{B,erase} = 1 - P_{b,correct}^8 - (1 - (1 - P_{b,error})^8) = (1 - P_{b,error})^8 - P_{b,correct}^8. \quad (5.22)$$

Let ξ_8 be the event be the event that the number of erasures plus twice the number of errors in the last 15 symbols is greater than or equal to 8. Thus, we have,

$$\begin{aligned}
Pr\{\xi_d\} &= Pr\{\xi_b \cap \xi_8\} \\
&= p \sum_{l=0}^{15} \sum_{\substack{k=8-2l \\ k \geq 0}}^{15-l} \binom{15}{k, l, 15-k-l} P_{B,erase}^k P_{B,error}^l (1 - P_{B,erase} - P_{B,error})^{15-l-k}.
\end{aligned} \tag{5.23}$$

where $\binom{15}{k, l, 15-k-l}$ is a multinomial coefficient [51] define as $\frac{15!}{l!k!(15-k-l)!}$.

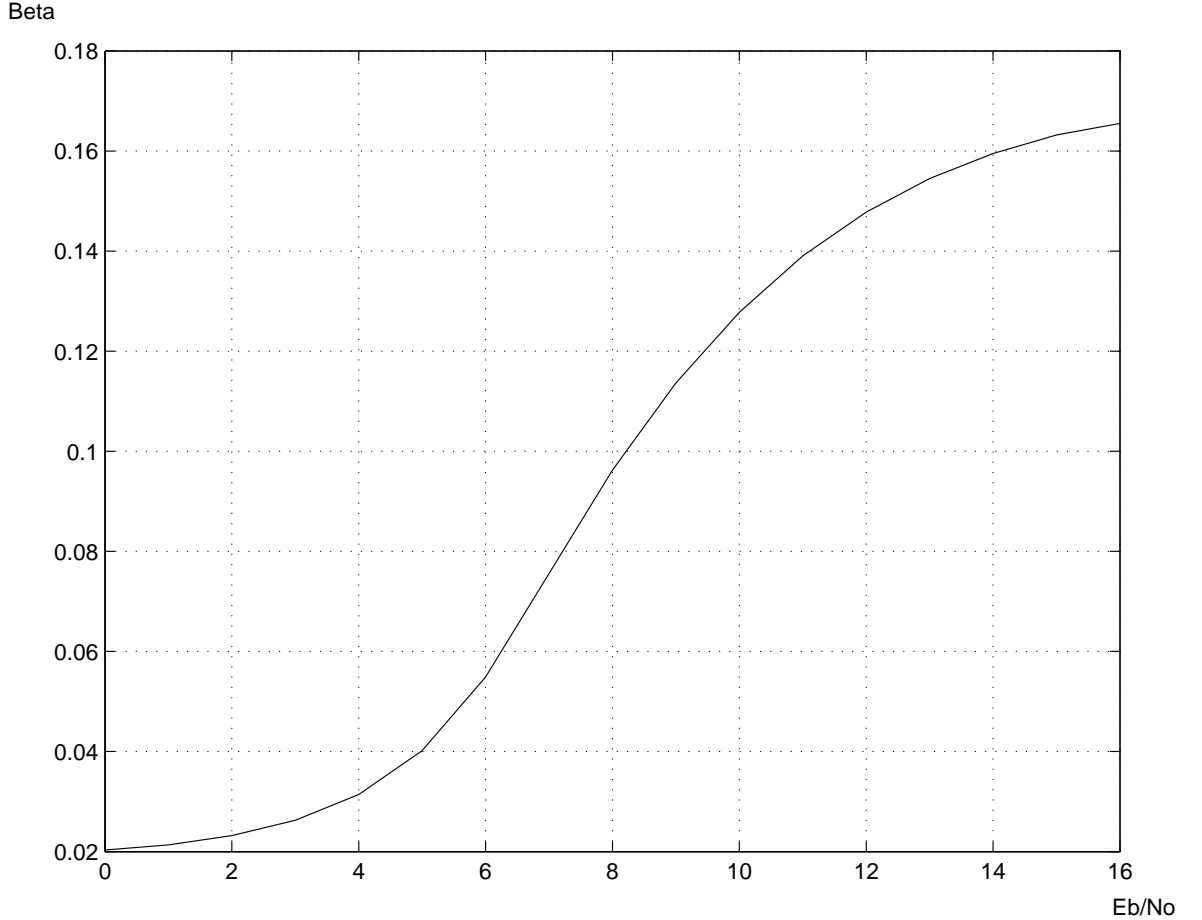


Figure 5.15: Optimal value of threshold β .

A numerical search technique known as the “golden section search” method was employed to find the optimal value of β that determine the lowest bit error probability. The optimal β value is shown as a function of E_b/N_0 in Fig. 5.15. It can be observed that as E_b/N_0 increases, β increases too. As β increases, it reduces both $P_{b,correct}$ and $P_{b,error}$. We can increase the value of β until the benefit of reducing $P_{b,error}$ over $P_{b,correct}$

is the highest. As E_b/N_0 increases, the signals are further apart, the optimum value of β also increases.

Assuming that the RS decoder knows E_b/N_0 , we can use the optimal β value with the corresponding E_b/N_0 for decoding. The bit error performance of the RS code using the optimal β value is compared with the case of no erasures (BSC) and perfect erasures (with the help of genie) is shown in Fig. 5.16. We observed that the bit error performance of the RS code using the optimal value of β for the erasure is very close to the case of the BSC model at low E_b/N_0 . A possible explanation is that at low E_b/N_0 , the value of β is close to 0, with small value of β the probability of a bit being erased is very small. At high SNR, the erasure channel with optimum β is about 1 dB better than the BSC model. But it is about 1.5 dB lower than the “perfect erasure” model.

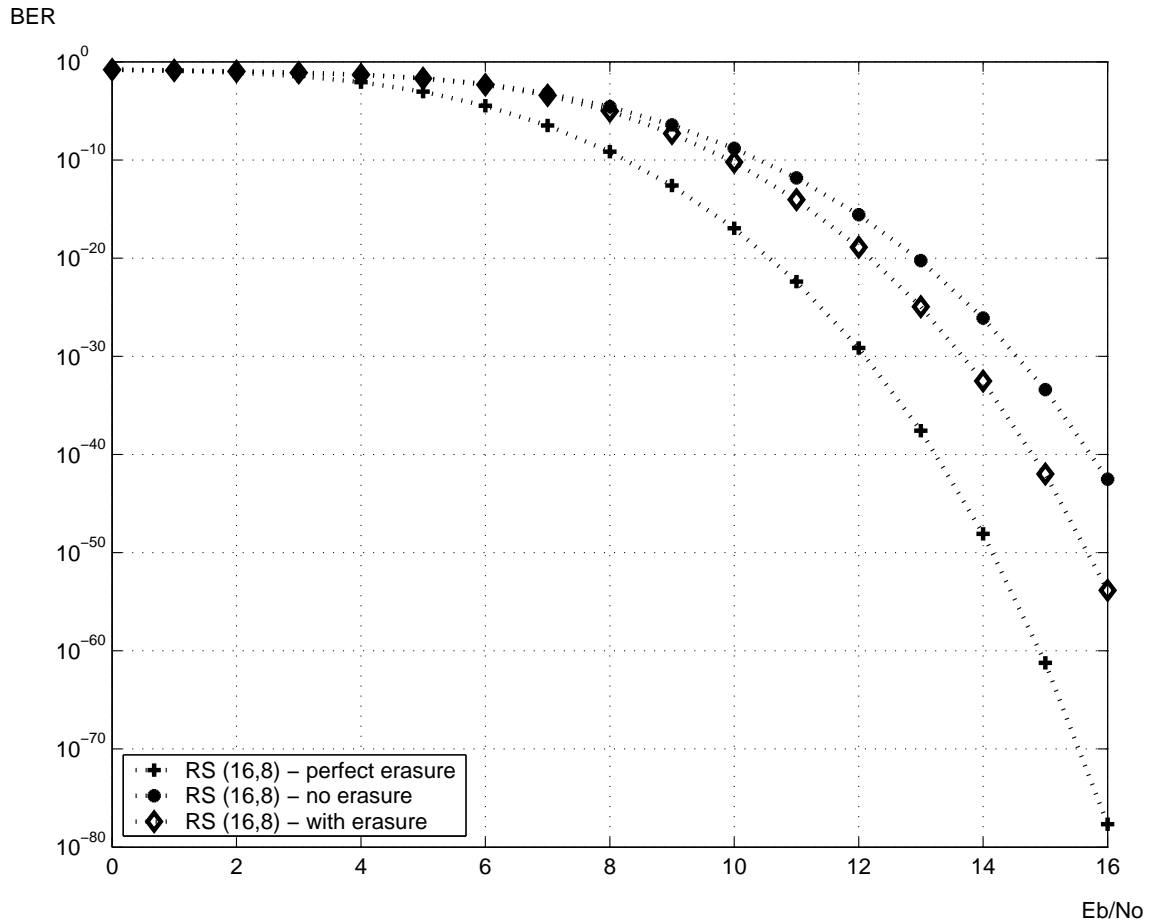


Figure 5.16: Bit Error Rate for the Three Cases of RS codes

5.8 Performance Comparison Over a Bursty Channel

For the bursty channel, we are considering the case when all the 8 bits are subjected to severe degradation with a probability of ρ such that each of the 8 bits has the worst cross-over probability of $p = 0.5$. That is, chances of a “0” being received as “1” is 0.5 and vice versa. As a string of 8-bits error can cause 1 or 2 error symbol, we assume that all the 8 errors bit happened in one byte for our RS codes. This will give the best performance for the RS code in bursty error condition. Let ξ_s be the event that {a 8-bit byte is in error}. For the hard decision TP codes with bursty noise, we let the output of the encoder go through an interleaver before transmission as shown in Figure 3.8. In this case, the probability of severely degraded bits will be scattered all over. As a result, we are able to assume a random occurrence of the severely degraded bits for the TP codes. Hence, the TP codes will see a resulting channel crossover probability p' as

$$p' = \frac{1}{2}\rho + (1 - \rho)p. \quad (5.24)$$

For the system using RS codes,

$$P_{Byte} = Pr\{\xi_s\} = \rho[1 - (0.5)^8] + (1 - \rho)[1 - (1 - p)^8]. \quad (5.25)$$

and

$$Pr\{\xi_d\} = \left[\frac{1}{2}\rho + (1 - \rho)p\right] \sum_{l=4}^{15} \binom{15}{l} P_{Byte}^l (1 - P_{Byte})^{15-l}. \quad (5.26)$$

We evaluate (5.26), considering $\rho = 0, 1/16$ and $2/16$; which corresponds to 0, 1 and 2 bytes being attacked by the burst noise. The performance of the system using hard decision TP codes and RS codes is shown in Fig. 5.17.

Again, as shown in Fig. 5.17, the system using TP codes with interleaver is much superior to RS codes.

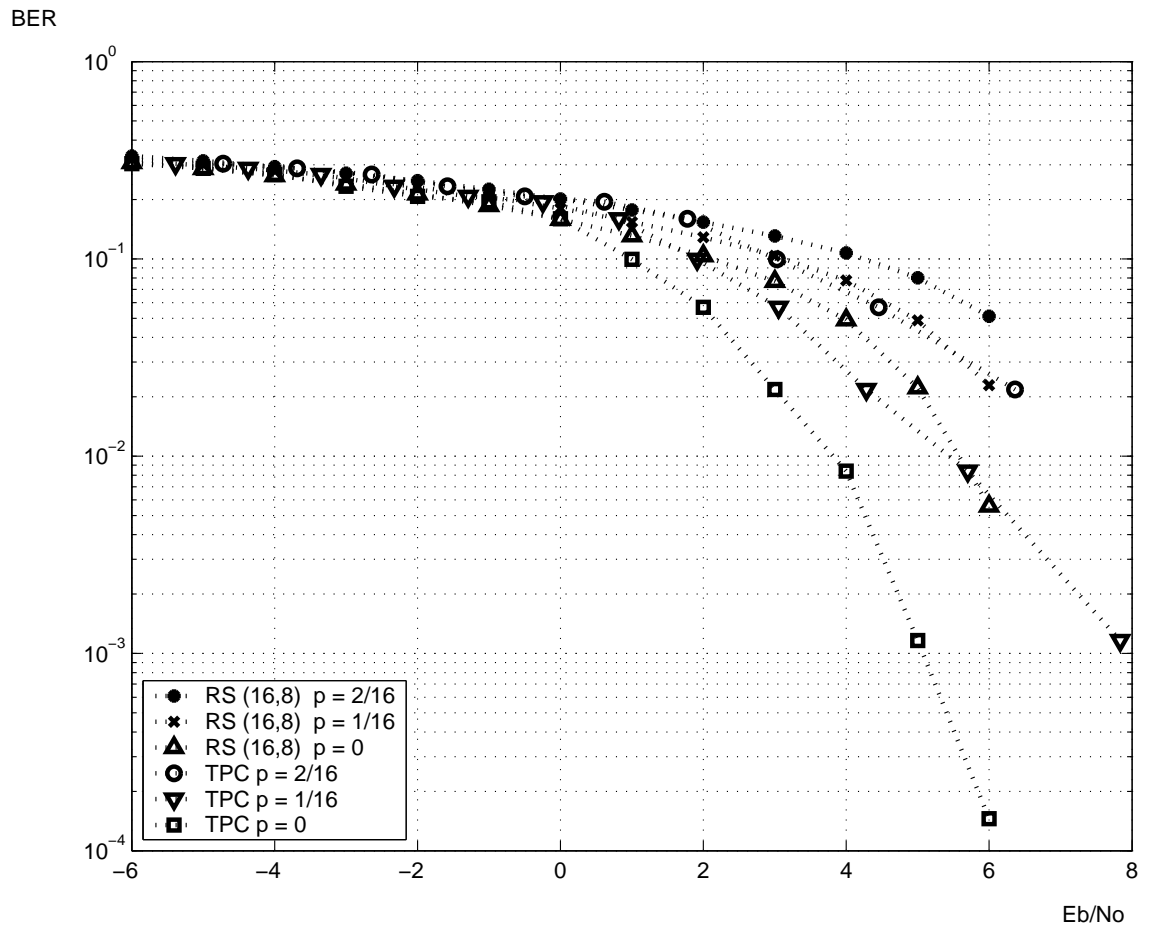


Figure 5.17: Bit error rate for the three Cases of RS codes

5.9 Conclusion

In this chapter, we compare the performance of product codes and RS codes over a BSC, a BSC with erasures, an AWGN channel and a bursty channel. We showed that turbo product codes have better than RS codes over a BSC, an AWGN channel and bursty channel. However, for a BSC with “perfect” erasures, RS codes have a better performance than product code when the SNR is greater than 5 dB.

CHAPTER 6

Conclusions and Future Research

In this chapter, we conclude this thesis by summarizing the content of the thesis and discussing possible future research directions.

6.1 Summary of Contributions

One of the important contributions of this thesis is the performance analysis of RS coded M -ary modulation system with symbol overlapping. We analyzed the bit error performance of this system using a Markov chain technique. We illustrated the bit error performance with specific examples using biorthogonal modulation with coherent detection and orthogonal modulation with coherent and noncoherent detection over an AWGN channel. In addition, we performed simulation on the bit error probability of RS codes concatenated with an NR code over an AWGN channel and compared it with the equivalent RS coded biorthogonal modulation. For the case of Rayleigh flat fading channel, we demonstrated the effect of RS coded modulation on the bit error performance using biorthogonal modulation. Our study showed that over an AWGN channel, a stronger inner code gives better bit error probability. However, in the case of Rayleigh flat fading and block fading channel, a stronger outer code gave a better bit error probability as there is a significant amount of errors present at the output of the demodulator.

We analyzed the throughput of a system using biorthogonal modulation over an

AWGN channel and a Rayleigh fading channel. We found that the minimum SNR in attaining maximum throughput is the lowest for system employing strong inner code for the case of an AWGN channel. However, the conclusion is different for the case of Rayleigh fading channel. In this case, strong outer code would result in the lowest SNR for maximum throughput.

As interleaving and iterative decoding may improve the bit error performance of a communication system, we proposed two novel low complexity coding strategies for RS coded modulation system - (i) bit interleaving with iterations and (ii) symbol interleaving with iterations. Our study demonstrated that the system with symbol interleaving has better bit error and packet error performance as compared to the case with bit interleaving over an AWGN channel and a Rayleigh channel. When we compare it to a system that did not employ symbol overlapping, there was a gain about 1 dB at bit error rate of 10^{-3} at a marginal increase in complexity (i.e. only 2 iterations).

We investigated the relationship between total energy consumed and channel code rate using the cutoff rate and capacity theorem. We derived a closed form expression for the optimal code rate over an AWGN channel at low rate using the cutoff rate theorem. We compare the performance using the cutoff rate theorem and the capacity theorem over an AWGN channel. It was found that they have identical performance when the code rate is high. For the case of Rayleigh fading channel, we used cutoff rate for noncoherent detection in our study. Both AWGN and Rayleigh channels show that a high code rate is desired when the contribution of processing energy is large. For practical coding, we present some numerical results using RS codes and convolutional codes. The results also show that to achieve minimum energy consumed, high code rate is required when processing energy is not insignificant. In addition, we notice that the performance of convolutional code is slightly inferior to the cutoff rate for both an AWGN channel and a Rayleigh channel.

Finally, we compared the performance of TP codes and RS codes when used on three different channels. We found that TP codes have a better performance than RS codes over an AWGN channel, a BSC, and a bursty channel. However, if we assume that an 8-bit RS symbol is erased, RS codes have a better performance than TP codes

using hard decision when the SNR is greater than 5 dB.

6.2 Future Research

In many important communication systems, the errors encountered in the channels are not independent but appear in bursts. The RS concatenated codes for the block fading case in our study is one specific case of bursty channel. One common model used for the bursty channel is the Gilbert-Elliott channel [52], [53]. It would be interesting to extend the research on RS concatenated codes with symbol overlapping using the Gilbert-Elliott channel model.

We demonstrated that for an RS coded M -ary modulation system, there is a performance gain with the use of an interleaver and iterating decoding. However, we presented the bit error performance using simulations. A possible research avenue is to derive its bit error performance analytically. An analytical expression for the bit error probability would benefit communication engineer from the time and resource spent on simulations.

Recently, interesting commercial applications of multi-hop wireless networks have emerged. One example of such applications is “community wireless networks” [54, 55, 56]. Several companies [57, 58] are field-testing wireless networks to provide broadband Internet access to communities that previously did not have such access. The research for energy analysis for short packet length data can be directed towards multi-hop systems. In addition, in our analysis, we assume that the amplifier efficiency is a fixed constant that is independent of the output power. However, in some communication systems that use a class-AB amplifier, the efficiency of the amplifier increases with output power until a certain threshold. Beyond that threshold, the efficiency begins to deteriorate [59]. Therefore, future research is needed to include a more realistic model for the amplifier.

APPENDICES

APPENDIX A

Computation of a 8-bits symbol error in block 1, 2th and 3th

In this section, we show the computation of $P_{1,j}$, $j = 1, 2, 3$.

$$\begin{aligned} P_{1,1} &= P(\overline{E_A}, \overline{E_B}, E_{A'}) + P(\overline{E_A}, E_B, \overline{E_{A'}}) + P(E_A, \overline{E_B}, \overline{E_{A'}}) \\ &= 2P(\overline{E_A}, \overline{E_B}, E_{A'}) + P(\overline{E_A}, E_B, \overline{E_{A'}}). \end{aligned} \quad (\text{A.1})$$

But

$$P(\overline{E_A}, \overline{E_B}, E_{A'}) = (1 - P_s)^2[(1 - P_s)P_s + 3P_{e,1}] \quad (\text{A.2})$$

and

$$P(\overline{E_A}, E_B, \overline{E_{A'}}) = (1 - P_s)^2[(15P_{e,1})(15P_{e,1}) + 2(1 - P_s)(15P_{e,1})]. \quad (\text{A.3})$$

Therefore, we have

$$\begin{aligned} P_{1,1} &= 2(1 - P_s)^2[(1 - P_s)P_s + 3P_{e,1}] + (1 - P_s)^2[(15P_{e,1})(15P_{e,1}) + 2(1 - P_s)(15P_{e,1})] \\ &= (1 - P_s)^2[2(1 - P_s)P_s + 6P_{e,1} + (15P_{e,1})(15P_{e,1} + 2 - 2P_s)]. \end{aligned} \quad (\text{A.4})$$

For $P_{1,2}$,

$$\begin{aligned} P_{1,2} &= P(\overline{E_A}, E_B, E_{A'}) + P(E_A, E_B, \overline{E_{A'}}) + P(E_A, \overline{E_B}, E_{A'}) \\ &= 2P(\overline{E_A}, E_B, E_{A'}) + P(E_A, \overline{E_B}, E_{A'}). \end{aligned} \quad (\text{A.5})$$

Now,

$$P(E_A, \overline{E_B}, E_{A'}) = P_s^2(1 - P_s + 3P_{e,1})^2 + [3P_{e,1}(1 - P_s)]^2 + 6P_sP_{e,1}(1 - P_s)(1 - P_s + 3P_{e,1}) \quad (\text{A.6})$$

Also

$$\begin{aligned} P(\overline{E_A}, E_B, E_{A'}) &= (1 - P_s)\{P_s[15P_{e,1} + (1 - P_s)(59P_{e,1} + P_{e,2})] \\ &\quad + (1 - P_s)[15P_{e,1}(47P_{e,1} + P_{e,2}) + (1 - P_s)(44P_{e,1} \\ &\quad + P_{e,2})]\}. \end{aligned} \quad (\text{A.7})$$

Thus

$$\begin{aligned} P_{1,2} &= 2(1 - P_s)\{P_s[15P_{e,1} + (1 - P_s)(59P_{e,1} + P_{e,2})] + (1 - P_s)[15P_{e,1}(47P_{e,1} + P_{e,2}) \\ &\quad + (1 - P_s)(44P_{e,1} + P_{e,2})]\} + P_s^2(1 - P_s + 3P_{e,1})^2 + [3P_{e,1}(1 - P_s)]^2 \\ &\quad + 6P_sP_{e,1}(1 - P_s)(1 - P_s + 3P_{e,1}). \end{aligned} \quad (\text{A.8})$$

Finally, using a similar derivation as above, we have

$$\begin{aligned} P_{1,3} &= P(E_A, E_B, E_{A'}) \\ &= P_s^2(59P_{e,1} + P_{e,2})(2 - P_s + 3P_{e,1}) + (1 - P_s)^2(44P_{e,1} + P_{e,2})(50P_{e,1} + P_{e,2}) \\ &\quad + 2P_s(1 - P_s)[(44P_{e,1} + P_{e,2}) + 3P_{e,1}(59P_{e,1} + P_{e,2})] \end{aligned} \quad (\text{A.9})$$

APPENDIX B

Computation of Bit Error Probability After Decoding

In this section, we show a detail computation for the bit error probability after decoding for (96,84) RS coded 64-ary biorthogonal modulation over an AWGN channel.

Define:

ϵ_2 : 2nd 8-bit symbol in a block is in error.

ϵ_3 : 3rd 8-bit symbol in a block is in error.

$$\begin{aligned}
 P(\epsilon_d) &= P_{bmb} \sum_{j=0}^2 P(\varepsilon_{j,2}) P(W_{32} \geq 6 - j) \\
 &= P_{bmb} [P(\varepsilon_{0,2}) P(W_{32} \geq 6) + P(\varepsilon_{1,2}) P(W_{32} \geq 5) + P(\varepsilon_{2,2}) P(W_{32} \geq 4)] \\
 &= P_{bmb} [P(W_{32} \geq 4) P(\epsilon_2, \epsilon_3) + P(W_{32} \geq 5) P(\bar{\epsilon}_2, \epsilon_3) + P(W_{32} \geq 5) P(\epsilon_2, \bar{\epsilon}_3) \\
 &\quad + P(W_{32} \geq 6) P(\bar{\epsilon}_2, \bar{\epsilon}_3)]. \tag{B.1}
 \end{aligned}$$

$$\begin{aligned}
 P(\epsilon_2, \epsilon_3) &= P_{smb} (59P_{e,1} + P_{e,2}) (2 - 59P_{e,1} - P_{e,2}) + (1 - P_{smb}) [(59P_{e,1} \\
 &\quad + P_{e,2}) (47P_{e,1} + P_{e,2}) + (1 - P_{smb} + 3P_{e,1}) (44P_{e,1} + P_{e,2})]. \tag{B.2}
 \end{aligned}$$

$$P(\bar{\epsilon}_2, \bar{\epsilon}_3) = (1 - P_{smb})^2 (1 - P_{smb} + 3P_{e,1}). \tag{B.3}$$

Similarly,

$$\begin{aligned} P(\varepsilon_{1,2}) &= P(\bar{\epsilon}_2, \epsilon_3) + P(\epsilon_2, \bar{\epsilon}_3) \\ &= P_{smb}(1 - P_{smb} + 3P_{e,1})^2 + 3P_{e,1}(1 - P_{smb})(1 - P_{smb} + 3P_{e,1}) \\ &\quad + (1 - P_{smb})[15P_{e,1} + (1 - P_{smb})(59P_{e,1} + P_{e,2})]. \end{aligned} \tag{B.4}$$

APPENDIX C

Proof On the Markov Chain for DPSK Error Probability

Let c_j be the event of correct decision for the j th bit. The decision variable for k th bit at the output of the receiver is

$$r_k = \sqrt{E_c} \exp(j\theta_k + \phi) + n_k \quad (\text{C.1})$$

where θ_k, ϕ is the phase angle and phase offset of the k th bit and $n_k = n_{kc} + jn_{ks}$ is a noise vector. Let $u_k = r_k \exp(-j\phi)$. Therefore, we have

$$u_k = \sqrt{E_c} \exp(j\theta_k) + n_k \exp(-j\phi). \quad (\text{C.2})$$

Hence, the statistic of u_k does not depend on ϕ since ϕ only rotates the noise component. Without loss of generality, we consider the all zero codeword is transmitted. A correct decision is made on k th bit if [10] $\Re(r_k r_{k-1}^*) > 0$ where $\Re(x)$ denotes the real part of x . Since $r_k r_{k-1}^* = u_k u_{k-1}^*$, the statistic of $r_k r_{k-1}^*$ is independent of ϕ . Hence, we have

$$\begin{aligned} P(c_m | c_{m-1}, \dots, c_k, \dots) &= P(\Re(r_m r_{m-1}^*) > 0 | \Re(r_{m-1} r_{m-2}^*) > 0, \dots, \Re(r_k r_{k-1}^*) > 0, \dots) \\ &= P(\Re(u_m u_{m-1}^*) > 0 | \Re(u_{m-1} u_{m-2}^*) > 0, \dots, \Re(u_k u_{k-1}^*) > 0, \dots) \\ &= P(\Re(u_m u_{m-1}^*) > 0 | \Re(u_{m-1} u_{m-2}^*) > 0). \end{aligned} \quad (\text{C.3})$$

The above expression is true since event c_m only depends on $\Re(u_m u_{m-1}^*)$. Therefore, given the event c_{m-1} , i.e. $\Re(u_{m-1} u_{m-2}^*) > 0$, it is independent of the event c_{m-2}, \dots, c_0 .

BIBLIOGRAPHY

BIBLIOGRAPHY

- [1] C. E. Shannon, "A mathematical theory of communication," *Bell Syst. Tech Journal*, vol. 27, pp. 623–656, October 1948.
- [2] R. W. Hamming, "Error detection and error correction codes," *Bell Syst. Tech. Journal*, vol. 29, pp. 147–160, April 1950.
- [3] S. Roman, *Coding and Information Theory*. Springer-Verlag, 1992.
- [4] G. D. Forney Jr., "Performance of concatenated codes," *Concatenated Codes*, pp. 1–6, 82–90, 1966.
- [5] C. Berrou, A. Glavieux, and P. Thitimajshima, "Near Shannon limit error-correcting coding and decoding: Turbo-codes," *Proceedings of the 1993 International Conference on Communications*, pp. 1064–1069, May 1993.
- [6] R. Gallager, "Low density parity check codes," *IEEE Trans. on Information Theory*, vol. IT-8, pp. 21–28, January 1962.
- [7] R. E. Blahut, *Theory and Practice of Error Control Codes*. Reading, MA: Addison-Wesley, 1983.
- [8] T. J. Richardson, M. A. Shokrollahi, and R. L. Urbanke, "Design of capacity-approaching irregular low-density parity-check codes," *IEEE Trans. on Information Theory*, vol. 47, pp. 619–637, February 2001.
- [9] T. Nakanishi and T. Ikegami, "Throughput performance of CDMA-ALOHA in S-band land mobile satellite channel," *Proceeding of the 2000 IEEE Sixth International Symposium on Spread Spectrum Techniques and Applications*, pp. 383–386, September 06-08 2000.
- [10] J. G. Proakis, *Digital Communications*, 3rd ed. McGraw Hill, 1995.
- [11] M. Rintamaki, H. Kovio, and I. Hartimo, "Adaptive closed-loop power control algorithms for CDMA cellular communication systems," *IEEE Trans. on Vehicular Technology*, vol. 53, no. 6, pp. 1756–1768, November 2004.
- [12] H. Su and E. Geraniotis, "Adaptive closed-loop power control with quantized feedback and loop filtering," *IEEE Trans. on Wireless Communications*, vol. 1, no. 1, pp. 76–86, January 2002.

- [13] R. H. Deng and M. L. Lin, "A type I hybrid ARQ system with adaptive code rates," *IEEE Trans. on Communications*, vol. 43, no. 234, pp. 733–737, February/March/April 1995.
- [14] S. B. Wicker and M. J. Bartz, "Type-II hybrid-ARQ protocols using punctured MDS codes," *IEEE Trans. on Communications*, vol. 42, no. 234, pp. 1431–1440, February/March/April 1994.
- [15] S. Lin and D. Costello, *Error Control Coding: Fundamentals and Applications*. Prentice-Hall, 1983.
- [16] A. Michelson and A. Levesque, *Error-control Techniques for Digital Communication*. New York: Wiley, 1985.
- [17] T. Kasami, T. Takata, T. Fujiwara, and S. Lin, "A concatenated coded modulation scheme for error control," *IEEE Trans. on Communications*, vol. 38, pp. 752–763, 1990.
- [18] B. Vucetic, "Bandwidth efficient concatenated coding schemes for fading channels," *IEEE Trans. on Communications*, vol. 41, pp. 50–61, January 1983.
- [19] R. D. Cideciyan and E. Eleftheriou, "Concatenated Reed-Solomon/convolutional coding scheme for data transmission in CDMA cellular systems," *IEEE Vehicular Technology conference*, pp. 1369–1373, June 8-10 1994.
- [20] Q. Wang, Q. Chen, V. K. Bhargava, and L. J. Mason, "Block and decoded error probabilities of DPSK in AWGN," *IEEE Trans. on Communications*, vol. 42, pp. 3065–3068, Dec 1994.
- [21] M. Zorzi and R. Rao, "Coding tradeoffs for reduced energy consumption in sensor networks," *PIMRC, PIMRC, Barcelona, Spain*, Sep 2004.
- [22] P. Elias, "Error-free coding," *IRE Trans. on Information Theory*, pp. 29–37, September 1954.
- [23] L. L. Joiner and J. J. Komo, "Soft decision Reed-Solomon coding for MPSK slow frequency hop spread spectrum multiple access communications," *Proceeding of the 2004 IEEE Military Communications Conference*, October 31 - November 3 2004.
- [24] T. Kasami and S. Lin, "On the probability of undetected error for the maximum distance separable codes," *IEEE Trans. Commun.*, vol. COM-32, no. 9, pp. 998–1006, September 1984.
- [25] K. M. Cheung, "More on the decoder error probability for Reed-Solomon codes," *IEEE Trans. on Information Theory*, vol. 35, pp. 895–900, July 1989.
- [26] D. J. Taipale and M. J. Seo, "An efficient soft-decision Reed-Solomon decoding algorithm," *IEEE Trans. on Information Theory*, vol. 40, pp. 1130–1139, July 1994.

- [27] J. Jing and K. R. Nnarayanan, "Iterative soft decoding of Reed-Solomon codes," *IEEE Communications Letters*, vol. 8, pp. 244–246, Apr 2004.
- [28] O. Aitsab and R. Pyndiah, "Performance of Reed-Solomon block turbo code," *Proc. Globecom Conf.*, vol. 1, pp. 121–125, Nov 1996.
- [29] H.-Y. Lee and I.-C. Park, "A fast Reed-Solomon product-code decoder without redundant computations," *Proc. ISCAS*, vol. 2, pp. 381–384, May 2004.
- [30] B. Sklar, *Digital Communications*. New Jersey: Prentice Hall, 1988.
- [31] S. G. Wilson, *Digital Modulation and Coding*. Englewood Cliffs, New Jersey: Prentice-Hall, 1995.
- [32] A. Goldsmith, *Wireless Communications*. New York, New York: Cambridge University Press, 2005.
- [33] M. Nafie, A. G. Dabak, T. M. Schmidl, and A. Gatherer, "Enhancements to the bluetooth specification," *Proceeding of the 2001 Thirty Fifth Asilomar Conference on Signals, Systems and Computers*, vol. 2, pp. 1591–1595, Nov 2001.
- [34] B. K. Poh and P. C. Phang, "High data rate MDPSK receiver architecture for indoor wireless application," *Proceeding of the 2002 IEEE Thirteenth International Symposium on Personal, Indoor and Mobile Radio Communications*, vol. 4, pp. 1718–1721, Sep 2002.
- [35] J. Goldman, "Multiple error performance of PSK systems with cochannel interference and noise," *IEEE Trans. on Commun. Technol*, vol. COM-19, pp. 420–430, Aug 1971.
- [36] J. F. Oberst and D. L. Schilling, "Double error probability in differential PSK," *Proc. IEEE*, vol. 56, pp. 1099–1100, Jun 1968.
- [37] Q. Wang and Q. Chen, "Block and decoded error probabilities of DPSK in AWGN," *Proceeding of the 25th Annual Conference on Information Science and Systems*, pp. 395–401, Mar 1991.
- [38] M. Weiser, B. Welch, A. Demers, and S. Shenker, "Scheduling for reduced CPU energy," *Proc. Symp. Operating System Design and Implementation (OSDI)*, pp. 13–23, Nov 1994.
- [39] R. Graybill and E. R. Melhem, *Power Aware Computing*. Kluwer, 2002.
- [40] F. Zhang and S. T. Chanson, "Processor voltage scheduling for real-time tasks with non-preemptible sections," *Proc. IEEE Real-Time Systems Symp. (RTSS)*, pp. 235–245, Dec 2002.
- [41] C. Rusu, R. Melhem, and D. Mosse, "Maximizing rewards for real-time applications with energy constraints," *ACM Trans. Embedded Comput. Syst.*, vol. 2, pp. 537–559, 2003.

- [42] J. L. Massey, “Coding and modulation in digital communications,” *Proc. Int. Zurich Sem. on Digital Communications*, March 1974.
- [43] J. M. Wozencraft and I. M. Jacobs, *Principles of Communication Engineering*. New York: Wiley, 1965.
- [44] T. S. Rappaport, *Wireless Communications: Principle and Practice*. New Jersey: Prentice-Hall, 1996.
- [45] R. G. Gallager, *Information theory and reliable communication*. New York: Wiley, 1968.
- [46] W. E. Stark, “Capacity and cutoff rate of noncoherent FSK with nonselective Rician fading,” *IEEE Transaction on Communications.*, vol. 33, no. 11, pp. 1153–1159, November 1985.
- [47] R. Tanner, “A recursive approach to low complexity codes,” *IEEE Trans. Information Theory*, vol. IT-27, no. 5, September 1981.
- [48] P. Sweeney, *Error Control Coding, from Theory to Practice*. John Wiley & Sons, 2002.
- [49] S. B. Wicker, *Error Control Systems for Digital Communication and Storage*. Englewood Cliffs, New Jersey: Prentice-Hall, 1995.
- [50] A. Dür, “On the computation of the performance probabilities for block codes with a bounded-distance decoding rule,” *IEEE Trans. on Information Theory*, vol. IT-34, pp. 70–78, January 1988.
- [51] S. Ross, *A First Course in Probability*. Prentice Hall, 2002.
- [52] E. N. Gilbert, “Capacity of a burst-noise channel,” *Bell Syst. Tech. Journal*, pp. 1253–1265, Sept. 1960.
- [53] E. O. Elliott, “Estimates of error rates for codes on burst-noise channels,” *Bell Syst. Tech. Journal*, pp. 1977–1997, Sept. 1963.
- [54] “Bay area wireless users group,” <http://www.bawug.org/>.
- [55] “Mit roofnet,” <http://www.pdos.lcs.mit.edu/roofnet/>.
- [56] “Seattle wireless,” <http://www.seattlewireless.net/>.
- [57] “Mesh networks inc.” <http://www.meshnetworks.com>.
- [58] “Radiant networks,” <http://www.radiantnetworks.com/>.
- [59] C. P. Liang, J. H. Jong, W. E. Stark, and J. R. East, “Nonlinear amplifier effects in communications systems,” *IEEE Trans. on Microwave Theory and Techniques*, vol. 47, pp. 1461–1466, Aug 1999.